VOL. 9 NO. 3 MARCH 1965

Journal of

ELECTROANALYTICAL CHEMISTRY

International Journal Dealing with all Aspects of Electroanalytical Chemistry, Including Fundamental Electrochemistry

ELSEVIER

GENERAL INFORMATION

See also Suggestions and Instructions to Authors which will be sent free, on request to the Publishers.

Types of contributions

(a) Original research work not previously published in other periodicals.
(b) Reviews on recent developments in various fields.
(c) Short communications.
(d) Bibliographical notes and book reviews.

Languages

Papers will be published in English, French or German.

Submission of papers

Papers should be sent to one of the following Editors:

Professor J. O'M. Bockris, John Harrison Laboratory of Chemistry, University of Pennsylvania, Philadelphia 4, Pa., U.S.A.
Dr. R. Parsons, Department of Chemistry, The University, Bristol 8, England.
Professor C. N. Reilley, Department of Chemistry, University of North Carolina, Chapel Hill, N.C., U.S.A.

Authors should preferably submit two copies in double-spaced typing on pages of uniform size. Legends for figures should be typed on a separate page. The figures should be in a form suitable for reproduction, drawn in Indian ink on drawing paper or tracing paper, with lettering etc. in thin pencil. The sheets of drawing or tracing paper should preferably be of the same dimensions as those on which the article is typed. Photographs should be submitted as clear black and white prints on glossy paper.
All references should be given at the end of the paper. They should be numbered and the numbers should appear in the text at the appropriate places.
A summary of 50 to 200 words should be included.

Reprints

Twenty-five reprints will be supplied free of charge. Additional reprints can be ordered at quoted prices. They must be ordered on order forms which are sent together with the proofs.

Publication

The *Journal of Electroanalytical Chemistry* appears monthly and has six issues per volume and two volumes per year, each of approx. 500 pages.

Subscription price (post free): £ 12.12.0 or $ 35.00 or Dfl. 126.00 per year; £ 6.6.0 or $ 17.50 or Dfl. 63.00 per volume.
Additional cost for copies by air mail available on request.
For advertising rates apply to the publishers.

Subscriptions

Subscriptions should be sent to:

ELSEVIER PUBLISHING COMPANY, P.O. Box 211, Amsterdam, The Netherlands.

SUMMARIES OF PAPERS PUBLISHED IN JOURNAL OF ELECTROANALYTICAL CHEMISTRY

Vol. 9, No. 3, March 1965

POINTS OF ZERO CHARGE IN EQUATIONS OF ELECTROCHEMICAL KINETICS

The reaction rate of the electron transfer is determined both by the electrode potential, φ, measured against a constant reference electrode and by the structure of the electric double layer, which to the first approximation depends on the electrode potential referred to the potential of zero charge, *i.e.*, $\varphi - \varphi_0$. It is shown that in order to make a rational comparison of the rates of reactions occurring on different electrodes it is not sufficient to know only the quantity $\varphi - \varphi_0$.

The effect of the presence of adsorbed hydrogen and oxygen on the electrode surface upon the process rate is considered.

A. N. FRUMKIN,
J. Electroanal. Chem., 9 (1965) 173–183

ELECTROLYTIC SEPARATION AND COLORIMETRIC DETERMINATION OF TRACES OF LEAD IN COBALT USING ISOTOPIC DILUTION ANALYSIS

Traces of lead in cobalt are determined colorimetrically with dithizone after a prior separation of the lead on to a mercury cathode using controlled potential analysis and subsequent distillation of the mercury in a nitrogen atmosphere. The total yield of lead is determined using the radio-isotope ^{210}Pb. The conditions, *i.e.*, electrolysis time, cathode potential, acidity, mercury volume, lead concentration, for electrodeposition of micro quantities were investigated. Interferences of cobalt, mercury, indium and bismuth are discussed.

A. LAGROU AND F. VERBEEK,
J. Electroanal. Chem., 9 (1965) 184–191

INFLUENCE OF MERCURY DROP GROWTH AND GEOMETRY ON THE A.C. POLAROGRAPHIC WAVE

Theoretical reassessment of the contributions of electrode growth and geometry on the a.c. polarographic wave is given. Examination of the theory for the 'quasi-reversible' a.c. wave indicates that these factors contribute significantly when the *d.c.* process is influenced by charge transfer kinetics. Generalization of these results leads to the conclusion that growth and geometry can be important when any rate process in addition to diffusion kinetically influences the d.c. process. If the d.c. process is diffusion-controlled or non-existent (zero direct current), theory predicts that these effects will be negligible, in agreement with earlier works of KOUTECKÝ and GERISCHER. An equation is given for the a.c. polarographic wave with a quasi-reversible process at the expanding spherical electrode. Derivation of similar exact expressions for more complex mechanisms is discussed. Implications of these results with regard to experimental approach and work with stationary electrodes are considered.

J. R. DELMASTRO AND D. E. SMITH,
J. Electroanal. Chem., 9 (1965) 192–217

REDUCTION OF IODATE IN SULPHURIC MEDIUM

I. THE REDUCTION MECHANISM

The iodic acid reduction in sulphuric medium on platinum micro-electrodes has been studied by polarographic, coulometric and chronopotentiometric methods. The influence of iodide ions, sulphuric acid protonic activity and of ligands of I^-, such as Tl(I) and Hg(II) on the reduction process has been extensively investigated. It is demonstrated that the iodate is not directly reduced but with a very high overtension and that reduction is strongly catalyzed by traces of I_2.

P. G. DESIDERI,
J. Electroanal. Chem., 9 (1965) 218–228

REDUCTION OF IODATE IN SULPHURIC MEDIUM
II. THE INFLUENCE OF THE SURFACE OF THE PLATINUM ELECTRODE

Iodic acid reduction on platinum micro-electrodes was studied with polarographic and chronopotentiometric methods with reference to the surface state of the electrodes. Treatment and treatment time of the electrodes and influence of sulphuric acidity, iodic acid concentration and iodine on the reduction process, were investigated. It is shown that the modification of the surface state of the electrode influences only the first stage of the reduction process. The role of the I_2/I^- system in the iodic acid reduction is confirmed.

P. G. DESIDERI,
J. Electroanal. Chem., 9 (1965) 229–236

THE ELECTRICAL DOUBLE LAYER ON INDIUM AMALGAMS IN 0.1 *M* $HClO_4$ AT 25°

The double-layer capacity of indium amalgams was measured at 25° in 0.1 *M* $HClO_4$ using a dropping electrode. Fourteen amalgams ranging in composition from 0.001–64.4 mole % In were studied. At indium concentrations below 0.001%, the capacity is identical to pure mercury; at higher concentrations, a pseudo-capacity due to the dissolution of indium is observed at potentials more positive than the $In-In^{3+}$ equilibrium potential. As the concentration of indium varies from 1–70%, the zero-charge potential shifts 0.4 V more negative, and the capacity–potential curve shows a corresponding shift. The capacity–surface charge curve in concentrated indium amalgams shows the same "hump" near the zero-charge point as in pure mercury.

At a surface charge of $-10\ \mu C/cm^2$, the capacity varies from $15\ \mu F/cm^2$ for mercury to $20\ \mu F/cm^2$ for 64% indium amalgam. At a surface charge of $+10\ \mu C/cm^2$, the capacity of a 64% indium amalgam is approximately twice that of mercury.

The potential drop across the diffuse double layer was calculated using the Gouy–Chapman theory. The influence of the diffuse double layer is greater for concentrated amalgams than for mercury. Previous data for hydrogen overvoltage on indium amalgams together with the capacity measurements was used to analyze the effect of the diffuse double layer on the hydrogen discharge reaction.

J. N. BUTLER, M. L. MEEHAN AND A. C. MAKRIDES,
J. Electroanal. Chem., 9 (1965) 237–250

POINTS OF ZERO CHARGE IN EQUATIONS OF ELECTROCHEMICAL KINETICS

A. N. FRUMKIN
Institute of Electrochemistry of the Academy of Sciences of the USSR, Moscow (USSR)
(Received December 21st, 1964)

INTRODUCTION

In equations of electrochemical kinetics expressing the dependence of the reaction rate upon the potential, the solution composition and the electrode nature, potentials can be referred to a constant reference electrode or to the potential of zero charge of the relevant electrode (rational potentials according to GRAHAME[1], the φ-scale of potentials according to ANTROPOV[2]). In the present communication I shall consider the advantages and drawbacks of a particular method of reference used in comparing the reaction rates on different electrodes. Closely associated with this, is the question of whether the electron work function at the metal–vacuum interfaces should appear in equations of electrochemical kinetics. Although the theoretical considerations presented here are not new in principle, it seemed necessary to return to this question as it has been treated inconsistently in the literature.

The expression for the rate of the electrochemical process containing potentials read from the point of zero charge was first proposed for the case of the hydrogen-ion discharge on mercury[3], but the effect of the nature of the metal upon the kinetics of the process was not then considered. ANTROPOV[2] proposed kinetic equations for the electro-reduction of organics taking into account the zero charge potential. According to BOCKRIS AND POTTER[4], the rate of processes on different electrodes should be compared at potentials of zero charge.

HYDROGEN-ION DISCHARGE

Let us consider in what form the value of the electrode potential appears in equations of electrochemical kinetics taking as example the much discussed reaction of the hydrogen-ion discharge in the simplest case when the process rate is determined by the discharge step at small coverage of the surface with adsorbed hydrogen. Let us suppose the interaction of the H_3O^+ ion with the electrode surface to be completely determined by coulombic forces. PARSONS has shown that the expression for the rate of discharge can be obtained by assuming formally that in the transition state of the reaction, a fraction α of the charge of the H_3O^+ ion is neutralized[5,6]. Let us assume that the potential in the bulk of the solution is zero; g_H is the standard free energy of

desorption of a hydrogen atom from the electrode surface (consequently, $g_H > 0$), φ is the electrode potential relative to the solution and ψ_1 is the potential in the solution at the point where the electric centre of the reacting particle in the transition state of the reaction is located. A more exact definition of the quantity φ will be given later. The reaction rate is determined by the difference in levels of the standard free energy in the transition and initial states of the system, which is equal to:

$$[(1-\alpha)\psi_1 F - (1-\alpha)\varphi F - \alpha g_H] - [-\varphi F] = \alpha(\varphi F - \psi_1 F - g_H) + \psi_1 F \quad (1)$$

as in the transition state, according to our assumption, the charge (per mol of substance) is equal to $(1-\alpha)F$, the electrode charge to $-(1-\alpha)F$, and the fraction, α, of the H mole appears on the electrode*. In the initial state, however, it is necessary to take into consideration the free energy of the electrons at the potential φ. This elementary consideration does not take into account the fact that the energy level (the Fermi level) of the electron depends not only on the electrode potential, but also on the nature of the metal. This does not lead to an error if we consider the behaviour of one metal electrode, *e.g.*, mercury[6]. If we use eqn. (1), however, to compare the electrode behaviour of two different metals and assume that φ is the metal–solution potential difference (Galvani potential), such an assumption will lead to erroneous results, as in the case of two electrodes made from different metals, equal values of the Galvani potential relative to the same solution correspond to different energy levels of the electron. On the other hand, if φ is the potential in some unchanging metal (*e.g.*, platinum) connected with the electrode metal and in electronic equilibrium with it (we shall call it the metal of the lead) equal values of φ will really correspond to identical energy levels of the electron. But in that case, φ will differ from the potential measured against any constant reference electrode by a constant quantity, independent of the metal of the electrode under consideration. In fact, this constant quantity is equal to the sum of the Galvani potentials at the solution–reference electrode and the reference electrode–platinum interfaces.

This conclusion becomes more convincing if the reaction rates of the hydrogen ion discharge $\vec{v}$ and of the inverse reaction of ionization of the adsorbed atom $\overleftarrow{v}$ are compared. In accordance with eqn. (1), we obtain

$$\vec{v} = k_1[H^+] \exp\left\{-\frac{\alpha F}{RT}\left[\varphi + \frac{1-\alpha}{\alpha}\psi_1\right]\right\} \exp\frac{\alpha g_H}{RT} \quad (2)$$

where $[H^+]$ is the concentration of the hydrogen ions in the solution.

It has already been noted that no account is taken explicitly in expression (1) of the term determined by the chemical potential of the electron in the electrode metal. However, if φ denotes the potential of the metal of the lead, referred to the solution or to a constant reference electrode, this term proves to be constant, which results in the appearance in k_1 of a constant factor, independent of the electrode metal. The other factor contained in k_1 is equal (if we stay within the frame of the theory of absolute reaction rates) to kT/h. Thus, k_1 under these conditions does not depend on the nature of the electrode metal.

* Putting the non-coulombic part of the standard free energy of desorption in the transition state equal to αg_H is a very rough approximation, which, however, is of no importance for the subsequent conclusions. The possible dependence of the value of α on the nature of the electrode will be neglected in the following discussion.

For the difference in levels of the transition state of the reaction and its final state we obtain instead of eqn. (1)

$$[(1-\alpha)\psi_1 F-(1-\alpha)\varphi F-\alpha g_H]-[-g_H]=[(1-\alpha)\psi_1 F-(1-\alpha)\varphi F+(1-\alpha)g_H] \quad (3)$$

whence for $\overleftarrow{v}$ we have:

$$\overleftarrow{v}=k_2[H]\exp\left\{-\frac{(1-\alpha)F}{RT}[-\varphi+\psi_1]\right\}\exp\frac{(\alpha-1)g_H}{RT} \quad (4)$$

where [H] is the surface concentration of H atoms.

The constant k_2, as well as k_1 under the same conditions, does not depend on the nature of the electrode metal.

By equating $\overrightarrow{v}$ to $\overleftarrow{v}$, we obtain the expression for the equilibrium value of φ

$$\varphi=\frac{RT}{F}\ln\frac{[H^+]}{[H]}+\frac{g_H}{F}+\frac{RT}{F}\ln\frac{k_1}{k_2} \quad (5)$$

It is clear from a comparison of eqn. (5) with the value of the reversible potential of adsorbed hydrogen at the atomic concentration [H] and the free energy of desorption g_H as deduced from thermodynamics,

$$\varphi_r=\frac{RT}{F}\ln\frac{[H^+]}{[H]}+\frac{g_H}{F}+\text{constant} \quad (6)$$

that the quantity φ, just as φ_r, should indeed be referred to a constant reference electrode rather than to the point of zero charge.

EQUATIONS OF ELECTROCHEMICAL KINETICS AND THE WORK FUNCTION

The physical sense of the conclusion, according to which the expression for the kinetics of the discharge (2) contains the potential referred to a constant reference electrode rather than the potential difference in the double layer at the metal–solution interface, becomes clear if we take into account that the expressions given here do not contain the work function of the metal, W_e. In fact, if instead of the potential referred to a constant reference electrode, the potential referred to the point of zero charge ($\varphi-\varphi_0$), is introduced into eqn. (2), the difference in the energy levels of the electrons in different metals should be taken into consideration and a factor containing the work function should be introduced into the expression for the reaction rate. When comparing the reaction rates of ethylene oxidation on different metals, DAHMS AND BOCKRIS[7], on the basis of the work of BOCKRIS AND POTTER[4], take into account a factor which contains in the exponent the quantity $\alpha W_e F/RT$. It should be borne in mind, however, that

$$\exp\left[-\frac{\alpha F}{RT}(\varphi-\varphi_0)\right]\exp\left(-\frac{\alpha W_e F}{RT}\right)=A\exp\left(-\frac{\alpha F}{RT}\varphi\right) \quad (7)$$

where A $\sim$ constant, since the relation between the work function and the potential of the point of zero charge

$$\varphi_0-W_e=\text{constant} \quad (8)$$

is approximately realized. This relation, and the equivalent one between the difference of potentials of the zero charge and the Volta potential, have been discussed in the literature[8–13]. The compensation of the effects associated with the change in the position of the point of zero charge and with that in the work function was first stated by FRUMKIN (cited in ref. 14). This problem* was also considered by RÜETSCHI AND DELAHAY[13]. TEMKIN AND FRUMKIN[15], in connection with a discussion with POLTORAK[16] who expressed a different point of view, showed that the difference in the heats of the discharge Q of hydrogen ions on two different metals, measured at the same potential relative to a reference electrode, is given (if we neglect the temperature coefficient of the Volta potential between the metals) by

$$Q_{\mathrm{I}} - Q_{\mathrm{II}} = u_{\mathrm{I}} - u_{\mathrm{II}} \tag{9}$$

where u_{I} and u_{II} are the energies of the H atom bond with the metals I and II, respectively; the difference in the electron work functions of metals I and II does not enter into this expression.

As the relation (8) is an approximate one, it could be possible that the compensation considered here is incomplete; but this is not the case. In fact, if we want to introduce into equations of electrochemical kinetics the electron work function as some quantity characterizing the relevant metal**, we should take into consideration the work function referring to the escape of the electron into the solution, $W_e{}^s$, rather than into the vacuum. Evidently, $W_e{}^s$ is a function of the electrode potential. The quantity $\vec{v}$ can depend only on the value of $W_e{}^s$ at the potential φ, which is equal to $\varphi - \varphi_0 + (W_e{}^s)_{\varphi_0}$. At a definite potential, φ, however, measured against a constant reference electrode, this work function cannot depend on the nature of the metal. Otherwise, the equilibrium between two electrodes immersed in the same solution and having the same potentials relative to a reference electrode, would be disturbed if traces of an electronic conductivity appeared in the solution. Hence it follows that

$$W_e{}^s = (W_e{}^s)_{\varphi_0} + \varphi - \varphi_0 = \text{constant} \tag{10}$$

and does not depend on the nature of the metal.

The same conclusion can be arrived at in a somewhat different way. Considering the cyclic process where the electron passes from the metal to the vacuum, then from a point near the metal surface to one near the surface of the solution, then through the surface of the solution and finally returns to the metal through the metal–solution interface, we find

$$W_e{}^s = W_e + V_{Me-s} - U_e{}^s \tag{11}$$

where V_{Me-s} is the electrode–solution Volta potential at a given electrode potential φ and $U_e{}^s$ is the real free energy of hydration of the electron.

By applying eqn. (11) to the two metals I and II, we obtain

$$(W_e{}^s)_{\mathrm{I}} - (W_e{}^s)_{\mathrm{II}} = (W_e)_{\mathrm{I}} - (W_e)_{\mathrm{II}} + V_{Me_{\mathrm{I-II}}} \tag{12}$$

where $V_{Me_{\mathrm{I-II}}}$ is the Volta potential between metals I and II.

---

* The recently published paper of BUTLER AND MAKRIDES[40] also contains the conclusion that these two effects should compensate each other.

** The question as to what kind of work function should appear in equations of electrochemical kinetics was posed recently by BOCKRIS AND WROBLOWA[17].

As metals I and II have the same potential φ relative to the reference electrode, nothing will change if they are connected with a metal wire and the right-hand side of eqn. (12) must vanish. Hence W_e^s is independent of the nature of the metal.

Thus, the quantity φ in eqn. (2) should be referred to a constant reference electrode. It should be emphasized that the result obtained here does not depend on the assumptions made in deducing eqn. (2). If we want, however, to refer φ to the potential of zero charge, it is advisable (see ref. 7*) to introduce into the equation for the reaction rate the term $\exp(-\alpha W_e F/RT)$. In practice, this correction presents difficulties because data for the value of W_e for most metals are not reliable. Moreover, this correction is only an approximate one because of the approximate character of eqn. (8). If the measurements of the process rate are performed at the potentials of zero charge (which has certain advantages, see below), it is logical to compare the results after multiplying them by the quantity $\exp(\alpha\varphi_0 F/RT)$. In this case, as follows from eqn. (2), the nature of the metal affects the resulting quantity *via* the value of g_H, which is a measure of the electrochemical activity of the electrode relative to the reaction of the hydrogen-ion discharge. It is obviously incorrect to use for the reaction rate relations containing, instead of φ, the potential referred to the point of zero charge, without introducing a term containing W_e, *e.g.* as in references 18 and 19.

The above considerations are invalid if, before interacting with the solution, the electron upon leaving the electrode has to overcome an activation barrier comparable with or greater than the quantity W_e^s. The kinetics on a metal covered with a thin semiconducting film is such a case and requires special consideration[20].

The dependence of the pre-exponential factor k_1 (or k_2) upon the nature of the metal for the simplest case of a reaction occurring without the breaking of a chemical bond was treated by DOGONADSE, CHISMADZEV AND LEVICH[21], who did not resort to the assumptions of the theory of the absolute reaction rates. According to these authors, the above dependence seems to be not strongly expressed; at any rate, it does not contain the quantity W_e.

ELECTRO-REDUCTION OF ANIONS

By taking the log of the right-hand side of eqn. (2) and generalizing for the case of a particle with the charge n, we obtain for the current density, i[22,23]

$$\ln i = \frac{\alpha(-\varphi F + g)}{RT} + \frac{(\alpha - n)F}{RT}\psi_1 + \ln c + \text{constant} \qquad (13)$$

where c is the concentration of the reacting particle and g the non-coulombic part of the free energy of desorption of the reaction product. In the absence of concentration polarization, eqn. (13) is applicable to an irreversible reaction of the first order if the rate-determining step of the process is the electron transfer, the specific (non-coulombic) adsorption of the reacting particle can be neglected and the coverage of the electrode surface with reaction products is small. According to the above it is possible

* DAHMS AND BOCKRIS[7] consider oxidation and not reduction reactions; therefore, the sign before W_e is an opposite one.

to the first approximation to neglect the dependence of the constant upon the nature of the metal. The first term in the right-hand side of eqn. (13) contains the quantity φ referred to a constant reference electrode; it takes account of the dependence of the kinetics of the electrochemical process upon its thermodynamics in the spirit of the transition state theory with the accuracy which is possible without taking into consideration the double-layer structure. The second term, containing the quantity ψ_1, expresses the effect of the adsorption factors for the given simplest case. It vanishes at the point of zero charge and at potentials equidistant from the point of zero charge should be only slightly dependent on the nature of the metal (see below). Thus, according to eqn. (13), in order to compare the behaviour of two electrodes it is necessary to use both the usual scale of potentials and that referred to the corresponding points of zero charge.

In the absence of specific adsorption of the reaction product ($g = 0$) it follows from eqn. (13) that

$$\ln i + \frac{n\psi_1 F}{RT} = -\frac{\alpha F}{RT}(\varphi - \psi_1) + \ln c + \text{constant} \qquad (14)$$

According to eqn. (14), the polarization curve in the co-ordinates $\ln i + n\psi_1 F/RT$, $(\varphi - \psi_1)$—the corrected Tafel plot—to the first approximation should be independent of the electrode material, as was pointed out by DELAHAY *et al.*[24]. However, there is little experimental evidence as yet to support this conclusion[22,24,25]. The fulfilment of the condition $g = 0$ limits the applicability of the above criterion to the reduction of anions at negatively charged electrodes.

In discussing the expediency of referring the electrode potential to the potential of zero charge we have assumed until now that at potentials equidistant from the point of zero charge the values of ψ_1 on different electrodes are equal or close to one another, which points to a similar structure of the electric double layer. Similar assumptions are made also in other cases when using the potential of zero charge in electrochemical kinetics. The investigation of the electrocapillary behaviour of gallium[26] showed, however, that this assumption is not always justified. Thus, the difference in the potentials of zero charge of mercury and gallium is *ca.* 0.5 V, whereas the difference in the potentials corresponding to identical, if they are high enough, negative surface charges of mercury and gallium is 0.17 V. This phenomenon is probably due to different dependences of the orientation of the water molecules upon the potential on both electrodes. No matter whether this explanation is correct or not, the possibility of such a phenomenon may require that additional corrections are made in using the values of the potential of zero charge in electrochemical kinetics.

REACTIONS OCCURRING WITH THE PARTICIPATION OF ADSORBED NEUTRAL MOLECULES

Another case with should be considered here is the kinetics of the electron transfer to a neutral molecule in the adsorbed state. Let us assume that the quantity ψ_1 can be neglected and that the surface coverage with the adsorbed substance is small. The dependence of the adsorption of organic molecules upon the potential at a given concentration in the solution is expressed by a bell-shaped curve, the maximum of

which lies close to the potential of zero charge, although in the general case it does not coincide with it[27,28]. Taking into account this dependence of adsorption upon the potential, we obtain for $\ln i$[29,30]

$$\ln i = -\frac{\alpha\varphi F}{RT} - \frac{1}{2RT\Gamma_\infty (C - C')}[C(\varphi - \varphi_0) - C'(\varphi - \varphi_N)]^2 + \ln c + \frac{g_m}{RT} + \text{constant} \quad (15)$$

where Γ_∞ is the limiting value of adsorption of the initial substance, C—the capacity of the electric double layer*, C'—the capacity of the electric double layer when the surface is covered with the adsorbed particles, φ_N—the potential of zero charge under the same conditions, g_m—the value of the free energy of desorption of the adsorbed particle in the transition state of the reaction at the potential at which adsorption is a maximum**. It would be more correct to refer not only g_m, but also the other quantities contained in eqn. (15) (Γ_m, φ_N and C') to the transition state of the reaction rather than to the initial one. In the case of large particles, however, the error due to this approximation should be small.

Along with the first term including the potential φ measured against the constant reference electrode, the right-hand side of eqn. (15) (as that of eqn. (13)) contains a second term depending upon $(\varphi - \varphi_0)$ and $(\varphi - \varphi_N)$, *i.e.*, upon the potential measured against the points of zero charge for the uncovered and covered surfaces. The quantity g_m contained in the third term is a measure of the electrochemical activity of the electrode. The question of the potentials at which the kinetics of processes on different electrodes should be compared is therefore not unambiguously settled in this case either. At potentials equidistant from φ_0, in particular at $\varphi = \varphi_0$, adsorption occurs under comparable conditions. The rates of the electron transfer referred to the same adsorption value should be compared, however, at φ = constant, if no corrections are made for the work function or for the position of the point of zero charge, as indicated above. Only in the case of a process with a rate determined by a preceding chemical step do we obtain a complete picture by comparing the rates at the potentials of zero charge.

INFLUENCE OF ADSORPTION OF PARTICLES NOT PARTICIPATING IN THE PROCESS

So far, we have not considered the possible influence of the presence or absence in the surface layer, of foreign adsorbed particles (*e.g.*, halogen anions, organic cations used as inhibitors, etc.) upon the adsorption of the reacting particle and the kinetics of the electrochemical process. In a number of cases a pronounced dependence of adsorption of these particles upon the sign and magnitude of the surface charge is observed and, consequently, in establishing the factors determining the process kinetics attention should be given to the position of the point of zero charge. In-

* The relations presented here were deduced assuming C = a constant, which is a rough approximation. The dependence of adsorption upon the potential in the general case is considered in ref. 28.

** If g_0 denotes the same quantity at $\varphi = \varphi_0$, to the same approximation, we have

$$g_m = g_0 + \frac{1}{2\Gamma_\infty}\frac{(C')^2}{C - C'}(\varphi_N - \varphi_0)^2 \quad (16)$$

stances of such adsorption effects have often been considered in recent literature[2,6,31,32] and will not, therefore, be discussed further here.

Somewhat different relations are observed in the case of adsorption of atomic hydrogen and oxygen, which are present in considerable concentration on the surface of many electrodes, *e.g.*, platinum, over definite potential ranges. Evidently, the activity of adsorbed hydrogen and oxygen (or of the adsorbed OH radical) in equilibrium with water at a given adsorption energy depends on the electrode potential as referred to the reversible hydrogen-electrode or some other reference electrode in the same solution. As a result of the polarity of the bond between the adsorbed atoms and the metal, the position of the point of zero charge also exerts an influence. Although, for example, hydrogen adsorption on platinum in acid solutions depends essentially upon the structure of the electric double layer[32,33], it is, nevertheless, the value of φ which is of principal importance for any given pH of the solution.

The surface coverage with adsorbed hydrogen and oxygen hinders the adsorption of organic molecules. The thermodynamics of the adsorption of an organic substance on a hydrogen-adsorbing metal has been considered[34]. The result can be written in the following form:

$$\left(\frac{\partial g_{org}}{\partial \varphi}\right)_{\Gamma_{org}} = \left(\frac{\partial q}{\partial \Gamma_{org}}\right)_{\varphi} - F\left(\frac{\partial A_H}{\partial \Gamma_{org}}\right)_{\varphi} \tag{17}$$

Here, g_{org} is the standard free energy of desorption of the organic substance, q—the charge per unit surface, A_H—the quantity of adsorbed atomic hydrogen per cm^2 that does not go into the bulk of the solution as ions, and Γ_{org}—the Gibbs adsorption of the organic substance per cm^2 (assuming $\Gamma_{H_2O} = 0$). Equation (17) was deduced assuming the adsorption of the organic substance to be reversible.-This is not always true in the case of adsorption of organic substances on metals of the platinum group, but is a necessary premise in the thermodynamic treatment of the problem. The first term in the right-hand side of eqn. (17) expresses the effects associated with the existence of the electric double layer; by taking this term into consideration, we obtain the relations used in the deduction of eqn. (15). A rough calculation shows, however, that in the presence of appreciable hydrogen adsorption, the second term should considerably exceed the first. The presence of this term in eqn. (17) leads to a decrease in the adsorption of the organic substance with increasing surface coverage with hydrogen. The appearance of adsorbed oxygen on the surface has a similar effect*. Therefore a maximum adsorption of organic molecules on metals adsorbing hydrogen and oxygen, would be expected in the range of potentials where the surface coverage with adsorbed hydrogen and oxygen is a minimum. If not, there must be, at any rate, a shift in the potential of maximum adsorption from the point of zero charge in the

* For an electrode which adsorbs oxygen and the organic substance reversibly and acts as an oxygen electrode, we should have instead of eqn. (17),

$$\left(\frac{\partial g_{org}}{\partial \varphi}\right)_{\Gamma_{org}} = \left(\frac{\partial q}{\partial \Gamma_{org}}\right)_{\varphi} + 2F\left(\frac{\partial A_O}{\partial \Gamma_{org}}\right)_{\varphi} \tag{18}$$

where A_O is the quantity of g-atoms of oxygen adsorbed on 1 cm^2 of the surface, that have not gone into the bulk of the solution as OH^- ions.

direction of this potential range*.

Summarising, we conclude that in comparing the electrochemical characteristics of two electrodes, we may proceed both from the rate values of the electron transfer process at the same potential values and from the values referred to the point of zero charge. In the former case, in making the comparison we should introduce a correction associated with different values of the reacting particle adsorption or of the ψ_1-potential at a given φ-potential. In the latter case, the conditions of adsorption on both electrodes become similar, but for a reasonable comparison of the kinetics of the electron transfer process, it is necessary to correct the rate observed in the case of an electro-reduction reaction using the factor $\exp \alpha\varphi_0 F/RT$. The possible effect of the presence of adsorbed hydrogen or oxygen on the electrode surface upon the adsorption value of the reacting particle should also be taken into consideration in this case.

ACKNOWLEDGEMENT

I thank B. G. LEVICH, L. I. KRISHTALIK and B. B. DAMASKIN for their helpful discussions in the preparation of this paper**.

SUMMARY

The reaction rate of the electron transfer is determined both by the electrode potential, φ, measured against a constant reference electrode and by the structure of the electric double layer, which to the first approximation depends on the electrode potential referred to the potential of zero charge, *i.e.*, $\varphi - \varphi_0$. It is shown that in order to make a rational comparison of the rates of reactions occurring on different electrodes it is not sufficient to know only the quantity $\varphi - \varphi_0$.

The effect of the presence of adsorbed hydrogen and oxygen on the electrode surface upon the process rate is considered.

ADDED IN PROOF. Using eqn. (11), one may try to estimate the value of W_e^s for mercury. According to BAXENDALE[41], the gain in the total energy in the process of electron hydration is 1.75 V. By substituting, as a rough approximation, this quantity for U_e^s into eqn. (11) and assuming $W_e = 4.52$ and $V_{Me-s} = -0.26$ at $\varphi = \varphi_0$ (according to the data of RANDLES[42,43]), we find that at this potential $W_e^s \approx 2.5$ V. From this value and assuming the general laws of thermal electron emission

* The considerations presented would be, apparently, of importance in interpreting some of the results obtained by BOCKRIS, GREEN AND SWINKELS[35], who studied the dependence of the adsorption of naphthalene on a number of metals upon the potential and composition of the solution. According to these authors, the adsorption maximum on platinum in acid solutions is located at 0.1–0.4 V (N.H.E.) depending on the naphthalene concentration, whereas $\varphi_0 = 0.11$–0.17[36]. In alkaline solutions the adsorption maximum is at -0.4 V (N.H.E.); the authors compare this value with the data of KHEĬFETS AND KRASIKOV[37], in which this potential corresponds to the point of zero charge. Actually, in the absence of surface active anions it is impossible to fix the position of the point of zero charge in the usual sense of the word on a platinum electrode in alkaline solutions, as the surface charge in the potential range -0.7–$+0.5$ V remains negative (the electrode adsorbs cations) and the change in the potential is apparently determined mainly by the change in the dipole moment of the bond between platinum and chemisorbed hydrogen and oxygen atoms[38].

** When the present paper was ready for publication, by the kindness of Dr. R. PARSONS I was able to read his article[39], the results of which, although deduced in a different way, partly coincide with ours.

from metals into the vacuum to be applicable to the mercury-solution interface, one would expect the current of electron emission into the solution at $\varphi - \varphi_0 = -2.2$ V to reach a value of the order of 10^{-2} A/cm^2. Such an effect is apparently not observed; at $\varphi = \varphi_0$, W_e^s should probably exceed 3 V. It is not possible as yet to ascertain which approximations and assumptions in our calculations are responsible for this discrepancy.

REFERENCES

1 D. C. GRAHAME, *Chem. Rev.*, 41 (1947) 441.
2 L. I. ANTROPOV, *Tr. Erevansk. Polytechn. Inst.*, 2 (1946) 7, 96; *Proceedings of the 4th Conference on Electrochemistry, Moscow, 1956*, Academy of Sciences, 1959, p. 34; *Kinetics of Electrode Processes and Null Points of Metals*, C.S.I.R., New Delhi, 1960; *Zh. Fiz. Khim.*, 25 (1951) 1494; 37 (1963) 965; *Ukr. Khim. Zh.*, 29 (1963) 557.
3 A. FRUMKIN, *Z. Physik. Chem. Leipzig*, 164 (1933) 121.
4 J. O'M. BOCKRIS AND E. C. POTTER, *J. Electrochem. Soc.*, 99 (1952) 169.
5 R. PARSONS, *Trans. Faraday Soc.*, 47 (1951) 1332.
6 A. N. FRUMKIN, *Advances in Electrochemistry*, Vol. 1, Interscience, New York, 1961, p. 65.
7 H. DAHMS AND J. O'M. BOCKRIS, *J. Electrochem. Soc.*, 111 (1964) 728.
8 A. FRUMKIN AND A. GORODETSKAYA, *Z. Physik. Chem. Leipzig*, 136 (1928) 451; A. N. FRUMKIN, V. S. BAGOTSKII, Z. A. IOFA AND B. KABANOV, *Kinetics of Electrode Processes*, Moscow University Press, 1952, p. 32; A. N. FRUMKIN, *J. Electrochem. Soc.*, 107 (1960) 461.
9 M. TEMKIN, *Izv. Akad. Nauk SSSR, Otd. Khim. Nauk*, (1946) 235.
10 V. M. NOVAKOVSKII, E. A. UKSHE AND A. I. LEVIN, *Zh. Fiz. Khim.*, 29 (1955) 1847.
11 R. M. VASENIN, *Zh. Fiz. Khim.*, 27 (1953) 878; 28 (1954) 1672, 1872.
12 B. JAKUSZEWSKI, *Bull. Acad. Polon. Sci., Ser. Sci. Chim.*, 9 (1961) 11.
13 P. RÜETSCHI AND P. DELAHAY, *J. Chem. Phys.*, 23 (1955) 195, 1167.
14 J. HORIUTI AND M. POLANYI, *Acta Physicochim. URSS*, 2 (1935) 505.
15 M. TEMKIN AND A. N. FRUMKIN, *Zh. Fiz. Khim.*, 29 (1955) 1515; 30 (1956) 1162.
16 O. M. POLTORAK, *Zh. Fiz. Khim.*, 28 (1954) 1845; 29 (1955) 2249.
17 J. O'M. BOCKRIS AND H. WROBLOWA, *J. Electroanal. Chem.*, 7 (1964) 428.
18 V. L. KHEĬFETS AND N. E. POLYAKOVA, *Zh. Prikl. Khim.*, 22 (1949) 801.
19 R. M. VASENIN, *Zh. Fiz. Khim.*, 30 (1956) 629.
20 R. R. DOGONADZE AND A. M. KUZNETSOV, *Izv. Akad. Nauk SSSR, Otd. Khim. Nauk*, (1964) 1253; R. R. DOGONADZE, A. M. KUZNETSOV AND YU. A. CHIZMADZHEV, *Zh. Fiz. Khim.*, 38 (1964) 1195.
21 B. LEVICH, *Advances in Electrochemistry*, Vol. 4, in press; R. R. DOGONADZE AND YU. A. CHIZMADZHEV, *Dokl. Akad. Nauk SSSR*, 145 (1962) 849.
22 A. N. FRUMKIN AND G. M. FLORIANOVICH, *Dokl. Akad. Nauk SSSR*, 80 (1951) 907; G. M. FLORIANOVICH AND A. N. FRUMKIN, *Zh. Fiz. Khim.*, 29 (1955) 1827.
23 A. N. FRUMKIN, O. A. PETRII AND N. V. NIKOLAEVA-FEDOROVICH, *Dokl. Akad. Nauk SSSR*, 147 (1962) 878; *Electrochim. Acta*, 8 (1963) 177; O. A. PETRII AND A. N. FRUMKIN, *Dokl. Akad. Nauk SSSR*, 146 (1962) 1121; 147 (1962) 418.
24 K. ASADA, P. DELAHAY AND A. K. SUNDARAM, *J. Am. Chem. Soc.*, 83 (1961) 3396; P. DELAHAY AND M. KLEINERMAN, *ibid.*, 82 (1960) 4509.
25 B. N. RYBAKOV, N. V. NIKOLAEVA-FEDOROVICH AND G. V. ZHUTAEVA, *Zh. Fiz. Khim.*, 38 (1964) 500.
26 A. N. FRUMKIN, N. B. GRIGOR'EV AND I. A. BAGOTSKAYA, *Dokl. Akad. Nauk SSSR*, 157 (1964) 957; A. N. FRUMKIN, N. S. POLYANOVSKAYA AND N. B. GRIGOR'EV, *Dokl. Akad. Nauk SSSR*, 157 (1964) 1455; A. N. FRUMKIN, N. S. POLYANOVSKAYA, N. B. GRIGOR'EV AND I. A. BAGOTSKAYA, *Electrochim. Acta*, in press.
27 A. FRUMKIN, *Z. Physik*, 35 (1926) 792.
28 A. N. FRUMKIN AND B. B. DAMASKIN, *Modern Aspects of Electrochemistry*, Vol. 3, Academic Press, New York, 1964.
29 A. B. ERSHLER, G. A. TEDORADZE AND S. G. MAIRANOVSKII ,*Dokl. Akad. Nauk SSSR*, 145 (1962) 1324.
30 A. N. FRUMKIN, *Electrochim. Acta*, 9 (1964) 465.
31 A. N. FRUMKIN, *Usp. Khim.*, 24 (1955) 933; *Z. Elektrochem.*, 59 (1955) 807; *Proc. Intern. Congr. Surface Activity, 2nd, London, 1957*; *Electrical Phenomena*, Butterworth, London, p. 58; *Trans. Faraday Soc.*, 55 (1959) 156.
32 A. N. FRUMKIN, *Advances in Electrochemistry*, Vol. 3, Interscience, New York, 1963, p. 288.

33 A. FRUMKIN AND A. SHLYGIN, *Izv. Akad. Nauk SSSR, Otd. Mat. Estestven. Nauk*, (1936) 773; *Acta Physicochim. URSS*, 5 (1936) 819.
34 A. N. FRUMKIN, *Dokl. Akad. Nauk. SSSR*, 154 (1964) 1432.
35 J. O'M. BOCKRIS, M. GREEN AND D. A. J. SWINKELS, *J. Electrochem. Soc.*, 111 (1964) 743.
36 V. E. KASARINOV AND N. A. BALASHOVA, *Dokl. Akad. Nauk SSSR*, 157 (1964) 1174; A. SHLYGIN, A. FRUMKIN AND V. MEDVEDOVSKII, *Acta Physicochim. URSS*, 4 (1936) 911.
37 V. L. KHEĬFETS AND B. S. KRASIKOV, *Zh. Fiz. Khim.*, 31 (1957) 1992.
38 V. E. KASARINOV, *Z. Physik. Chem. Leipzig*, 226 (1964) 167.
39 R. PARSONS, *Surface Sci.*, 2 (1964) 418.
40 J. N. BUTLER AND A. C. MAKRIDES, *Trans. Faraday Soc.*, 60 (1964) 1656.
41 J. BAXENDALE, *Rad. Res. Suppl.*, 4 (1964) 139.
42 J. RANDLES, *Trans. Faraday Soc.*, 52 (1956) 1573.
43 A. N. FRUMKIN, *Electrochim. Acta*, 2 (1960) 351.

J. Electroanal. Chem., 9 (1965) 173–183

ELECTROLYTIC SEPARATION AND COLORIMETRIC DETERMINATION OF TRACES OF LEAD IN COBALT USING ISOTOPIC DILUTION ANALYSIS

A. LAGROU AND F. VERBEEK
Laboratory for Analytical Chemistry, Ghent University, Ghent (Belgium)
(Received October 23rd, 1964)

Traces of lead can be determined colorimetrically with dithizone[1]. For the determination of lead in cobalt, however, prior separation of lead is necessary. Immediate extraction with dithizone in slightly alkaline citrate–cyanide medium in the presence of a large excess of cobalt is impossible because the cyanide concentration may not exceed 0.1 M[1] (formation of lead cyanide complexes) and this concentration is insufficient to mask the cobalt completely. By electrolysis at a controlled cathode potential, lead was deposited on to a mercury cathode and thus separated from the solution. After the mercury had been removed by distillation, the lead remaining was dissolved and determined colorimetrically. The yield was controlled radiometrically with ^{210}Pb and corrections were made for losses. The ideal conditions for deposition, the influence of several variables and the possible interferences of other elements have also been investigated.

APPARATUS AND REAGENTS

Potentiostat, Tacussel type ASA4C.

Multi-range microammeter Kipp, type Microva AL4. This was connected in series between the potentiostat and the non-working electrode of the electrolysis cell to control the current density (of the order of a few mA).

pH meter Radiometer type pHM 22. A supplementary control enabled the potential to be measured accurately to within 5 mV.

Electrolysis cell: microcell of the H-type about 10 cm high with a diameter of $\pm$ 2 cm. A stopcock permitted withdrawal of the mercury. The anode was a platinum plate measuring 1 $\times$ 2 cm, and 0.5 ml of twice-distilled mercury was used as cathode. A sintered-glass disk between the two compartments with an agar-gel plug on the side of the saturated calomel electrode (S.C.E.) prevented all possible diffusion.

Spectrophotometer, Beckman D.U. and 1.000-cm quartz cuvettes.

Gamma Spectrometer, type Oak Ridge with a NaI(Tl) well-type crystal.

^{210}Pb solution. 1 mC of RaD (^{210}Pb; γ-energy = 47 keV; β-energy = 25 keV; T 1/2 = 22 years) with decay products in approximate equilibrium in 2.5 N nitric acid and a total lead concentration of about 0.2 mg in 0.5 ml was obtained from U.K.A.E.A. (Amersham, England). A stock solution was prepared by diluting 0.100

ml to 100 ml with 1 N hydrochloric acid. The activity of this solution was approximately 1.5×10^5 counts/min.ml and the lead concentration about 5×10^{-6} M.

^{60}Co was obtained by irradiation of metallic cobalt in the BR-1 reactor (at a neutron flux of 10^{12} neutron sec^{-1} cm^{-2} during 11 days).

Analytical-grade products and twice-distilled water were used for the preparation of reagents. Diluted lead solutions ($< 10^{-4}$ M), radioactive or not, were freshly prepared and stored in polyethylene containers.

EXPERIMENTAL

Sorption

Before investigating the quantitative aspect of the deposition of traces of lead on the mercury cathode, the possibility of losses arising from sorption on the walls of the apparatus used was checked. STOCK[2-4] and other authors[5-8] have drawn attention to this possibility.

The lead concentration in the electrolysis cell for each experiment was 3.5×10^{-7} M. After contact times of 1, 2, 3, 6, 18 and 24 h, the activity of 1 ml of the solution (A_e) was compared with that of 1 ml of the original solution (A_0). No sorption was observed after 24 h in 1 M HCl, 10^{-1} M HCl, 10^{-2} M HCl and 0.1 M NaCl–0.5 M tartrate, whilst the highest sorption (over 40%, after 1 h) was obtained in a neutral medium (0.1 M KCl). It is, therefore, impossible to study lead deposition on to a mercury cathode in a neutral medium.

Conditions of electrolysis

Various authors[9-15] have examined the electrolysis of quantities of lead from milligrams to macroquantities using a mercury cathode. The deposition appears to

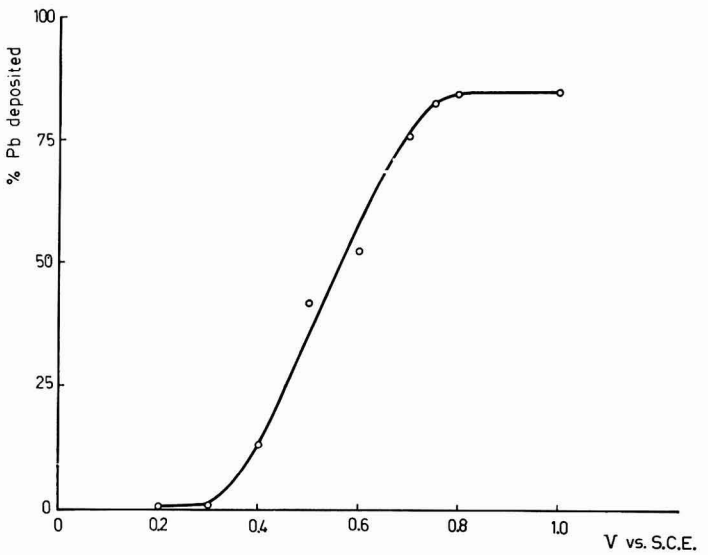

Fig. 1. Percentage of lead deposited as a function of cathode potential (V). Lead concn., 3.5×10^{-7} M in 1 M HCl; electrolysis time, 1 h.

be affected by several factors and in this investigation the influence of each factor has been studied separately for microgram quantities of lead.

Cathode potential. All the following experiments were carried out using 25 ml 1 *M* HCl and 2 ml ^{210}Pb stock solution. The quantity of mercury used was 0.5 ml. The mercury was stirred with a glass rod dipped about 2 mm in the mercury. The activity before electrolysis was 10^4 counts/min.ml and the initial lead concentration 3.5×10^{-7} *M*. The electrolysis was performed at different cathode potentials during one hour using rapid stirring (600 rev./min) and the decrease of the activity in the cell was followed. The percentage of deposited lead as a function of the cathode potential is given in Fig. 1.

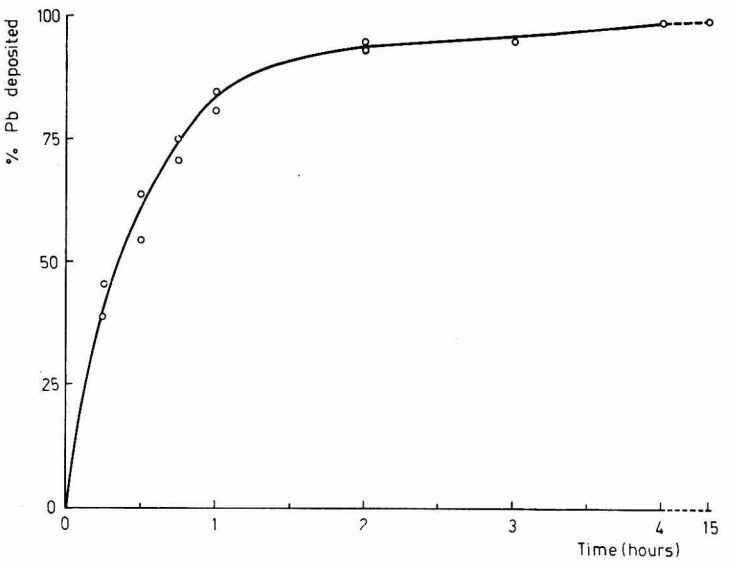

Fig. 2. Percentage of lead deposited as a function of electrolysis time (h). Lead concn. 3.5×10^{-7} *M* in 1 *M* HCl.

Electrolysis time. The working conditions were the same as those used in previous experiments. The deposition at a fixed potential (−0.800 V *vs.* S.C.E.) was followed as a function of time and the results are given in Fig. 2.

Acidity of the solution. The electrolysis was performed in solutions of varying hydrochloric acid concentration. The results after one hour electrolysis, at a cathode potential of −0.800 V *vs.* S.C.E. are given in Fig. 3. Very dilute lead solutions may easily become colloidal in weakly acidic solutions and for this reason, all further experiments were carried out in 1 *M* HCl.

Lead concentrations. Increasing amounts of lead were added to the original ^{210}Pb solution (3.5×10^{-7} *M*). The results are shown in Table 1. The conditions of electrolysis were as before.

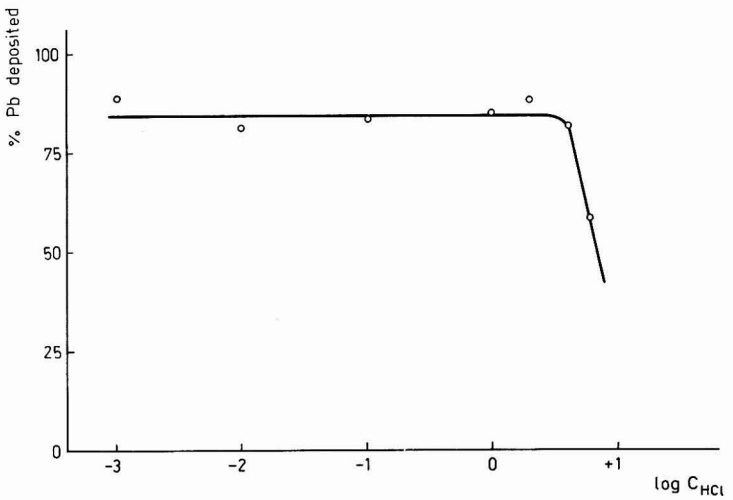

Fig. 3. Percentage of lead deposited as a function of HCl molarity. Lead concn., 3.5×10^{-7} *M*, electrolysis time 1 h.

TABLE 1

INFLUENCE OF LEAD CONCENTRATION ON DEPOSITION

Lead concn. in 25 ml (mg)	A_0 *(cpm/ml)*	A_e *(cpm/ml)*	*Lead remaining (%)*	*Lead deposited (%)*
0.002	8896	1274	14.32	85.68
0.400	8780	1389	15.82	84.18
4	8721	1313	15.28	84.72
20	8978	1425	15.87	84.13

TABLE 2

INFLUENCE OF MERCURY VOLUME ON ELECTRODEPOSITION OF LEAD

Vol. Hg (ml)	A_0 *(cpm/ml)*	A_e *(cpm/ml)*	*Lead remaining (%)*	*Lead deposited (%)*
0.25	8972	2868	31.96	68.04
0.50	9107	1755	19.27	80.73
1.00	8915	1794	20.12	79.88

Mercury volume. Different volumes of mercury were used for the same ^{210}Pb solution (3.5×10^{-7} *M*). The results are given in Table 2. The conditions of electrolysis were as before.

These experiments show that lead, in 1 *M* HCl medium, is almost completely deposited after a 4 h electrolysis at −0.800 V *vs.* S.C.E. Increasing amounts of lead

do not influence the deposition, at least not in the concentration range investigated. Increasing the amount of mercury makes no difference, but a very small volume lowers the deposition yield. Dilute lead solutions (10^{-6}–10^{-7} *M*) more than one week old, gave a decreased deposition on electrolysis, probably because of colloid formation. The yield improved by evaporating the solution to dryness and redissolving.

Decomposition of the lead amalgam

The lead amalgam has first to be separated from the cobalt in the solution; to do this the electrolysed solution was removed from the cell and the amalgam was washed. This manipulation, however, was difficult when working with very dilute amalgams. Washing with water, 1 *M* HCl or alcohol, all gave unsatisfactory results, as a large amount of the radioactivity was lost in the wash water. Finally, a system of continuous washing was used. Without interrupting the electrolysis and under continuous suction, 1 *M* HCl was led into the electrolysis compartment. Care was taken that the end of the suction tube did not come too close to the mercury cathode. In this way, satisfactory results were obtained.

Complete separation of lead from the mercury may be carried out by treating the amalgam with an oxidising agent[16], by distilling off the mercury[17] or by stripping it at a controlled potential or at a controlled current[18]. The second method was applied after the electrolysis and washing of the amalgam. The mercury was withdrawn from the cell and transferred to a small silica boat, which was placed in a silica tube heated by a horizontal tube furnace. The mercury was distilled at 365° in a stream of nitrogen, to prevent possible oxidation and finally collected under water. The residue containing lead was dissolved in nitric acid and analysed colorimetrically.

The electrodeposition of lead is practically complete (99%, Fig. 2). After washing, and distilling the mercury, the yield was 80–90% (see Table 3). The loss is mainly due to the lead remaining on the walls and stopcock of the electrolysis cell when withdrawing the mercury.

PROCEDURE

Add to the electrolysis cell, 25 ml of a $CoCl_2$–1 *M* HCl solution, and 2 ml of ^{210}Pb stock solution. Electrolyse during 5 h at a cathode potential of −0.800 V *vs.* S.C.E. Control the completeness of deposition by measuring the cell activity remaining. After continuous washing, distil the mercury as described above. Dissolve the remaining lead in twice-distilled nitric acid.

Evaporate the solution to dryness with an infrared lamp, redissolve in 1:100 nitric acid and transfer quantitatively to a calibrated flask. Determine in one volume of the solution the total recovered radioactivity and use another quantity for the colorimetric determination with dithizone[1] of total lead. Correct the amount found for the amount of lead lost in the processes of the determination.

A blank determination is necessary for the lead present in the 2 ml of radioactive solution added before the electrolysis.

INTERFERENCES

In the colorimetric determination of lead in slight alkaline cyanide medium,

interferences by traces of bismuth, indium, tin(II), thallium(I)[1] and excesses of cobalt and mercury, are possible.

The influence of increasing quantities of cobalt on the photometric determination of lead was investigated since the deposition of traces of cobalt by electrolysis at −0.800 V cannot be completely excluded. Curve 1 in Fig. 4 shows the extinction

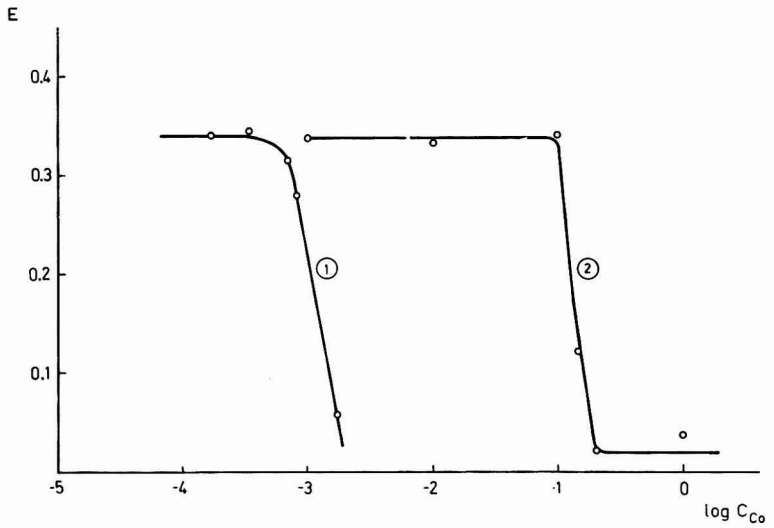

Fig. 4. Influence of cobalt concn. on the colorimetric determination of lead (10 μg in 10 ml) with dithizone: curve 1, without prior extraction with dithizone; curve 2, after prior extraction with dithizone.

at a wavelength of 525 mμ of 10 μg of lead in 10 ml of solution containing amounts of cobalt between 25 μg and 1 mg. Below 200 μg of cobalt the extinction remains constant, while a systematic error occurs above this limit[19]. When the cobalt concentration exceeds this limit, prior separation of the lead is necessary but isolation of the lead by extraction with dithizone[1] appeared to be impossible when the cobalt concentration was higher than 0.1 *M* (Fig. 4, curve 2). Therefore the cobalt–lead separation had to be done electrolytically for the determination of trace amounts of lead. An electrolysis of a 2 *M* Co–1 *M* HCl solution was performed at −0.800 V after adding ^{210}Pb and ^{60}Co. On a 400-channel gamma-spectrometer, a spectrum was taken before and after the electrolysis. This showed that cobalt remained almost completely in solution, and thus did not interfere in the colorimetric determination of lead.

Divalent mercury reacts readily with excess dithizone in a fairly acid medium to give an orange-coloured complex, but it can also interfere in alkaline medium[1]. Twice-distilled mercury was introduced into a silica boat and distilled as described earlier. The extinction of the residue was determined, and proved the distillation to be quantitative.

To avoid interference by bismuth a preliminary electrolysis was carried out

at a cathode potential of −0.200 V *vs.* S.C.E. Bismuth was deposited quantitatively whilst lead remained in the solution (*cf.* Fig. 1).

Experiments showed that indium was not deposited in 1 *M* HCl at −0.800 V *vs.* S.C.E. and would therefore not interfere.

The electrolytic separation of lead from thallium and tin will also be studied although interference from these elements is unlikely, as they have seldom been present in similar analyses.

The deposition of micro quantities of bismuth, indium and thallium and their colorimetric determination will be discussed in a later paper.

RESULTS

A number of analyses have been performed on synthetic samples by adding a known quantity of a standardised lead solution to a cobalt solution freed from lead by electrolysis at a mercury cathode in a Melaven cell. The results are summarised in Table 3. Correction was made for the lead present in the 2 ml of tracer solution amounting to 1.98 μg. The determination of 2–25 μg of lead in 25 ml was possible with an average error of 5%. This method allows the determination of 10^{-4}–$5 \cdot 10^{-5}$% of lead in cobalt when electrolysing 25 ml of a 2 *M* cobalt solution.

TABLE 3

DETERMINATION OF LEAD IN COBALT

Pb added (μg)	*Co added (g)*	*Yield (%)*	*Pb found (μg)*	*Pb found (corr. blank) (μg)*
25	2.9495	82.46	27.78	25.80
20	2.9495	86.32	22.66	20.68
10	2.9495	81.53	11.96	9.98
5	2.9495	75.60	7.76	5.78
2.5	2.9495	89.80	4.50	2.52
0	2.9495	81.80	1.98	0

It is not really necessary to determine the correction for the yield radiochemically. Although this yield can vary as much as 10% or more, as shown in Table 3 these variations can be decreased considerably by performing the electrolyses immediately one after another with freshly prepared solutions and under the same conditions. The yield of 4 successive electrolyses of solutions each containing 25 μg of Pb, were, respectively, 93.47 — 90.25 — 90.91 — 89.75%, with an average value of 91.90 ± 1.2% and of three successive electrolyses of solutions containing 10 μg, 81.53 — 83.74 — 84.07%, with an average value of 83.10 ± 1.10%. In this way a satisfactory colorimetric determination of the yield is possible. After the determination of the lead content of the unknown sample, the yield is determined under the same conditions for a standard lead solution.

ACKNOWLEDGEMENTS

The authors thank Prof. DR. J. HOSTE for his kind interest in this work and to Mrs. F. VAN DEN ABEELE for technical asisstance. This investigation has partly been sponsored by the Inter-university Institute for Nuclear Sciences (I.I.K.W.), Belgium.

SUMMARY

Traces of lead in cobalt are determined colorimetrically with dithizone after a prior separation of the lead on to a mercury cathode using controlled potential analysis and subsequent distillation of the mercury in a nitrogen atmosphere. The total yield of lead is determined using the radio-isotope ^{210}Pb. The conditions, *i.e.*, electrolysis time, cathode potential, acidity, mercury volume, lead concentration, for electrodeposition of micro quantities were investigated. Interferences of cobalt, mercury, indium and bismuth are discussed.

REFERENCES

1 E. B. SANDELL, *Colorimetric Determination of Traces of Metals*, 3rd ed., Interscience Publishers Inc., New York, 1959, pp. 563–571.
2 A. STOCK, *Mikrochim. Acta*, 30 (1942) 128.
3 A. STOCK, *Z. Angew. Chem.*, 42 (1929) 999.
4 A. STOCK, *Z. Physik. Chem. Leipzig*, A 189 (1941) 63.
5 E. B. SANDELL, *Colorimetric Determination of Traces of Metals*, 3rd ed., Interscience Publishers Inc., New York, 1959, pp. 19.
6 I. L. PREISS AND R. W. FINK, *Nucleonics*, 15, No. 10 (1957) 108.
7 T. SCHÖNFELD AND E. BRODA, *Mikrochim. Acta*, 36–37 (1951) 537.
8 J. H. YOE AND H. J. KOCH, JR., *Trace Analysis*, John Wiley and Sons Inc., New York, 1957, pp. 645–651.
9 J. J. LINGANE, *Electroanalytical Chemistry*, 2nd ed., Interscience Publishers Inc., New York, 1958, pp. 430 and 462.
10 H. FUNK AND H. SCHÄFER, *Chem. Tech., Berlin*, 8 (1956) 718.
11 L. MEITES, *Anal. Chem.*, 27 (1955) 1114.
12 P. R. SEGATTO, *J. Am. Ceram. Soc.*, 45 (1962) 102.
13 J. J. LINGANE, *Ind. Eng. Chem., Anal. Ed.*, 16 (1944) 147.
14 J. J. LINGANE, *J. Am. Chem. Soc.*, 67 (1945) 1916.
15 J. J. LINGANE, *Anal. Chim. Acta*, 2 (1948) 584.
16 N. H. FURMAN AND W. C. COOPER, *J. Am. Chem. Soc.*, 72 (1950) 5667.
17 *National Nuclear Energy Series*, Division VIII, Vol. I, *Analytical Chemistry of the Manhattan Project*, Editor C. J. RODDEN, McGraw-Hill Book Co. Inc., New York, 1950, pp. 513 and 520–521.
18 W. E. SCHMIDT AND C. E. BRICKER, *J. Electrochem. Soc.*, 102 (1955) 623.
19 F. ADAMS, private communication.

INFLUENCE OF MERCURY DROP GROWTH AND GEOMETRY ON THE A.C. POLAROGRAPHIC WAVE

JOSEPH R. DELMASTRO AND DONALD E. SMITH
Department of Chemistry, Northwestern University, Evanston, Illinois (U.S.A.)
(Received November 2nd, 1964)

INTRODUCTION

The majority of experimental a.c. polarographic investigations of electrode processes have employed the dropping mercury electrode (D.M.E.). Nevertheless, neglect of the influence of curvature (electrode geometry) and movement relative to the solution (electrode growth) of the electrode surface characterize most theoretical treatments of the small amplitude a.c. polarographic wave which are applied to these data. The fact that a.c. wave equations applicable strictly only to the stationary planar electrode may be considered accurate for work with the D.M.E. is suggested by the theoretical treatments of KOUTECKÝ[1] and GERISCHER[2], as well as intuitive rationalization. KOUTECKÝ considered the contribution of drop growth in his theory for the diffusion-controlled (reversible) a.c. polarographic wave. He showed that for normal conditions of mercury flow, drop life and alternating potential frequency, the influence of drop growth is negligible. GERISCHER derived equations for the faradaic impedance with a stationary spherical electrode at the equilibrium potential (zero direct current) for a process kinetically controlled by diffusion and charge transfer (the quasi-reversible case). His equations showed that the spherical correction is insignificant for normal drop radii and frequency of alternating potential. These theoretical results appear to support two simple intuitive concepts: (a) the rapidly changing alternating potential renders negligible the influence of the slow movement of the electrode surface relative to the solution; (b) the short distance which the a.c. concentration wave extends into the solution at frequencies usually employed ($>$ 10 c/sec) renders electrode geometry unimportant. The diffusing particles involved in the a.c. concentration profile are so close to the electrode that they do not 'see' the curvature of the electrode surface.

Thus, although the theoretical treatments of KOUTECKÝ and GERISCHER are applicable to the rather specific cases of the reversible process and the quasi-reversible process in absence of direct current, their results combined with the foregoing intuitive ideas apparently led most workers concerned with the theory of the a.c. polarographic wave to ignore possible influence of mercury drop growth and geometry. One exception is the classic paper by MATSUDA[3] on the quasi-reversible system. MATSUDA employed the expanding plane approximation which accounts for drop growth. His final equation showed that drop growth can influence the magnitude of the quasi-

reversible a.c. wave under normal experimental conditions. This is evidenced, among other ways, by the presence of the ubiquitous factor, $\sqrt{\frac{7}{3}}$, (see eqn. (14)). Closer examination of these equations indicates that the term responsive to drop growth, $F(\lambda t^{\frac{1}{2}})$, reduces to unity when the *d.c.* process is reversible. Under these conditions influence of drop growth disappears, and the equations for the expanding plane and stationary plane become identical. Thus, MATSUDA's predictions are not in conflict with the work of KOUTECKÝ which was applicable only to reversible systems. The source of a contribution due to drop growth when the d.c. process is quasi-reversible and the reason for its negligibility when the d.c. process is reversible can be rationalized without difficulty. Primary factors in determining the cell impedance under a.c. polarographic conditions are the magnitudes and ratio of the d.c. (or mean) concentrations of the oxidized and reduced forms of the electroactive couple at the electrode surface. In a.c. polarography, these parameters are varied *in situ* through the d.c. polarographic process. When the d.c. process is reversible, movement of the electrode surface into the solution is unimportant because the mean concentrations of the two redox forms are determined primarily by thermodynamic considerations, *i.e.*, the electrode potential. However, when charge transfer kinetics influence the d.c. process, non-equilibrium conditions exist with regard to the d.c. surface concentrations. A competition between mass transfer and charge transfer ensues and the magnitude of the deviation from equilibrium is influenced by movement of the electrode into the solution which enhances mass transfer. Thus, one concludes that drop growth influences the a.c. wave indirectly through its effect on the d.c. process, when the latter is subject to kinetic effects of charge transfer. The previously expressed intuitive ideas arguing that the a.c. wave would not be responsive to drop growth do not represent an incorrect concept of the a.c. process. They simply fail to take account of the coupling between the d.c. and a.c. polarographic processes.

Implications of this analysis of MATSUDA's equation go beyond the conclusion that drop growth can be important. The same arguments expressed to rationalize the prediction of a contribution from drop growth lead one to conclude that electrode geometry can also be important when the d.c. process is quasi-reversible. Electrode geometry affects the d.c. concentration gradient at the interface. Thus, deviations from equilibrium of the mean surface concentrations will be dependent upon electrode geometry.

The purpose of the work presented is to reassess the influence of electrode geometry and drop growth on the small amplitude a.c. polarographic wave, emphasizing the quasi-reversible case. The magnitude of these influences is examined by comparing calculated a.c. waves for various mass transfer models (planar diffusion, spherical diffusion, etc.) employing a wide range of rate parameters. An a.c. polarographic wave equation applicable to the D.M.E. with a quasi-reversible system is presented. Implications of the theoretical results regarding a.c. polarographic studies with stationary electrodes, studies of time-dependence of the a.c. wave, investigations of more complicated mechanisms and other aspects of a.c. polarography are considered.

THEORY

Equations presented here for the quasi-reversible system represented by the reaction scheme

$$O + n\,e \rightleftharpoons R$$

incorporate the assumptions: (a) Fick's law is applicable to each diffusing species independently; (b) the theory of absolute reaction rates as applied to electrode reaction kinetics[4] is applicable; (c) charge transfer involves one rate-determining step; (d) the electrode process is influenced kinetically solely by charge transfer and diffusion; (e) each reacting species is soluble either in the solution or electrode phase; (f) adsorption effects are negligible; (g) double-layer influences not encompassed by the Frumkin theory[5] are negligible; (h) the potentiostatic approximation for the d.c. potential is accurate, *i.e.*, the scan rate is so slow that the change in d.c. potential is negligible over the life of a single mercury drop; (i) steady state is achieved in the a.c. concentration profile[6]; (j) small amplitudes ($\Delta E \leq 8/n$ mV) of alternating potential are employed.

Equations presented here do not include terms accounting for double-layer corrections of the Frumkin type or activity corrections. However, these are introduced conveniently. Multiplying k_h in the following equations by $\exp[(\alpha n - Z_O)F\Delta\phi_E/RT]$ effects the double-layer correction[6] and multiplying k_h by $f_O^{\beta} f_R^{\alpha}$ introduces the activity corrections[3,7]. A list of notation definitions is given in Appendix 1.

A. Stationary planar electrode

Equations based on this electrode model have been applied to data obtained with the D.M.E. simply by introducing the time-dependence of electrode area [eqn. (12)]. As indicated above, this practice amounts to neglecting curvature and motion relative to the solution of the surface of the D.M.E.

For an applied potential

$$E(t) = E_{\text{d.c.}} - \Delta E \sin \omega t \tag{1}$$

the small amplitude a.c. polarographic wave equation for planar diffusion and a quasi-reversible system may be written, for only the oxidized form of the redox couple present initially[7,8]

$$I_P(\omega t) = I_{\text{rev.}} F_P(\lambda t^{\frac{1}{2}}) G_P(\omega^{\frac{1}{2}}\lambda^{-1}) \sin(\omega t + \theta_P) \tag{2}$$

where

$$I_{\text{rev.}} = \frac{n^2F^2AC_O^*(\omega D_O)^{\frac{1}{2}}\Delta E}{4RT\cosh^2\left(\frac{j}{2}\right)} \tag{3}$$

$$F_P(\lambda t^{\frac{1}{2}}) = 1 + (\alpha\, e^{-j} - \beta)\, e^{\lambda^2 t}\operatorname{erfc}(\lambda t^{\frac{1}{2}}) \tag{4}$$

$$G_P(\omega^{\frac{1}{2}}\lambda^{-1}) = \left[\frac{2}{1 + \left(1 + \frac{\sqrt{2\omega}}{\lambda}\right)^2}\right]^{\frac{1}{2}} \tag{5}$$

$$\theta = \cot^{-1}\left(1 + \frac{\sqrt{2\omega}}{\lambda}\right) \tag{6}$$

$$j = \frac{nF}{RT}(E_{\text{d.c.}} - E_{\frac{1}{2}}^r) \tag{7}$$

$$\lambda = \frac{k_h}{D^{\frac{1}{2}}} (e^{-\alpha j} + e^{\beta j}) \tag{8}$$

$$D = D_O{}^{\beta} D_R{}^{\alpha} \tag{9}$$

$$E_{\frac{1}{2}}{}^{r} = E^{o} - \frac{RT}{nF} \ln \left(\frac{f_R}{f_O}\right)\left(\frac{D_O}{D_R}\right)^{\frac{1}{2}} \tag{10}$$

$$\beta = 1 - \alpha \tag{11}$$

$$A = 0.8515(mt)^{\frac{2}{3}} \qquad \text{(at } 25°\text{)} \tag{12}$$

The term $I_{\text{rev.}}$ is the amplitude of the reversible a.c. polarographic wave. The functions $F_P(\lambda t^{\frac{1}{2}})$ and $G_P(\omega^{\frac{1}{2}}\lambda^{-1})$ represent 'correction' terms accounting for deviations from reversibility. The term $F_P(\lambda t^{\frac{1}{2}})$ is dependent on the influence of charge transfer kinetics on the d.c. process, *i.e.*, it differs from unity when the mean concentrations of the electroactive species at the interface deviate from their Nernstian values. The term $G_P(\omega^{\frac{1}{2}}\lambda^{-1})$ responds to charge transfer kinetic effects on the a.c. process and differs from unity when the alternating component of the surface concentrations deviate from the Nernst equation. Similar terms will appear in equations for other electrode models. While they may differ in magnitude, their significance is the same. The symbol $F(\lambda t^{\frac{1}{2}})$ will refer to the term related to the d.c. process while $G(\omega^{\frac{1}{2}}\lambda^{-1})$ will be the term due to the a.c. process. Subscripts, such as employed above, will designate to which electrode model the term applies.

B. Expanding planar electrode

MATSUDA's derivation of the a.c. polarographic wave equation for a quasi-reversible system employed this approximation which takes account of contributions due to drop growth, but neglects drop curvature. He showed for normal conditions of mercury flow, drop life, scan rate and alternating potential frequency, that the a.c. polarographic wave with the reduced form initially absent from the solution is given by the expression[3]

$$I_{EP}(\omega t) = I_{\text{rev.}} F_{EP}(\lambda t^{\frac{1}{2}}) G_{EP}(\omega^{\frac{1}{2}}\lambda^{-1}) \sin(\omega t + \theta_{EP}) \tag{13}$$

where

$$F_{EP}(\lambda t^{\frac{1}{2}}) = 1 + \left(\frac{7}{3\pi}\right)^{\frac{1}{2}} (\alpha e^{-j} - \beta) \frac{(1.61 + \lambda t^{\frac{1}{2}})}{(1.13 + \lambda t^{\frac{1}{2}})^2} \tag{14}$$

$$G_{EP}(\omega^{\frac{1}{2}}\lambda^{-1}) = G_P(\omega^{\frac{1}{2}}\lambda^{-1}) \tag{15}$$

$$\theta_{EP} = \theta_P \tag{16}$$

and $I_{\text{rev.}}$ is given by eqn. (3). It should be noted that only the term responsive to kinetic influence of the d.c. process, $F_{EP}(\lambda t^{\frac{1}{2}})$, differs from the analogous term for the stationary plane model. The $G(\omega^{\frac{1}{2}}\lambda^{-1})$ and phase angle terms are identical. It is to be expected under rather extreme experimental conditions (*e.g.*, very low frequency, very short drop life, etc.) that $G_{EP}(\omega^{\frac{1}{2}}\lambda^{-1})$ and θ_{EP} would differ from $G_P(\omega^{\frac{1}{2}}\lambda^{-1})$ and θ_P, respectively. MATSUDA did not derive closed-form expressions for these quantities applicable to all experimental conditions, but assumed normal conditions and proceeded to prove eqns. (15) and (16).

A more exact form for $F_{EP}(\lambda t^{\frac{1}{2}})$ is obtained[3] by replacing $\lambda t^{\frac{1}{2}}$ by $(\lambda t^{\frac{1}{2}})^{1.04}$. The latter form was employed in calculations reported here. Differences between the two alternatives are usually small, except for the slowest charge transfer rates considered (*e.g.*, $k_h = 5 \cdot 10^{-4}$ cm sec^{-1}).

C. Stationary spherical electrode

By introducing the time-dependence of electrode area one can apply this electrode model to the D.M.E. This amounts to considering the contribution due to drop curvature, but neglecting drop growth. A complete a.c. polarographic wave equation for this electrode with a quasi-reversible system has not been reported to our knowledge. GERISCHER's equations[2] for the faradaic impedance at a stationary spherical electrode do not apply rigorously to conditions of both alternating and direct current flow which exist in a.c. polarography. The derivation of the a.c. polarographic wave equation for diffusion to a stationary sphere with both redox forms soluble in solution, the reduced form absent initially and equal diffusion coefficients, is given in Appendices II and III. Equations for the case of the reduced form soluble in the electrode (as in metal ion–metal amalgam systems), where one must consider the finite volume of the diffusing medium, will not be given here. This important case is treated in the derivation of equations for the D.M.E., to follow. The equations obtained in the Appendix may be written

$$I_S(\omega t) = I_{\text{rev.}} F_S(\lambda t^{\frac{1}{2}}) G_S(\omega^{\frac{1}{2}}\lambda^{-1}) \sin(\omega t + \theta_S) \tag{17}$$

where

$$F_S(\lambda t^{\frac{1}{2}}) = 1 + \frac{(\alpha e^{-j} - \beta)}{(D_O^{\frac{1}{2}} r_O^{-1} + \lambda)} \times \{\lambda \exp([D_O^{\frac{1}{2}} r_O^{-1} + \lambda]^2 t) \operatorname{erfc}([D_O^{\frac{1}{2}} r_O^{-1} + \lambda] t^{\frac{1}{2}}) + D_O^{\frac{1}{2}} r_O^{-1}\} \tag{18}$$

$$G_S(\omega^{\frac{1}{2}}\lambda^{-1}) = \left[\frac{2}{\left(\frac{\sqrt{2\omega}}{\lambda} + 1 - P\right)^2 + (1-Q)^2}\right]^{\frac{1}{2}} \tag{19}$$

$$\theta_S = \cot^{-1}\left(\frac{\frac{\sqrt{2\omega}}{\lambda} + 1 - P}{1 - Q}\right) \tag{20}$$

$$P = \frac{y^2}{1 + y^4}(1 - \sqrt{2}y + y^2) \tag{21}$$

$$Q = \frac{y}{1 + y^4}(\sqrt{2} - y + y^3) \tag{22}$$

$$y = \frac{D_O^{\frac{1}{2}}}{\omega^{\frac{1}{2}} r_O} \tag{23}$$

and $I_{\text{rev.}}$ is given by eqn. (3). Examination of these relations indicates for

$$y \ll 1 \tag{24}$$

that

$$P \ll 1 \tag{25}$$

$$Q \ll 1 \tag{26}$$

so that P and Q are negligible leading to the results

$$G_S(\omega^{\frac{1}{2}}\lambda^{-1}) = G_P(\omega^{\frac{1}{2}}\lambda^{-1}) \tag{27}$$

$$\theta_S = \theta_P \tag{28}$$

Substitution of typical experimental values of r_o, D_0 and ω indicates that the above inequalities will be obeyed for usual experimental conditions, so eqns. (27) and (28) will apply. This result is analogous to that obtained for the expanding plane model, *i.e.*, the only term dependent on the geometry contribution is the term responsive to deviations of the d.c. process from reversibility, $F_S(\lambda t^{\frac{1}{2}})$.

Although direct derivation of equations assuming inequality of diffusion coefficients is possible, diffusion coefficients were assumed equal in deriving the above equations to avoid much algebraic complexity. The important result expressed by eqns. (27) and (28) is not dependent on the assumption of equality of diffusion coefficients.

D. Expanding spherical electrode (D.M.E.)

It would be desirable to solve the mass transfer relations considering simultaneously contributions due to electrode geometry and growth. However, complete and direct solution of the MacGillavry–Rideal[9] differential equation for a.c. polarography appears extremely cumbersome. In view of certain results obtained for the cases considered above, a direct approach also appears unnecessary. It has been shown for normal experimental conditions, that only the $F(\lambda t^{\frac{1}{2}})$ function retains terms characteristic of the specific electrode model employed. All other components of the solution are adequately expressed on the basis of the stationary plane. In addition, *for any of the cases considered* it can be shown that the $F(\lambda t^{\frac{1}{2}})$ function can be written

$$F(\lambda t^{\frac{1}{2}}) = 1 + \frac{(\alpha e^{-j} - \beta)D^{\frac{1}{2}} i_{d.c.}(t)}{nFAC_o^* D_o^{\frac{1}{2}} k_h e^{-\alpha j}} \tag{29}$$

where $i_{d.c.}(t)$ is the direct current corresponding to the electrode model under consideration. This result can be derived directly for all the cases considered above (*cf.*, *e.g.*, ref. 7 for the stationary plane and Appendix II for the stationary sphere). Alternatively, one can show that eqn. (29) is consistent with eqns. (4), (14) and (18) by substituting the appropriate solutions for the direct current into eqn. (29). The direct currents for a stationary planar electrode[10], an expanding plane[3] and a stationary sphere (both redox forms soluble in the solution, diffusion coefficients equal) are, respectively,

$$i_{d.c.}(t) = nFAC_o^* \left(\frac{D_o}{D}\right)^{\frac{1}{2}} k_h e^{-\alpha j} e^{\lambda^2 t} \operatorname{erfc}(\lambda t^{\frac{1}{2}}) \tag{30}$$

$$i_{d.c.}(t) = nFAC_o^* D_o^{\frac{1}{2}} \sqrt{\frac{7}{3\pi}} \frac{\lambda(1.61 + \lambda t^{\frac{1}{2}})}{(1 + e^j)(1.13 + \lambda t^{\frac{1}{2}})^2} \tag{31}$$

$$i_{\text{d.c.}}(t) = nFAC_O^* k_h e^{-\alpha j} \left(\frac{1}{D_O^{\frac{1}{2}} r_O^{-1} + \lambda}\right)$$

$$\times \{\lambda \exp[(D_O^{\frac{1}{2}} r_O^{-1} + \lambda)^2 t] \operatorname{erfc} [(D_O^{\frac{1}{2}} r_O^{-1} + \lambda) t^{\frac{1}{2}}] + D_O^{\frac{1}{2}} r_O^{-1}\} \quad (32)$$

Substituting eqns. (30), (31) and (32) in eqn. (29) yields eqns. (4), (14) and (18), respectively. A simple approach to an expression for the D.M.E. is suggested by the facts that: (a) $F(\lambda t^{\frac{1}{2}})$ is the only term significantly dependent on the electrode model; (b) $F(\lambda t^{\frac{1}{2}})$ can be expressed in the general form of eqn. (29); (c) substitution of the appropriate expression for the direct current with a particular electrode model into eqn. (29) yields $F(\lambda t^{\frac{1}{2}})$ for that electrode. We submit that to obtain an equation for the a.c. polarographic wave adequately accounting simultaneously for geometry and growth of the mercury drop, one simply substitutes into eqn. (29) the eqns. of KOUTECKÝ AND ČÍŽEK for the d.c. polarographic wave at the D.M.E. with a quasi-reversible system[11]. This leads to the results

$$I_{\text{D.M.E.}}(\omega t) = I_{\text{rev.}} F_{\text{D.M.E.}}(\lambda t^{\frac{1}{2}}) G_P(\omega^{\frac{1}{2}} \lambda^{-1}) \sin(\omega t + \theta_P) \quad (33)$$

where $I_{\text{rev.}}$, $G_P(\omega^{\frac{1}{2}}\lambda^{-1})$ and θ_P are given by eqns. (3), (5) and (6), respectively,

$$F_{\text{D.M.E.}}(\lambda t^{\frac{1}{2}}) = 1 + \sqrt{\frac{7}{3\pi t}} \frac{(\alpha e^{-j} - \beta)}{\lambda} \left\{1 + \frac{0.7868(1 + \delta^{\frac{1}{2}} e^{j})}{(1 + e^{j})} \xi_1\right\}$$

$$\times \left\{F(X) - \xi_1 \left[0.7868 \frac{(1 + \delta^{\frac{1}{2}} e^{j})}{(1 + e^{j})} F(X) - G_A(X)\right]\right\} \quad (34)$$

for both redox forms soluble in the solution and

$$F_{\text{D.M.E.}}(\lambda t^{\frac{1}{2}}) = 1 + \sqrt{\frac{7}{3\pi t}} \frac{(\alpha e^{-j} - \beta)}{\lambda} \left\{1 + \frac{0.7868(1 - \delta^{\frac{1}{2}} e^{j})}{(1 + e^{j})} \xi_1\right\}$$

$$\times \left\{F(X) - \xi_1 \left[0.7868 \frac{(1 - e^{j})}{(1 + e^{j})} F(X) - G_B(X)\right]\right\} \quad (35)$$

for the reduced form soluble in the mercury drop. $F(X)$, $G_A(X)$, $G_B(X)$ and ξ_1, are defined in KOUTECKÝ AND ČÍŽEK's manuscript[11]. The other new quantities are

$$X = \sqrt{\frac{12}{7}} \lambda t^{\frac{1}{2}} \quad (36)$$

$$\delta = \frac{D_R}{D_O} \quad (37)$$

These equations are quite cumbersome and application in data analysis appears difficult. This matter is discussed later. However, it is proposed that they represent an exact a.c. polarographic wave equation for the D.M.E. and thus permit theoretical assessment of the importance of the combined contribution of drop growth and geometry.

The concepts invoked to obtain the equations for the D.M.E. lead also to some important conclusions regarding a.c. polarography at stationary electrodes. These are discussed below.

COMPARISON OF A.C. POLAROGRAPHIC WAVES PREDICTED FOR THE VARIOUS ELECTRODE MODELS

It is apparent that the theoretical equations differ for various approximations to the D.M.E. It has not been established that these differences are important under conditions where a.c. polarographic waves normally are observed with quasi-reversible systems. To investigate this aspect, numerous calculations of a.c. waves predicted by the various models have been performed. An IBM 709 digital computer was utilized to facilitate this work. Calculations were limited to the range of heterogeneous charge transfer rate constants between 10^{-4} and 10^{-2} cm sec^{-1}. For rate constants much larger than 10^{-2} cm sec^{-1}, the d.c. process is reversible and differences between predictions for different electrode models prove negligible. Rate constants much smaller than 10^{-4} cm sec^{-1} yield a.c. waves prohibitively small so that accurate measurement proves difficult. Although the two-decade range for rate constants of interest in this investigation may appear rather small, numerous systems have been found to exhibit rates in this range as evidenced by data presented in a recent extensive discussion of a.c. polarography[12]. In addition to a.c. polarograms calculated from equations given above, theoretical polarograms based on the assumption that the d.c. process is reversible, $[F(\lambda t^{\frac{1}{2}}) = 1]$, were included in the comparison of theoretical models. The latter correspond to polarograms predicted by the Breyer–Bauer–Kambara expression[13,14]. Comparing these with polarograms not subject to this assumption permits assessment of the contribution of non-Nernstian conditions in the d.c. surface concentrations. BREYER AND BAUER clearly indicate the limitation of their equation, but belittle the importance of considering conditions where the d.c. process is not reversible[13].

Figures 1–11 and Tables 1–4 illustrate a sampling of the results of our calculations. In equations for spherical electrodes, it is assumed that both redox forms are soluble in solution. All calculations assume reduced form initially absent from solution. Results are given for charge transfer rate constants of 1.00×10^{-2}, 1.00×10^{-3} and 5.00×10^{-4} cm sec^{-1} and α values of 0.200, 0.500 and 0.800. Calculated a.c. polarograms correspond to the instantaneous alternating current at end of drop life. Some calculated alternating current–time curves for the life of a single drop [$I(\omega t)$–t curves] are also presented. The study of i–t curves over the life of a single drop has recently received much attention in d.c. polarography[15,16,17]. Advantageous application of similar investigations in a.c. polarography has not been suggested to date. However, because it is perhaps inevitable that experiments of this nature will be suggested, calculation of such curves was performed to establish the importance of electrode geometry in such studies.

It is apparent from brief perusal of the figures and tables that a number of general conclusions can be reached. Contributions of quasi-reversibility in the d.c. process, drop growth and geometry will be of notable importance when k_h becomes less than 10^{-2} cm sec^{-1}. For rate constants of 10^{-3} or smaller, these effects can be

remarkably large. The magnitude and form of these influences on the a.c. wave is strongly dependent on the value of α for any particular magnitude of k_h. In all cases, the expanding plane equation lies closest to the exact (D.M.E.) expression, with the stationary sphere model next, and the stationary plane showing greatest deviations. This indicates that the contribution of drop growth is more important than electrode geometry, the result expected because this is the situation known to exist in d.c. polarography. Geometry and drop growth contribute significantly to the position and magnitude of the peak of the a.c. wave, a parameter of considerable interest to most experimentalists. Some typical predicted differences in magnitude and position of the a.c. polarographic peak between the various approximate models [eqns. (2), (13) and (17)] and the exact solution [eqn. (33)] are given in Table 1. Contributions of electrode

TABLE 1

PEAK CURRENTS AND PEAK POTENTIALS FOR VARIOUS ELECTRODE MODELS

Rate parameters	$k_h = 1.0 \times 10^{-3}$ *cm sec*$^{-1}$, $\alpha = 0.50$		$k_h = 5.0 \times 10^{-4}$ *cm sec*$^{-1}$, $\alpha = 0.20$		$k_h = 5.0 \times 10^{-4}$ *cm sec*$^{-1}$, $\alpha = 0.50$	
	Peak current (μ*amp*)	$[(E_{d.c.})_{Peak} - E_{\frac{1}{4}}^{r}]$ (*V*)	*Peak current* (μ*amp*)	$[(E_{d.c.})_{Peak} - E_{\frac{1}{4}}^{r}]$ (*V*)	*Peak current* (μ*amp*)	$[(E_{d.c.})_{Peak} - E_{\frac{1}{4}}^{r}]$ (*V*)
Breyer–Bauer–Kambara model	0.310	0.000	0.189	+0.031	0.160	0.000
Planar diffusion	0.325	−0.022	0.156	+0.046	0.198	−0.056
Spherical diffusion	0.330	−0.024	0.153	+0.048	0.209	−0.068
Expanding plane	0.336	−0.030	0.149	+0.049	0.224	−0.080
Expanding sphere	0.346	−0.036	0.145	+0.050	0.247	−0.095

geometry and growth are most significant on the cathodic portion of the a.c. wave. This phenomena appears because the polarograms apply to the case where only the oxidized form is initially present in the solution. It manifests the greater width and steepness of the d.c. concentration profile at negative potentials where interface concentrations deviate most from bulk concentrations. Exactly the opposite result is obtained (*i.e.*, greater influence at positive potentials) if one assumes only reduced form initially present. An intermediate situation is expected for the case in which both redox forms exist in the bulk of the solution. It should be noted that there is always one d.c. potential (sometimes difficultly discernible for large α) along the a.c. wave at which all of the equations predict the same current and the directions of the contributions due to drop growth, etc. reverse. This potential corresponds to $(\alpha e^{-j} - \beta) = 0$. It is the same d.c. potential at which dependence of the a.c. wave on mercury column height disappears[8]. The determination of this potential has been suggested for evaluation of α.[8] The equation based on neglecting the influence of non-Nernstian d.c. behavior predicts a.c. waves considerably different in magnitude, position of the peak, and half-width of the wave, as compared to the equations accounting for this effect. Differences in position and width are not surprising because neglect of quasi-reversibility of the d.c. process neglects the shift in potential and decreased slope (*i.e.*, broadening) of the d.c. wave for such conditions. As expected,

TABLE 2

ALTERNATING CURRENTS PREDICTED BY VARIOUS MODELS $k_h = 1.0 \times 10^{-2}$ cm sec^{-1}, $\alpha = 0.20$; values of other parameters as in Fig. 1

$E_{d.c.} - E_{\frac{1}{2}}^r$	*Breyer–Bauer–Kambara model*	*Stationary plane*	*Stationary sphere*	*Expanding plane*	*Expanding sphere*
−0.10	0.164	0.198	0.204	0.209	0.220
−0.08	0.317	0.348	0.353	0.358	0.368
−0.06	0.588	0.610	0.614	0.617	0.624
−0.04	1.015	1.020	1.021	1.021	1.023
−0.02	1.552	1.535	1.532	1.529	1.524
0.00	1.976	1.946	1.940	1.936	1.926
+0.02	2.001	1.974	1.969	1.966	1.956
+0.04	1.598	1.583	1.580	1.579	1.570
+0.06	1.040	1.034	1.033	1.033	1.030
+0.08	0.584	0.582	0.582	0.582	0.581
+0.10	0.299	0.298	0.298	0.298	0.298

TABLE 3

ALTERNATING CURRENTS PREDICTED BY VARIOUS MODELS $k_h = 1.0 \times 10^{-2}$ cm sec^{-1}, $\alpha = 0.50$; values of other parameters as in Fig. 1

$E_{d.c.} - E_{\frac{1}{2}}^r$	*Breyer–Bauer–Kambara model*	*Stationary plane*	*Stationary sphere*	*Expanding plane*	*Expanding sphere*
−0.10	0.254	0.298	0.305	0.310	0.327
−0.08	0.478	0.531	0.541	0.547	0.567
−0.06	0.836	0.893	0.904	0.911	0.930
−0.04	1.314	1.362	1.371	1.377	1.398
−0.02	1.776	1.801	1.805	1.809	1.817
0.00	1.976	1.976	1.976	1.976	1.976
+0.02	1.776	1.765	1.763	1.761	1.757
+0.04	1.314	1.304	1.303	1.301	1.298
+0.06	0.836	0.831	0.830	0.829	0.827
+0.08	0.478	0.478	0.475	0.475	0.474
+0.10	0.254	0.253	0.253	0.253	0.252

TABLE 4

ALTERNATING CURRENTS PREDICTED BY VARIOUS MODELS $k_h = 1.0 \times 10^{-2}$ cm sec^{-1}, $\alpha = 0.80$; values of other parameters as in Fig. 1

$E_{d.c.} - E_{\frac{1}{2}}^r$	*Breyer–Bauer–Kambara model*	*Stationary plane*	*Stationary sphere*	*Expanding plane*	*Expanding sphere*
−0.10	0.299	0.325	0.330	0.331	0.343
−0.08	0.584	0.626	0.634	0.637	0.656
−0.06	1.040	1.101	1.112	1.118	1.143
−0.04	1.598	1.668	1.681	1.689	1.715
−0.02	2.001	2.059	2.069	2.077	2.097
0.00	1.976	2.007	2.012	2.016	2.026
+0.02	1.552	1.560	1.561	1.562	1.565
+0.04	1.015	1.014	1.014	1.014	1.014
+0.06	0.588	0.586	0.586	0.585	0.585
+0.08	0.317	0.316	0.315	0.315	0.315
+0.10	0.164	0.163	0.163	0.163	0.163

variations between the a.c. waves predicted by the different models become quite small for $k_h = 1.00 \times 10^{-2}$ cm sec^{-1}. The small differences discourage graphical illustration so results for this value of k_h are given in tabular form (Tables 2–4). However, the contributions of drop growth etc. may still be greater than experimental uncertainty, *e.g.*, peak currents in Table 4. The effect of increasing drop life (decreasing mercury column height) on the differences between the various models is illustrated for a particular set of rate parameters in Figs. 2, 3 and 4. It is seen that the variations between the predicted a.c. waves tend to decrease as drop life increases. This occurs because longer times permit the interface concentrations to approach more closely Nernstian conditions. Figures 9–11 illustrate the importance of the effects under consideration on studies of $I(\omega t)$–t curves in a.c. polarography. For the $\log I(\omega t)$ *vs.* $\log t$ plots, the Breyer–Bauer–Kambara theory neglecting non-Nernstian d.c. behavior predicts a linear plot with a slope of 2/3. The theoretical equations accounting for this effect predict slopes differing significantly from $\frac{2}{3}$, and in some cases the log–log plots are non-linear. In addition, the latter equations all

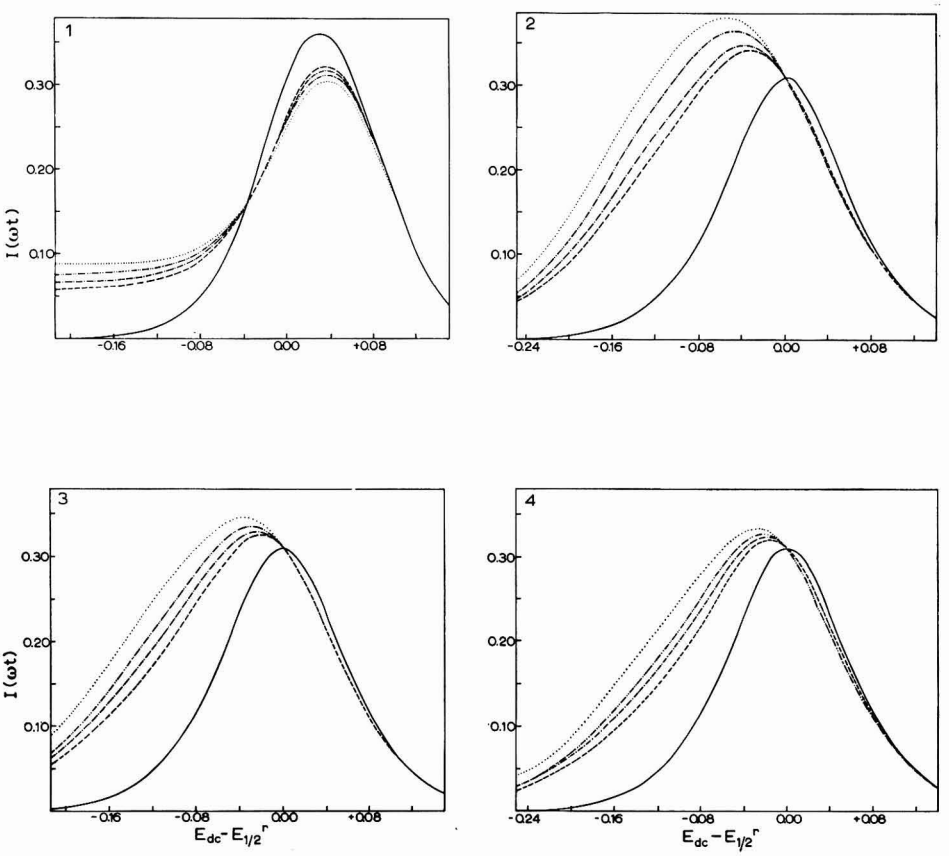

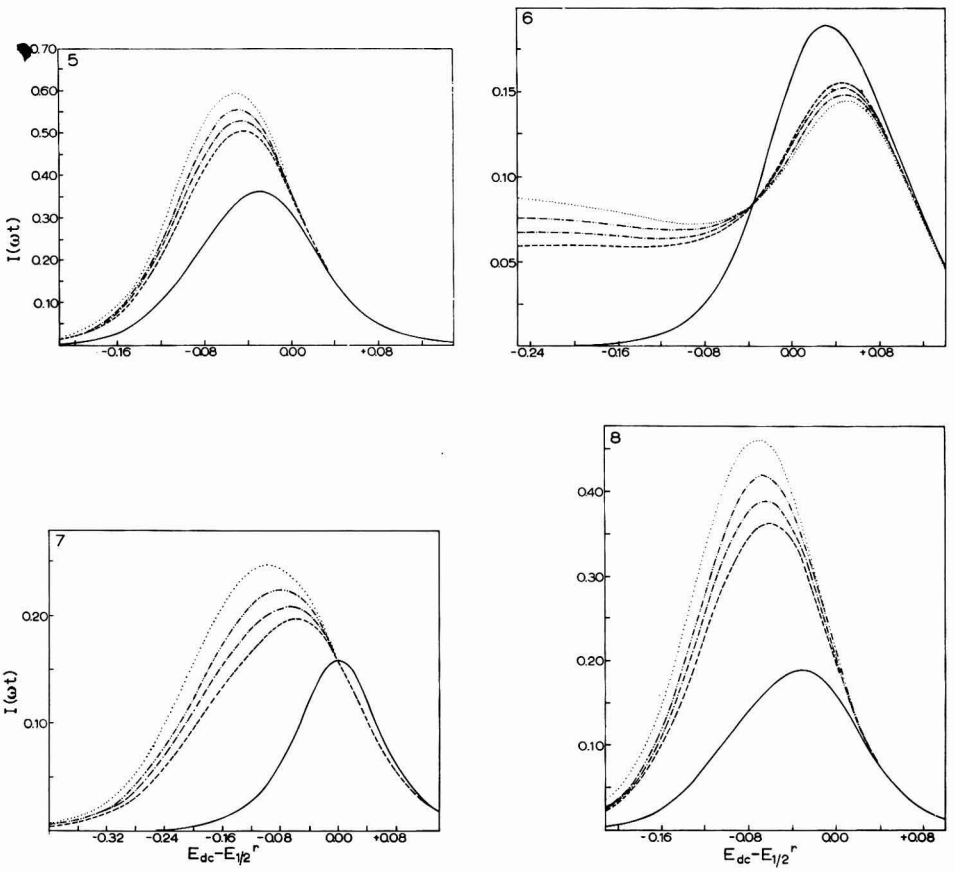

Fig. 1–8. Calculated a.c. polarograms for the quasi-reversible system with various electrode models: ——, Breyer–Bauer–Kambara model; – –, planar diffusion; — · —, spherical diffusion; — · · —, expanding plane; . . . ., expanding sphere. $n = 1$, $T = 25°$, $\Delta E = 5.00$ mV, $\omega = 125.66$, $C_O^* = 1.00 \times 10^{-3}$ M, $m = 1.40$ mg sec^{-1}, $D_O = D_R = 5.00 \times 10^{-6}$ cm^2 sec^{-1}. Values of k_h, α, and droptime are given in the following table

Figure	k_h *(cm sec^{-1})*	α	*drop-time (sec)*	*Figure*	k_h *(cm sec^{-1})*	α	*drop-time (sec)*
1	1.00×10^{-3}	0.200	6.0	2	1.00×10^{-3}	0.500	3.0
3	1.00×10^{-3}	0.500	6.0	4	1.00×10^{-3}	0.500	9.0
5	1.00×10^{-3}	0.800	6.0	6	5.00×10^{-4}	0.200	6.0
7	5.00×10^{-4}	0.500	6.0	8	5.00×10^{-4}	0.800	6.0

predict approximately the same slopes (or tangents to the curve in non-linear plots) for the $\log I(\omega t) - \log t$ plots. This implies that electrode growth and geometry significantly alter the magnitude of the alternating current, but not the form of the time dependence. Thus, one contemplating the determination of kinetic parameters

from the *slope* of $\log I(\omega t) - \log t$ plots may consider equations for the stationary plane adequate. This type of result was expected because in theoretical treatment of the d.c. wave it is found that the approximate approaches usually predict with relative accuracy the form of the time dependence, while they fare poorly in predicting current magnitude.

The levelling off or increase in alternating current at very negative potentials for systems with small values of α (Figs. 1 and 6) represent secondary peaks or shoulders predicted by the theory (*cf.*, MATSUDA's manuscript[3]). While not shown in Figs. 1 and 6, the predicted current eventually decays to zero at sufficiently negative potentials. This feature of the a.c. polarographic wave has been observed experimentally in at least one instance[18].

IMPLICATIONS OF THEORETICAL RESULTS

The results of this theoretical study suggest some important implications related to the theory and practice of a.c. polarography. These are the concern of the remainder of this discussion.

A. More complex reaction schemes

The above development was concerned with the kinetically simple quasi-reversible system in which only diffusion and charge transfer exert kinetic control. However, the same ideas used to rationalize influence of electrode geometry and growth when the d.c. process is influenced kinetically by charge transfer lead one to similar conclusions regarding systems with coupled chemical reactions and/or adsorption. One is led to conclude that when the d.c. process is influenced kinetically by either charge transfer, chemical reaction or adsorption, contributions of electrode geometry and growth may exert significant influence on the a.c. polarographic wave. When any of these rate processes is sufficiently slow, deviations from equilibrium of the mean surface concentrations may occur. Through their effects on the d.c. mass transfer process, electrode geometry and growth will influence the magnitude of deviations from equilibrium for both chemical and electrochemical steps. Thus, a system with a coupled preceding chemical reaction

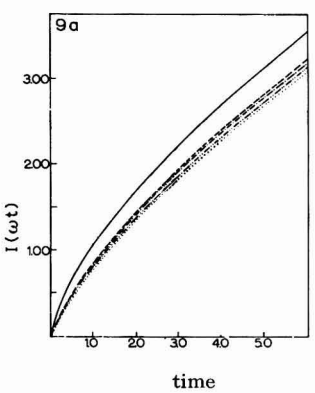

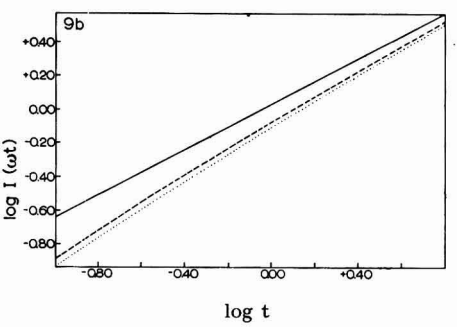

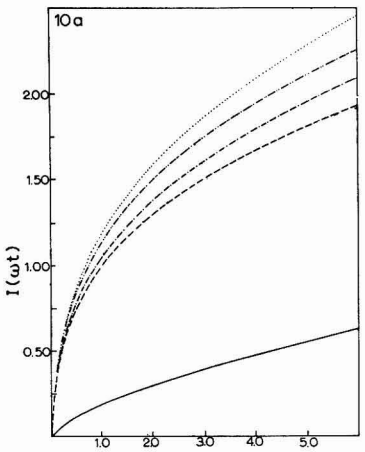

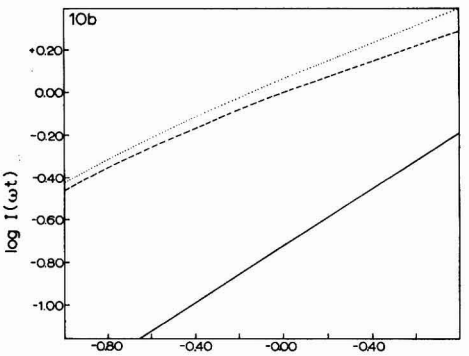

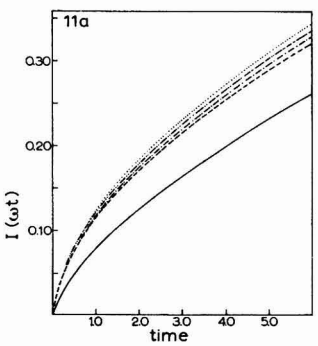

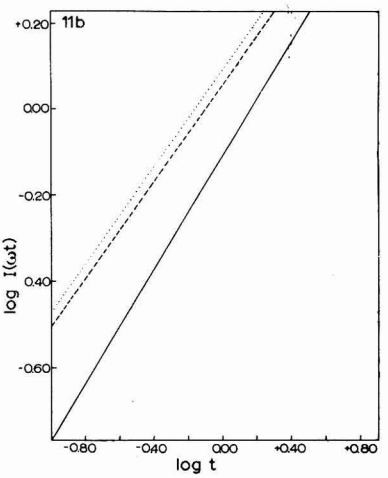

Fig. 9a–11a. Calculated instantaneous alternating current–time curves for the quasi-reversible system with various electrode models. Fig. 9b–11b. Calculated log $I(\omega t)$ *vs.* log t curves for the quasi-reversible system with various electrode models (curves for spherical and expanding plane lie between those for planar and expanding drop). Parameters and legend, see Fig. 1–8. Values of k_h, α, $E_{d.c.} - E_{\frac{1}{2}}{}^r$ and $C_O{}^*$ are given in the following table

Figure	k_h(*cm sec*$^{-1}$)	α	$E_{d.c.} - E_{\frac{1}{2}}{}^r$(*V*)	$C_O{}^*$ (*M*)
9a,b	1.00×10^{-3}	0.200	+0.040	1.00×10^{-2}
10a,b	5.00×10^{-4}	0.500	−0.080	1.00×10^{-2}
11a,b	1.00×10^{-3}	0.500	−0.030	1.00×10^{-2}

$$Y \underset{k_2}{\overset{k_1}{\rightleftharpoons}} O + n\,e \rightleftharpoons R$$

can yield an a.c. wave dependent on electrode growth and geometry if the preceding chemical reaction and/or charge transfer kinetically influence the d.c. process. As an example, the contribution of drop growth will be illustrated in a more formal manner.

Employing the stationary plane diffusion model, the a.c. polarographic wave equation for a system with a coupled preceding chemical reaction is given by[7,8]

$$I(\omega t) = I_{\text{rev.}} G_P(t)\, H(\omega^{\frac{1}{2}}\lambda^{-1}, g) \sin\left(\omega t + \cot^{-1}\frac{V}{S}\right) \tag{38}$$

where

$$G_P(t) = (1 + e^{-j})\left\{\frac{\alpha D^{\frac{1}{2}} Q_O(t)}{k_h e^{-\alpha j}} + e^{j}\int_0^t \frac{Q_O(t-u)\,du}{(\pi u)^{\frac{1}{2}}}\right\} \tag{39}$$

$$Q_O(t) = \frac{i_{\text{d.c.}}(t)}{nFAC_O^* D_O^{\frac{1}{2}}} \tag{40}$$

$$H(\omega^{\frac{1}{2}}\lambda^{-1}, g) = \left[\frac{2}{V^2 + S^2}\right]^{\frac{1}{2}} \tag{41}$$

$$V = \frac{\sqrt{2\omega}}{\lambda} + \frac{1}{(1 + e^{j})}\left\{e^{j} + \frac{K}{1+K} + \frac{1}{1+K}\left[\frac{(1+g^2)^{\frac{1}{2}} + g}{1+g^2}\right]^{\frac{1}{2}}\right\} \tag{42}$$

$$S = \frac{1}{(1 + e^{j})}\left\{e^{j} + \frac{K}{1+K} + \frac{1}{1+K}\left[\frac{(1+g^2)^{\frac{1}{2}} - g}{1+g^2}\right]^{\frac{1}{2}}\right\} \tag{43}$$

$$g = \frac{k_1 + k_2}{\omega} \tag{44}$$

$$K = \frac{k_1}{k_2} \tag{45}$$

and $I_{\text{rev.}}$ is given by eqn. (3). The term dependent on direct current, $G_P(t)$, is analogous to $F(\lambda t^{\frac{1}{2}})$ in the quasi-reversible case. It is dependent upon deviations from equilibrium (chemical or electrochemical) of the d.c. surface concentrations. Employing the expanding plane model and proceeding as in MATSUDA's derivation[3], one obtains a result differing from the stationary plane model only in the $G(t)$ term. For an expanding plane one obtains in place of $G_P(t)$

$$G_{EP}(t) = (1 + e^{-j})\left\{\frac{\alpha D^{\frac{1}{2}} Q_O(t)}{k_h e^{-\alpha j}} + e^{j}\sqrt{\frac{7}{3\pi}}\int_0^t \frac{u^{\frac{2}{3}} Q_O(u)\,du}{(t^{7/3} - u^{7/3})^{\frac{1}{2}}}\right\} \tag{46}$$

The difference in the integrals in $G_P(t)$ and $G_{EP}(t)$ manifest one difference in stationary and expanding plane models. A different form of $Q_O(t)$ also is expected for the two models. Whereas with the quasi-reversible system, $F(\lambda t^{\frac{1}{2}})$ expressed in terms of

$i_{a.c.}(t)$ could be written in an identical fashion for any electrode model [eqn. (29)], this does not hold for the system with a coupled preceding chemical reaction. The term dependent on electrode geometry and growth differs for the stationary and expanding plane models and is expected to exhibit other forms for stationary sphere and D.M.E. models. The variations appear in the integral. For a number of reasons this complication renders somewhat ineffective the approach employed to obtain the 'exact' a.c. wave equation for the quasi-reversible system at the D.M.E. [eqns. (33), (34) and (35)]. We have been unable to deduce the form of $G(t)$ in terms of $i_{a.c.}$ for the D.M.E. model. Even if this were achieved, the form of the integral may prove so complicated that integration of the appropriate expression for $i_{a.c.}(t)$ may prove difficult. This is implied by the complexity of the integral obtained for the expanding plane. Finally, the problem of deriving equations for the entire d.c. polarographic wave considering kinetic effects of charge transfer and chemical reaction, as well as the contribution of electrode geometry and growth, has not been solved.

For the special case in which only chemical reaction kinetically influences the d.c. process, the $G(t)$ function with a preceding chemical reaction assumes the form[7]

$$G_P(t) = (1 + e^j) \int_0^t \frac{Q_O(t - u)\,du}{(\pi u)^{\frac{1}{2}}} \tag{47}$$

for the stationary plane and

$$G_{EP}(t) = (1 + e^j)\sqrt{\frac{7}{3\pi}} \int_0^t \frac{u^{\frac{3}{7}} Q_O(u)\,du}{(t^{7/3} - u^{7/3})^{\frac{1}{2}}} \tag{48}$$

for the expanding plane. The integral still appears so the $G(t)$ function differs in form for various electrode models and many of the problems discussed for the general case still apply, although solution of the d.c. polarographic problem should prove less difficult.

For the case where the preceding chemical reaction is so rapid that it exerts only thermodynamic influence on the d.c. process, but charge transfer is kinetically important, the integral term disappears and $G_P(t)$ and $G_{EP}(t)$ have the form

$$G_{EP}(t) = G_P(t) = \frac{(1 + e^j)(1 + K)}{K + (1 + K)e^j} \left[1 + \left(\frac{\alpha K e^{-j}}{1 + K} - \beta\right) \frac{D^{\frac{1}{2}} Q_O(t)}{k_h e^{-\alpha j}}\right] \tag{49}$$

This applies for all electrode models and the problem of theoretically accounting for electrode geometry and growth can be handled as for the quasi-reversible case. As expected, when neither chemical reaction nor charge transfer kinetics influence the d.c. wave, the $G(t)$ term is independent of direct current and, thus, electrode growth becomes unimportant. For these conditions

$$G(t) = \frac{(1 + e^j)(1 + K)}{K + (1 + K)e^j} \tag{50}$$

for any electrode model. The factors causing $G(t)$ to differ from unity arise because of the shift in the d.c. polarographic wave to negative potentials due to the thermodynamic influence of the coupled preceding chemical reaction.

It is evident that when a chemical reaction influences the d.c. wave, solution of the theoretical problem including contributions of electrode growth and geometry appears quite difficult, in comparison with systems in which the d.c. wave is quasi-reversible. This is due to increased complexity of the function responsive to non-equilibrium conditions in the d.c. process and difficulty associated with obtaining an exact solution for $i_{d.c.}(t)$. Only the simple catalytic process

$$O + n\,e \rightleftharpoons R$$
$$\uparrow\_\_\_\_\_|$$

retains the simplicity associated with the quasi-reversible system. The completely general result for $G(t)$ with the catalytic case has the same form as $F(\lambda t^{\frac{1}{2}})$ in eqn. (29)[7] and solution of the d.c. problem has proven less difficult than for other types of mechanisms[19,20,21,22].

At this time we can say little regarding handling the problem under consideration for systems involving adsorption. There is every reason to believe that adequate theoretical treatment will prove even more complicated than for the foregoing cases.

B. Time dependence of a.c. polarographic currents

Time-dependent a.c. polarographic waves (waves dependent on mercury column height) and a.c. waves influenced by electrode geometry and growth arise from exactly the same effect; a d.c. polarographic process influenced kinetically by some rate process in addition to diffusion[8,23,24,25]. The two phenomena necessarily appear in unison. Thus, waves dependent on column height will be influenced by electrode geometry and growth. The absence of column height dependence assures one that these complicating factors need not be considered. Because contributions of electrode growth and geometry introduce significant complications into theoretical equations, quantitative kinetic studies based on the magnitude of the column height dependence are rendered difficult. However, certain types of measurements may yield useful quantitative results without the necessity of handling cumbersome theoretical relationships. Two examples are: (a) measurement of the potential of the 'cross-over point' with a quasi-reversible system[8] where column height dependence disappears together with contributions of electrode geometry and growth; (b) measurement of the slope of $\log I(\omega t) - \log t$ plots for which the simpler stationary plane model suffices.

C. Preferred experimental approaches

Because contributions of electrode geometry and growth can be significant when the d.c. process is not controlled solely by diffusion, sizeable errors in quantitative kinetic work may result from neglecting these factors. Inclusion of these contributions severely complicates theoretical expressions when such expressions are derivable. Further, one may reason that if drop growth and geometry are important, other perturbing influences known to be significant in the d.c. process may influence the a.c. wave for the same reasons. Among these are electrode shielding[26,27] and depletion[15,16], both of which are difficult to treat theoretically. Such considerations lead us to conclude that in experiments designed for quantitative kinetic studies, conditions under which electrode geometry and growth are important should be avoided, if at all possible. In most situations this should not be difficult. For some systems with slow kinetics, proper choice of experimental parameters such as electrolyte

concentration, pH, temperature etc. may effect a d.c. process controlled solely by diffusion. However, altering solution conditions may prove unsatisfactory because large deviations from experimental conditions of interest may be required to obtain the desired result. Then other approaches are required.

One of the more encouraging aspects of a.c. polarographic theory is the prediction that phase angles often will not be subject to contributions of electrode geometry and growth, even when the d.c. process is kinetically controlled. This is seen in equations for the quasi-reversible system and the system with a preceding chemical reaction. The terms responsive to electrode geometry and growth, $F(\lambda t^{\frac{1}{2}})$ and $G(t)$, do not appear in the phase angle expression. It is predicted that phase angles will be independent of such terms for systems with any number and type of coupled first-order chemical reaction[7]. Systems of this type, as well as the simple quasi-reversible case, encompass a wide range of systems which one may encounter. By restricting quantitative data analysis to phase angles when charge transfer or chemical reaction influence the d.c. wave, one may avoid the problem of accounting for contributions of electrode geometry and growth, while retaining the accuracy inherent in the a.c. methods. This represents another noteworthy advantage for phase angle measurements. Advantages pointed out previously are frequent relative simplicity of theoretical expressions for phase angle[28,29] and greater sensitivity of the phase angle to various kinetic influences[30]. On the other hand, with kinetically complicated electrode processes, phase angle measurements alone may not suffice to yield unambiguous values of rate parameters; then additional information furnished by current amplitude data will be required. In addition, not all electrode reaction mechanisms allow the simplicity of phase angle expression inherent in the systems mentioned above. Mechanisms involving multi-charge transfer steps and second- or higher-order chemical reactions can be shown to yield phase angle expressions dependent on $i_{\text{d.c.}}(t)$ when the d.c. process is not solely diffusion-controlled[8,30] so electrode geometry and growth can influence the phase angle. The same result is expected for systems involving adsorption effects. These are the same kinetic schemes which yield time-dependent phase angles[8].

To employ experimental conditions common to the classical faradaic impedance measurement is obviously a useful way of avoiding electrode geometry and growth considerations. In this experiment both forms of the redox couple are present in solution and measurements are confined to the equilibrium d.c. potential where zero direct current flows (if one neglects the small contribution due to faradaic rectification). The d.c. process is virtually non-existent and coupling of electrode growth and geometry contributions to the a.c. process *via* the d.c. process cannot occur. This method is applicable only when both forms of the redox couple are stable in solution.

Thus, if systems with slow kinetic steps influence the d.c. wave, adjustment of solution conditions, confining quantitative measurements to phase angles and/or employing measurements only at the equilibrium d.c. potential often will allow one to avoid problems associated with contributions of electrode geometry and growth. If it is necessary to employ data subject to these influences, one simplifying approach appears useful in some cases. Rather than utilizing the a.c. wave equation in which the complicated theoretical relation for the d.c. wave has been substituted [*e.g.*, eqns. (33), (34) and (35)], one employs equations expressed in terms of $i_{\text{d.c.}}(t)$ and

experimental values of this parameter. As an example, consider the quasi-reversible system. Instead of employing eqn. (34) or (35) for $F(\lambda t^{\frac{1}{2}})$, one applies eqn. (29) and substitutes experimental values of direct current for $i_{\text{d.c.}}(t)$. Use of experimental values should incorporate contributions of electrode geometry, growth, shielding, etc. This approach appears readily applicable to the analysis of a.c. polarographic waves with a quasi-reversible process, a simple catalytic process, all systems with first-order coupled chemical reactions in which *only* charge transfer influences the *d.c.* process and some systems with coupled higher-order reactions[7,30] where the steady state approximation[31] is valid. In these cases the $i_{\text{d.c.}}(t)$ term arises in the a.c. wave equations in a non-integral form [as opposed to eqns. (39), (46), (47) and (48)]. With the exception of the catalytic case, theoretical relations for systems where coupled first-order chemical reactions exert kinetic influence on the d.c. wave exhibit terms involving integrals of the direct current as in eqns. (39), (46), (47) and (48). This complicates the use of experimental values of direct current, particularly since the appropriate integral for the exact electrode model (D.M.E.) is unknown. In addition, evaluation of the integral requires knowledge of the detailed $i_{\text{d.c.}}(t)$ *vs.* t relation. Thus, for systems in which such integrals appear, the use of experimentally determined direct current values does not represent a simplification of the data analysis problem.

D. Stationary electrodes

Intuitively one is led to believe that equations for a.c. polarography derived assuming a constant d.c. potential, might be applied also to a.c. polarography at stationary electrodes under conditions of linear scan d.c. potential, if the scan rate is small compared to the rate of change of alternating potential. UNDERKOFLER AND SHAIN[32] examined this problem quantitatively for the diffusion controlled a.c. polarographic wave. Their equations supported intuitive expectations as did their experimental results. They found no variation of the a.c. wave characteristics for d.c. scan rates ranging from 2–150 mV per sec with ferric ion in oxalate media. Because their equations and experiments were concerned with a reversible system, they did not consider the problem of concern here, *i.e.*, the influence of a d.c. process subject to kinetic control by rate processes in addition to diffusion. Placing the theory for a.c. polarography at stationary electrodes with linear potential scan on a quantitative basis for more complicated schemes is not difficult. If one assumes that scan rate is slow relative to alternating potential changes, a.c. polarographic wave equations may be derived for various mechanisms in the same manner as for the potentiostatic model. The assumption of slow scan rate is invoked when evaluating integrals such as

$$\int_0^t \frac{A(u)\,\sin \omega u\,\mathrm{d}u}{(\pi u)^{\frac{1}{2}}}$$

and

$$\int_0^t \frac{\mathrm{e}^{-ku}\,A(u)\,\sin \omega u\,\mathrm{d}u}{(\pi u)^{\frac{1}{2}}}$$

etc. [*e.g.*, ref. 29, eqns. (40–45)] by assuming $A(t)$ is a slowly changing function of time (slow scan rate) so that it may be factored outside the integral [*cf.*, MATSUDA[3]].

Final results for a.c. wave equations under linear scan conditions are identical in form to equations given here and in the literature[7,8,29,33] for constant d.c. potential when the functions responsive to conditions in the d.c. process are expressed in terms of $i_{d.c.}(t)$, as in eqns. (29) and (39). The term $i_{d.c.}(t)$ is the linear scan voltammetric current for the particular reaction mechanism. $E_{d.c.}$ is expressed as

$$E_{d.c.}(t) = E_i - vt \tag{51}$$

As with the potentiostatic model, deviations from equilibrium in the d.c. process can have a marked influence on the a.c. wave. Since the magnitudes of such deviations are influenced by d.c. potential scan rate, it is apparent that characteristics of the a.c. wave can be markedly affected by this variable if the d.c. process is not solely diffusion-controlled. This applies even when slow scan rate conditions as defined by UNDERKOFLER AND SHAIN are fulfilled. For the quasi-reversible case, criteria given by MATSUDA AND AYABE[34] may be invoked to determine conditions under which an a.c. wave dependent on scan rate will appear due to a non-Nernstian d.c. process. In addition to producing an a.c. wave dependent on scan rate, a kinetically influenced d.c. process at a stationary electrode introduces a dependence on electrode geometry. Arguments essentially identical to those employed above lead to the conclusion that in the a.c. wave equations for stationary electrodes, the $i_{d.c.}(t)$ term represents the direct current in linear scan voltammetry *for the particular electrode geometry employed.*

The above method of derivation and final form of equations for the a.c. polarographic wave with linear potential scan is essentially the same as given by OKAMOTO[35] for oscillographic square-wave polarography.

E. A.c. polarography at large amplitudes

We wish to re-emphasize that all equations and discussion presented apply only for small amplitudes of applied alternating potential ($\Delta E \leq 8/n$ mV). Such conditions are achieved readily. A.c. polarograms uninfluenced by electronic noise problems have been obtained with amplitudes an order of magnitude less than the approximate upper limit of $8/n$ mV[36]. If amplitudes much larger than this limit are employed, the basic conditions for the appearance of an a.c. wave influenced by electrode geometry and growth remains unchanged. However, whatever simplicity remained in the a.c. wave equations for such conditions is destroyed by application of large amplitudes. For example, when the direct current is kinetically influenced by processes other than diffusion, phase angle expressions for large amplitudes are dependent on $i_{d.c.}(t)$ and thus on electrode growth and geometry for any electrode reaction mechanism.

APPENDIX I

Notation definitions

A = electrode area.
D_i = diffusion coefficient of species i.
C_O^* = initial concentration of oxidized form.
E^o = standard redox potential in European convention.
E_i = initial potential.
$E(t)$ = instantaneous value of potential.

ΔE = amplitude of applied alternating potential.
$E_{d.c.}$ = d.c. potential.
$E_{\frac{1}{4}}^{r}$ = reversible polarographic half-wave potential.
f_i = activity coefficient of species i.
F = Faraday's constant.
R = ideal gas constant.
T = absolute temperature.
n = number of electrons transferred in heterogeneous charge transfer step.
$i_{d.c.}(t)$ = instantaneous direct faradaic current (cathodic current positive).
$I(\omega t)$ = fundamental harmonic faradaic alternating current (subscripts used to designate electrode model — see text).
θ = phase angle of fundamental harmonic alternating current relative to applied alternating potential (subscripts also used).
ω = angular frequency.
t = time.
u = auxiliary variable of integration.
s = Laplace transform variable.
k_h = apparent heterogeneous rate constant for charge transfer at E^o.
α = charge transfer coefficient.
k_1, k_2 = first-order chemical rate constants.
m = mercury flow rate.
Z_O = ionic valence of oxidized form.
$\Delta\phi_E$ = Difference of potential between the plane of closest approach and the bulk of the solution outside the diffuse double layer at potential $E_{d.c.}$.
v = scan rate.
r = distance from the center of spherical electrode.
r_o = spherical electrode radius.

APPENDIX 2

Derivation of a.c. polarographic current with diffusion to a stationary spherical electrode

For diffusion to a stationary spherical electrode and the electrode reaction

$$O + n\,e \rightleftharpoons R$$

the system of partial differential equations, initial and boundary conditions is:

$$\frac{\partial C_O}{\partial t} = D_O\left[\frac{\partial^2 C_O}{\partial r^2} + \frac{2}{r}\frac{\partial C_O}{\partial r}\right] \tag{A1}$$

$$\frac{\partial C_R}{\partial t} = D_R\left[\frac{\partial^2 C_R}{\partial r^2} + \frac{2}{r}\frac{\partial C_R}{\partial r}\right] \tag{A2}$$

$$t = 0,\ \text{any } r;\ C_O = C_O^* \tag{A3a}$$

$$C_R = 0 \tag{A3b}$$

$$t > 0,\ r \to \infty;\ C_O = C_O^* \tag{A4a}$$

$$C_R = 0 \tag{A4b}$$

$$t > 0;\ r = r_0;\ D_O \frac{\partial C_O}{\partial r} = -D_R \frac{\partial C_R}{\partial r} = \frac{i(t)}{nFA} \tag{A5}$$

This boundary value problem has been solved previously[37,38] for the surface concentrations. The results are:

$$C_{O_{r=r_O}} = C_O^* - \int_0^t \frac{i(t-u)}{nFAD_O^{\frac{1}{2}}} \left\{ \frac{1}{\sqrt{\pi u}} - D_O^{\frac{1}{2}} r_O^{-1} \, e^{D_O r_O^{-2} u} \operatorname{erfc}(D_O^{\frac{1}{2}} r_O^{-1} u^{\frac{1}{2}}) \right\} du \tag{A6}$$

$$C_{R_{r=r_O}} = \int_0^t \frac{i(t-u)}{nFAD_R^{\frac{1}{2}}} \left\{ \frac{1}{\sqrt{\pi u}} - D_R^{\frac{1}{2}} r_O^{-1} e^{D_R r_O^{-2} u} \operatorname{erfc}(D_R^{\frac{1}{2}} r_O^{-1} u^{\frac{1}{2}}) \right\} du \tag{A7}$$

Substituting eqns. (A6) and (A7) into the absolute rate expression[4]

$$\frac{i(t)}{nFAk_h} = C_{O_{r=r_O}} \exp\left\{\frac{-\alpha nF}{RT}[E(t) - E^o]\right\} - C_{R_{r=r_O}} \exp\left\{\frac{(1-\alpha)nF}{RT}[E(t) - E^o]\right\} \tag{A8}$$

where the instantaneous potential, $E(t)$, is given by eqn. (1) and employing step-by-step operations identical to those used by MATSUDA[3], one obtains the system of integral equations

$$\frac{D^{\frac{1}{2}} Q_d(t)}{k_h} = \alpha^d e^{-\alpha j} \frac{(\sin \omega t)^d}{d!} - \sum_{h=0}^{d} \left\{ \alpha^h e^{-\alpha j} \frac{(\sin \omega t)^h}{h!} \times \int_0^t Q_{d-h}(t-u) \left[\frac{1}{\sqrt{\pi u}} - D_O^{\frac{1}{2}} r_O^{-1} e^{D_O r_O^{-2} u} \operatorname{erfc}(D_O^{\frac{1}{2}} r_O^{-1} u^{\frac{1}{2}}) \right] du \right.$$

$$\left. + (-1)^h \beta^h e^{\beta j} \frac{(\sin \omega t)^h}{h!} \int_0^t Q_{d-h}(t-u) \left[\frac{1}{\sqrt{\pi u}} - D_R^{\frac{1}{2}} r_O^{-1} e^{D_R r_O^{-2} u} \operatorname{erfc}(D_R^{\frac{1}{2}} r_O^{-1} u^{\frac{1}{2}}) \right] du \right\} \tag{A9}$$

where $d = 0, 1, 2, 3 \ldots$

$$Q(t) = \frac{i(t)}{nFAC_O^* D_O^{\frac{1}{2}}} = \sum_{d=0}^{\infty} Q_d(t) \left(\frac{nF}{RT} \Delta E \right)^d \tag{A10}$$

j, D, $E_{\frac{1}{2}}^r$ and β are defined by eqns. (7), (9), (10) and (11), respectively. The significance of the system of integral equations represented by eqn. (A9) has been discussed elsewhere[29]. In the following derivation, equality of diffusion coefficients is assumed for simplicity.

The small amplitude fundamental harmonic alternating current is given by

$$I_s(\omega t) = nFAC_O^* D_O^{\frac{1}{2}} \left(\frac{nF\Delta E}{RT} \right) Q_1(t) \tag{A11}$$

[note omission of the factor $nF\Delta E/RT$ in eqn. (37) of an earlier paper[29]] where $Q_1^{(t)}$ is the solution of eqn. (A9) for $d = 1$.

$$Q_1(t) =$$

$$\frac{k_h}{D_O^{\frac{1}{2}}}\left\{F_O(t)\sin\omega t - \int_0^t Q_1(t-u)\left[\frac{1}{\sqrt{\pi u}} - D_O^{\frac{1}{2}}r_O^{-1}e^{D_O r_O^{-2}u}\operatorname{erfc}(D_O^{\frac{1}{2}}r_O^{-1}u^{\frac{1}{2}})\right]du\right\} \tag{A12}$$

where

$$F_O(t) = \alpha\, e^{-\alpha j} - (\alpha e^{-\alpha j} - \beta e^{\beta j}) \times \int_0^t Q_O(t-u)\left[\frac{1}{\sqrt{\pi u}} - D_O^{\frac{1}{2}}r_O^{-1}e^{D_O r_O^{-2}u}\operatorname{erfc}(D_O^{\frac{1}{2}}r_O^{-1}u^{\frac{1}{2}})\right]du \tag{A13}$$

The solution for $Q_O(t)$ is given in Appendix 3. The solution to eqn. (A12) contains only fundamental harmonic alternating current components and hence $Q_1^{(t)}$ has the form

$$Q_1^{(t)} = A(t)\cos\omega t + B(t)\sin\omega t \tag{A14}$$

Substituting eqn. (A14) in eqn. (A12) and making use of the trigonometric identities

$$\sin\omega(t-u) = \sin\omega t\cos\omega u - \cos\omega t\sin\omega u \tag{A15}$$

$$\cos\omega(t-u) = \cos\omega t\cos\omega u + \sin\omega t\sin\omega u \tag{A16}$$

yields an expression integrable by neglecting the slight time dependence of $A(t)$ and $B(t)$. The steady state approximation[6] ($\int_0^t = \int_0^\infty$) and the identities

$$\int_0^\infty \frac{\cos\omega u\,du}{(\pi u)^{\frac{1}{2}}} = \int_0^\infty \frac{\sin\omega u\,du}{(\pi u)^{\frac{1}{2}}} = \left(\frac{1}{2\omega}\right)^{\frac{1}{2}} \tag{A17}$$

are employed. Evaluation of the other integrals by using the convolution theorem[40] and neglecting transient terms yields

$$\int_0^t e^{D_O r_O^{-2}u}\operatorname{erfc}(D_O^{\frac{1}{2}}r_O^{-1}u^{\frac{1}{2}})\cos\omega(t-u)\,du =$$

$$\frac{1}{\omega^2 + D_O^2 r_O^{-4}}\left\{\left[\omega - \frac{\omega D_O^{\frac{1}{2}}r_O^{-1}}{(2\omega)^{\frac{1}{2}}} + \frac{D_O^{\frac{3}{2}}r_O^{-3}}{(2\omega)^{\frac{1}{2}}}\right]\sin\omega t - \left[Dr_O^{-2} - \frac{\omega D_O^{\frac{1}{2}}r_O^{-1}}{(2\omega)^{\frac{1}{2}}} - \frac{D_O^{\frac{3}{2}}r_O^{-3}}{(2\omega)^{\frac{1}{2}}}\right]\cos\omega t\right\} \tag{A18}$$

$$\int_0^t e^{D_O r_O^{-2}u}\operatorname{erfc}(D_O^{\frac{1}{2}}r_O^{-1}u^{\frac{1}{2}})\sin\omega(t-u)\,du =$$

$$\frac{1}{\omega^2 + D_O^2 r_O^{-4}}\left\{\left[\frac{D_O^{\frac{3}{2}}r_O^{-3}}{(2\omega)^{\frac{1}{2}}} + \frac{D_O^{\frac{1}{2}}r_O^{-1}\omega}{(2\omega)^{\frac{1}{2}}} - D_O r_O^{-2}\right]\sin\omega t + \left[\frac{D_O^{\frac{1}{2}}r_O^{-1}\omega}{(2\omega)^{\frac{1}{2}}} - \frac{D_O^{\frac{3}{2}}r_O^{-3}}{(2\omega)^{\frac{1}{2}}} - \omega\right]\cos\omega t\right\} \tag{A19}$$

Equating coefficients of $\sin \omega t$ and $\cos \omega t$, solving for $A(t)$ and $B(t)$ and using the identity

$$a \sin \omega t + b \cos \omega t = (a^2 + b^2)^{\frac{1}{2}} \sin\left(\omega t + \cot^{-1} \frac{a}{b}\right) \tag{A20}$$

yields for $Q_1(t)$

$$Q_1(t) = \frac{(2\omega)^{\frac{1}{2}} F_O(t)}{(e^{-\alpha j} + e^{\beta j}) \left[\left(\frac{\sqrt{2\omega}}{\lambda} + 1 - P\right)^2 + (1 - Q)^2\right]^{\frac{1}{2}}} \sin(\omega t + \theta_S) \tag{A21}$$

where

$$\theta_S = \cot^{-1}\left(\frac{\frac{\sqrt{2\omega}}{\lambda} + 1 - P}{1 - Q}\right) \tag{A22}$$

$$P = \frac{y^2}{1 + y^4} (1 - \sqrt{2y} + y^2) \tag{A23}$$

$$Q = \frac{y}{1 + y^4} (\sqrt{2} - y + y^3) \tag{A24}$$

$$y = \frac{1}{r_O}\left(\frac{D_O}{\omega}\right)^{\frac{1}{2}} \tag{A25}$$

After algebraic rearrangement of the integral equation for $Q_O(t)$ and substitution of eqn. (A21) in eqn. (A11), one obtains the result

$$I_S(\omega t) = I_{\text{rev.}} F_S(\lambda t^{\frac{1}{2}}) G_S(\omega^{\frac{1}{2}} \lambda^{-1}) \sin(\omega t + \theta_S) \tag{A26}$$

where $I_{\text{rev.}}$, $F_S(\lambda t^{\frac{1}{2}})$, $G_S(\omega^{\frac{1}{2}} \lambda^{-1})$, and θ_S are given by eqns. (3), (29), (19) and (A22), respectively.

APPENDIX 3

Derivation of the d.c polarographic current with diffusion to a stationary spherical electrode

$Q_O(t)$ is the solution to the integral equation [eqn (A9) for $d = 0$].

$$\frac{D^{\frac{1}{2}} Q_O(t)}{k_h} = e^{-\alpha j} - e^{-\alpha j} \int_0^t Q_O(t - u) \left[\frac{1}{\sqrt{\pi u}} - D_O^{\frac{1}{2}} r_O^{-1} e^{D_O r_O^{-2} u} \operatorname{erfc}(D_O^{\frac{1}{2}} r_O^{-1} u^{\frac{1}{2}})\right] du -$$

$$- e^{\beta j} \int_0^t Q_O(t - u) \left[\frac{1}{\sqrt{\pi u}} - D_R^{\frac{1}{2}} r_O^{-1} e^{D_R r_O^{-2} u} \operatorname{erfc}(D_R^{\frac{1}{2}} r_O^{-1} u^{\frac{1}{2}})\right] du \tag{A27}$$

which is expressed in Laplace transform space as

$$Q_O(s) = \frac{k_h}{D^{\frac{1}{2}}} \left\{\frac{e^{-\alpha j}}{s} - \frac{e^{-\alpha j} Q_O(s)}{s^{\frac{1}{2}} + D_O^{\frac{1}{2}} r_O^{-1}} - \frac{e^{\beta j} Q_O(s)}{s^{\frac{1}{2}} + D_R^{\frac{1}{2}} r_O^{-1}}\right\} \tag{A28}$$

Algebraic rearrangement yields

$$Q_O(s) = \frac{k_h e^{-\alpha j}}{D^{\frac{1}{2}}}\left[\frac{s + r_O^{-1}(D_O^{\frac{1}{2}} + D_R^{\frac{1}{2}})s^{\frac{1}{2}} + r_O^{-2} D_O^{\frac{1}{2}} D_R^{\frac{1}{2}})}{s(s^{\frac{1}{2}} + a)(s^{\frac{1}{2}} + b)}\right] \tag{A29}$$

where

$$2a = r_O^{-1}(D_O^{\frac{1}{2}} + D_R^{\frac{1}{2}}) + \lambda - \left\{[r_O^{-1}(D_O^{\frac{1}{2}} + D_R^{\frac{1}{2}}) + \lambda]^2 - 4\left[r_O^{-2} D_O^{\frac{1}{2}} D_R^{\frac{1}{2}} + \frac{k_h r_O^{-1}}{D^{\frac{1}{2}}}(D_R^{\frac{1}{2}} e^{-\alpha j} + D_O^{\frac{1}{2}} e^{\beta j})\right]\right\}^{\frac{1}{2}} \tag{A30}$$

$$2b = r_O^{-1}(D_O^{\frac{1}{2}} + D_R^{\frac{1}{2}}) + \lambda + \left\{[r_O^{-1}(D_O^{\frac{1}{2}} + D_R^{\frac{1}{2}}) + \lambda]^2 - 4\left[r_O^{-2} D_O^{\frac{1}{2}} D_R^{\frac{1}{2}} + \frac{k_h r_O^{-1}}{D^{\frac{1}{2}}}(D_R^{\frac{1}{2}} e^{-\alpha j} + D_O^{\frac{1}{2}} e^{\beta j})\right]\right\}^{\frac{1}{2}} \tag{A31}$$

and λ has its usual significance [eqn. (8)]. Expansion of the right side of eqn. (29) by the method of partial fractions, inverse transformation and algebraic rearrangement yields

$$Q_O(t) = \frac{k_h e^{-\alpha j}}{D^{\frac{1}{2}}}\left\{\frac{1}{a-b}\left[a - r_O^{-1}(D_O^{\frac{1}{2}} + D_R^{\frac{1}{2}}) + \frac{r_O^{-2} D_O^{\frac{1}{2}} D_R^{\frac{1}{2}}}{a}\right] e^{a^2 t} \operatorname{erfc}(at^{\frac{1}{2}}) - \frac{1}{a-b}\left[b - r_O^{-1}(D_O^{\frac{1}{2}} + D_R^{\frac{1}{2}}) + \frac{r_O^{-2} D_O^{\frac{1}{2}} D_R^{\frac{1}{2}}}{b}\right] e^{b^2 t} \operatorname{erfc}(bt^{\frac{1}{2}}) + \frac{r_O^{-2} D_O^{\frac{1}{2}} D_R^{\frac{1}{2}}}{ab}\right\} \tag{A32}$$

If equality of diffusion coefficients is assumed, eqn. (A32) simplifies to

$$Q_O(t) = \frac{k_h e^{-\alpha j}}{D_O^{\frac{1}{2}}(D_O^{\frac{1}{2}} r_O^{-1} + \lambda)} \times \left\{\lambda \exp[(D_O^{\frac{1}{2}} r_O^{-1} + \lambda)^2 t] \operatorname{erfc}[(D_O^{\frac{1}{2}} r_O^{-1} + \lambda)t^{\frac{1}{2}}] + D_O^{\frac{1}{2}} r_O^{-1}\right\} \tag{A33}$$

Substitution of eqn. (A33) in eqn. (29) gives eqn. (18).

ACKNOWLEDGEMENTS

The authors are indebted to the National Science Foundation for support of this work and to the Northwestern University Computing Center for generous donation of computer time.

SUMMARY

Theoretical reassessment of the contributions of electrode growth and geometry on the a.c. polarographic wave is given. Examination of the theory for the 'quasi-reversible' a.c. wave indicates that these factors contribute significantly when the *d.c.* process is influenced by charge transfer kinetics. Generalization of these results leads to the conclusion that growth and geometry can be important when any rate process

in addition to diffusion kinetically influences the d.c. process. If the d.c. process is diffusion-controlled or non-existent (zero direct current), theory predicts that these effects will be negligible, in agreement with earlier works of KOUTECKÝ and GERISCHER. An equation is given for the a.c. polarographic wave with a quasi-reversible process at the expanding spherical electrode. Derivation of similar exact expressions for more complex mechanisms is discussed. Implications of these results with regard to experimental approach and work with stationary electrodes are considered.

REFERENCES

1 J. KOUTECKÝ, *Collection Czech. Chem. Commun.*, 21 (1956) 433.
2 H. GERISCHER, *Z. Physik. Chem. Leipzig*, 198 (1951) 286.
3 H. MATSUDA, *Z. Elektrochem.*, 62 (1958) 977.
4 S. GLASSTONE, K. J. LAIDLER AND H. EYRING, *The Theory of Rate Processes*, McGraw-Hill, New York, 1941, pp. 575–577.
5 A. N. FRUMKIN, *Z. Elektrochem.*, 59 (1955) 807.
6 P. DELAHAY, *Advances in Electrochemistry and Electrochemical Engineering*, Vol. 1, edited by P. DELAHAY AND C. W. TOBIAS, Interscience, New York, 1961, ch. 5.
7 D. E. SMITH, *Anal. Chem.*, 36 (1964) 962.
8 H. L. HUNG AND D. E. SMITH, *Anal. Chem.*, 36 (1964) 922.
9 D. MACGILLAVRY AND E. K. RIDEAL, *Rec. Trav. Chim.*, 56 (1937) 1013.
10 P. DELAHAY, *New Instrumental Methods in Electrochemistry*, Interscience, New York, 1954, p. 74.
11 J. KOUTECKÝ AND J. ČÍŽEK, *Collection Czech. Chem. Commun.*, 21 (1956) 836.
12 B. BREYER AND H. H. BAUER, *Chemical Analysis*, Vol. 13, edited by P. J. ELVING AND I. M. KOLTHOFF, Interscience, New York, 1963, ch. 4.
13 B. BREYER AND H. H. BAUER, *ibid.*, ch. 2.
14 T. KAMBARA, *Z. Physik. Chem., Frankfurt*, 5 (1955) 52.
15 J. KŮTA AND I. SMOLER, *Advances in Polarography*, Vol. 1, edited by I. S. LONGMUIR, Pergamon, New York, 1960, pp. 350–358.
16 J. KŮTA AND I. SMOLER, *Progress in Polarography*, Vol. 1, edited by P. ZUMAN with collaboration of I. M. KOLTHOFF, Interscience, New York, 1962, ch. 3.
17 C. N. REILLEY AND W. STUMM, *Progress in Polarography*, Vol. 1, edited by P. ZUMAN, with collaboration of I. M. KOLTHOFF, Interscience, New York, 1962, ch. 3.
18 M. ISHIBASHI AND T. FUJINAGA, *Bull. Chem. Soc. Japan*, 25 (1952) 238.
19 J. KOUTECKÝ, *Collection Czech. Chem. Commun.*, 18 (1953) 311.
20 J. ČÍŽEK AND J. KOUTECKÝ, *Collection Czech. Chem. Commun.*, 28 (1963) 2808.
21 J. KOUTECKÝ AND J. ČÍŽEK, *Collection Czech. Chem. Commun.*, 21 (1956) 1063.
22 J. DELMASTRO AND D. E. SMITH, unpublished work.
23 M. SENDA, *Kagaku No Ryoiki, Zokan*, 50 (1962) 15.
24 G. H. AYLWARD, J. W. HAYES AND R. TAMAMUSHI, *Proceedings 1st Australian Conference on Electrochemistry*, edited by J. A. FRIEND AND F. GUTMANN, Pergamon Press, Oxford, 1964, in press.
25 G. H. AYLWARD, J. W. HAYES, H. L. HUNG AND D. E. SMITH, *Anal. Chem.*, 36 (1964) 2218.
26 H. MATSUDA, *Z. Elektrochem.*, 61 (1957) 489.
27 D. C. GRAHAME, *Chem. Rev.*, 41 (1947) 441.
28 R. TAMAMUSHI AND N. TANAKA, *Z. Physik. Chem., Frankfurt*, 21 (1959) 89.
29 D. E. SMITH, *Anal. Chem.*, 35 (1963) 602.
30 D. E. SMITH, unpublished work.
31 J. KOUTECKÝ AND V. HANUŠ, *Collection Czech. Chem. Commun.*, 20 (1955) 124.
32 W. L. UNDERKOFLER AND I. SHAIN, *Anal. Chem.*, 37 (1965) 218.
33 H. L. HUNG, J. R. DELMASTRO AND D. E. SMITH, *J. Electroanal. Chem.*, 7 (1964) 1.
34 H. MATSUDA AND Y. AYABE, *Z. Elektrochem.*, 59 (1955) 494.
35 K. OKAMOTO, *Bull. Chem. Soc. Japan*, 36 (1963) 1381.
36 D. E. SMITH, *Anal. Chem.*, 35 (1963) 1811.
37 P. DELAHAY AND G. MAMANTOV, *J. Am. Chem. Soc.*, 76 (1954) 5323.
38 H. D. HURWITZ, *J. Electroanal. Chem.*, 7 (1964) 368.
39 *Handbook of Chemistry and Physics*, 41st ed., edited by C. D. HODGMAN, Chemical Rubber Publishing Co., Cleveland, 1959, p. 282.
40 R. V. CHURCHILL, *Modern Operational Mathematics in Engineering*, McGraw-Hill, New York, 1944.

REDUCTION OF IODATE IN SULPHURIC MEDIUM

I. THE REDUCTION MECHANISM

PIER GIORGIO DESIDERI
Institute of Analytical Chemistry, University of Florence (Italy)
(Received October 26th, 1964)

INTRODUCTION

Previous work on the reduction mechanism of iodate ion in acid medium can be grouped on the basis of the method used in the investigation.

Chemical methods. The fundamental works by ANDREWS[1] and JAMIESON[2].

Polarographic method. The work by KOLTHOFF AND ORLEMANN[3,4], LAITINEN AND SUBCASKY[5] with a dropping mercury electrode and BADOZ AND GUILLAUME[6] with a rotating platinum electrode.

Chronopotentiometric method. OSTERYOUNG *et al.*[7,8] and ANSON[9].

Kinetic method. The review by MORGAN *et al.*[10].

The discordant results obtained by many authors have led us to undertake the present work on the reduction mechanism of the iodate ion in sulphuric acid medium. In our investigation we have used the polarographic method with solid[11] micro-electrodes as well as millicoulometric and chronopotentiometric methods.

EXPERIMENTAL

Apparatus and reagents

The polarographic measurements were made using an AME polarograph. The half-wave potentials are referred to the S.C.E. The electrolytic controlled-potential reductions were made following the millicoulometric method; the micro-electrode used in the polarographic investigation was used as an indicating electrode. A chronopotentiograph derived from a Speedmax X_1X_2 recorder was used for chronopotentiometric measurements. An Amel Corrograph Amperostat was used as a constant current source. The KIO_3 solution was prepared by dissolving accurately weighed portions of pure KIO_3 in water twice distilled from alkaline permanganate. The KI solution, obtained by dissolving the salt in de-aerated, distilled water, was standardized according to Volhard and discarded whenever it showed the slightest trace of iodine. The platinum spherule of the bubbling electrode was 2.0 mm in diameter.

RESULTS AND DISCUSSION

The polarographic characteristics of IO_3^-

The standard potential of the HIO_3/I_2 couple is + 1.19 V *vs.* N.H.E.[12]. By reducing an iodate solution in 1*M* H_2SO_4 on the bubbling platinum electrode, a well-developed reduction wave is obtained in the potential range + 0.5 to − 0.1 V *vs.* S.C.E. The half-wave potential is + 0.350 V *vs.* S.C.E. Referring this half-wave potential value to the N.H.E. instead of the S.C.E., we obtain a value of about + 0.6 V.

This value denotes that the reduction of iodate shows a remarkable overtension on a smooth platinum electrode. The IO_3^- reduction wave in sulphuric acid is critically connected with iodate concentration. Unlike other oxidant ionic species such as MnO_4^-, Ce(IV), investigated in previous studies[13,14,15] on the bubbling platinum electrode, and iodine itself, the HIO_3^- reduction wave abruptly disappears at concentrations of the electroreducible species lower than $2 \cdot 10^{-3}$ *N*, when KIO_3 in the highest degree of purity is employed. If we exclude this anomalous behaviour from the remaining discussion, the reduction process seems to be controlled by diffusion as shown by the data relative to the limiting current in relation to the changes of bubble time and temperature given in Tables 1 and 2.

The shape of polarographic wave can be observed to change. With a new platinum electrode a single polarographic wave is found; with an electrode which has been used for some time (about a week) the polarographic wave is like that shown

TABLE 1

I_d VALUES FOR $5 \cdot 10^{-3}$ *N* IO_3^- IN 1 *M* H_2SO_4, AT 25°, AT VARIOUS BUBBLE TIMES

t (sec)	I_d (μA)	*t* (sec)	I_d (μA)
2.0	77.9	4.50	59.1
2.30	75.1	4.90	56.6
2.70	72.2	5.40	53.8
3.0	68.9	6.0	51.3
3.30	66.9	6.60	48.9
3.60	64.4	7.10	48.3
4.0	62.3	7.85	46
4.30	61.9	8.50	45

TABLE 2

I_d VARIATION WITH TEMPERATURE FOR $5 \cdot 10^{-3}$ *N* IO_3^- IN 1 *M* H_2SO_4

T (°C)	I_d (μA)	*T* (°C)	*Id* (μA)
5	32.5	50	95
10	39	60	109
20	53	70	122
30	67	80	136
40	81	90	150

Temp. coeff. = 1.5% per degree.

in Fig. 1. The half-wave potential of the first step has the value of about + 0.30 to 0.35 V *vs.* S.C.E., while $E_{\frac{1}{2}}$ of the second step is at less positive potentials. The appearance of the double wave can be explained by a slow but progressive change of the surface of the platinum electrode. This change is due to the absorption of I_2 on the

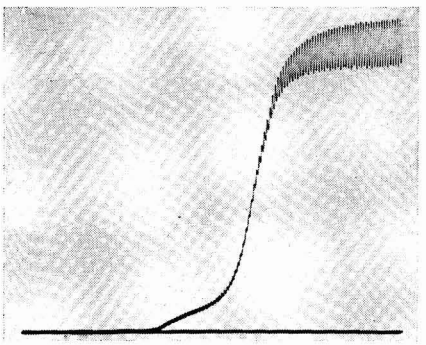

Fig. 1. Polarographic wave of $5 \cdot 10^{-3} N$ IO_3^- in 1 *M* H_2SO_4. The electrode had been used for a week.

surface of the electrode. Using a platinum electrode which had been plunged into hot iodine solution for a time (10–20 min), we obtained a wave like that shown in Fig. 1. HI, however, has no effect. The I_2 which has been absorbed by the electrode during the iodate reduction process can be eliminated by physical treatment (*e.g.*, a prolonged treatment of the electrode in hot water); after continued use, the electrode requires a treatment by chemical cleansing with strong or electrochemical oxidants.

The influence of I_2 on the reduction of HIO_3

The formation of I_2 on the electrode surface during the iodate reduction and its influence on the reduction process has suggested the extension of the investigation to iodate–iodine mixtures.

Iodate–iodine mixtures were obtained by adding to measured amounts of iodic acid solution increasing quantities of iodine. The behaviour of $E_{\frac{1}{2}}$ and I_d as C_{I_2} increases is shown in Figs. 2 and 3.

It can be seen that:

(a) for $C_{I_2} = 2.4 \cdot 10^{-4} N$, the double wave disappears;

(b) when iodide increases, the half-wave potential of the two waves gradually increases until a single wave appears.

Its $E_{\frac{1}{2}}$ progressively shifts towards more positive values till it reaches and exceeds, when $C_{I_2} = 1.2 \cdot 10^{-3} N$, the half-wave potential of a iodine solution having the same concentration.

The presence of I_2 in the solution can condition the iodate reduction process. We have seen that the iodate polarographic wave disappears for $C_{IO_3^-} < 2 \cdot 10^{-3} N$;

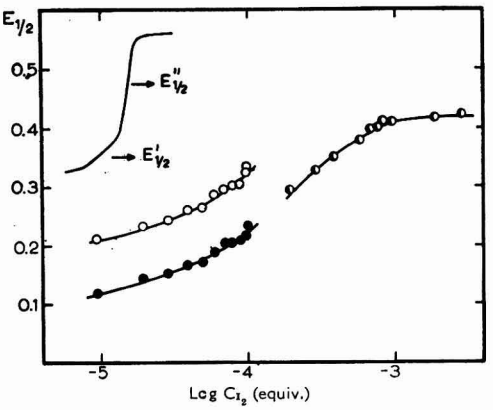

Fig. 2. Change in $E_{\frac{1}{2}}$ of the two steps as C_{I_2} increases; $5 \cdot 10^{-3} N$ IO_3^- in 1 M H_2SO_4. ○, $E'_{\frac{1}{2}}$; ●, $E''_{\frac{1}{2}}$; ◐, $E_{\frac{1}{2}}$ of single wave.

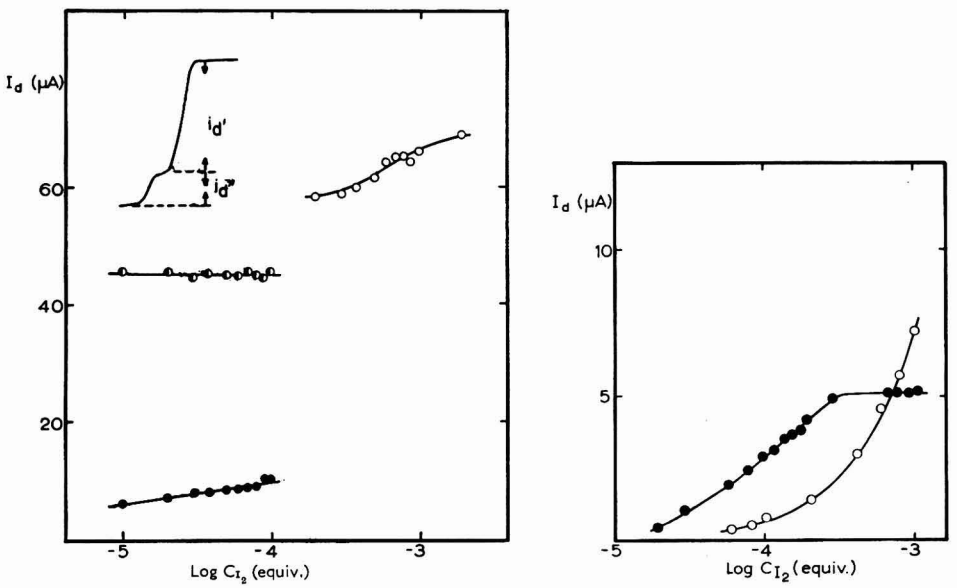

Fig. 3. Change in I_d of the two steps as C_{I^-} increases; $5 \cdot 10^{-3} N$ IO_3^- in 1 M H_2SO_4. ●, i_d''; ◐, i_d'; ○, i_d of single wave.

Fig. 4. Change in I_d as C_{I^-} increases: ●, $5 \cdot 10^{-4} N$ IO_3^-; ○, I_2.

in the presence of iodine we obtain well-developed waves for $C_{IO_3^-}$ up to $5 \cdot 10^{-4} N$, see Fig. 4 where the values of the diffusion current of solutions of equal iodine concentration are compared.

Iodine, added to iodate solution in such a quantity that the wave appears, is not able to give, by itself, an appreciable wave. Further additions of iodine lead to an increase of the wave height which is always greater than the corresponding heights obtained from solutions of equal iodine concentration.

From the data presented it follows that iodate reduction at the electrode occurs through the I_2/I^- system, probably *via* the following mechanism:

$$I_2 + 2e \rightleftharpoons 2I^- \quad (1)$$

$$HIO_3 + 5\,I^- + 5\,H^+ \rightleftharpoons 3\,I_2 + 3\,H_2O \quad (2)$$

To confirm the role of the I_2/I^- system in the iodate reduction, we tried to trap the iodide ion in order to prevent reaction (2). Among the ionic species able to bind the iodide ion, thallous and mercuric ions appeared to be the most suitable.

The influence of Tl(I) and Hg(II) on the reduction of HIO_3

By adding thallous ions to a $5 \cdot 10^{-3}$ *N* KIO_3 solution in 1 *M* H_2SO_4, for thallium concentrations between $3 \cdot 10^{-3}$ *N* and $5 \cdot 10^{-3}$ *N* we obtain a lowering of the wave up to a maximum of 70%. The reduction process is complicated by the appearance of current maxima due to a modification of the electrode surface by forming of a film of TlI.

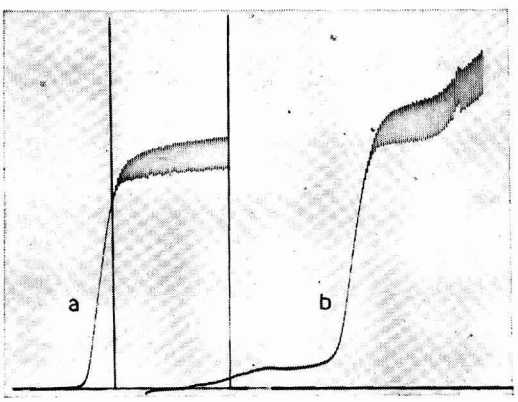

Fig. 5. Polarographic waves in 1*M* H_2SO_4 of: (a), $5 \cdot 10^{-3}N$ IO_3^-; (b) $5 \cdot 10^{-3}N$ IO_3^- + $1 \cdot 10^{-4}M$ Hg^{2+}. Abscissa, +0.3 V *vs.* S.C.E.

The influence of the addition of mercuric ions is shown in Fig. 5. When the Hg(II) concentration is equal to or greater than $1 \cdot 10^{-4}M$ the iodate wave is shifted 0.4 V towards more negative potentials. It should be noted that the wave does not develop until the electrode has reached the reduction potential of the iodomercuric complex, *i.e.*, the potential corresponding to the reappearance of iodide ions in the diffusion layer.

The influence of sulphuric acid concentration

As $C_{H_2SO_4}$ increases the diffusion current and half-wave potential reach maximum values which, for I_d (Fig. 6) is at 1*M* H_2SO_4, and for $E_{\frac{1}{2}}$ is at 3*M* H_2SO_4 (Fig.

7). For acid concentrations greater than $3M$ the wave divides into two steps (Fig. 8) of which the one with the less positive potential is smaller and badly defined. In Table 3 are given the heights of both waves and the percentage which the smaller step contributes to the total of both. From this data the following conclusions can be drawn.

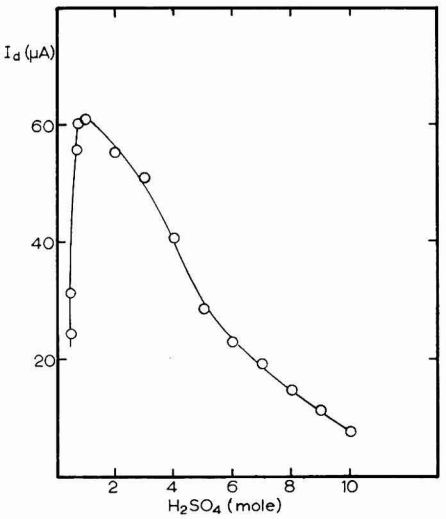

Fig. 6. Change in I_d as $C_{H_2SO_4}$ increases.

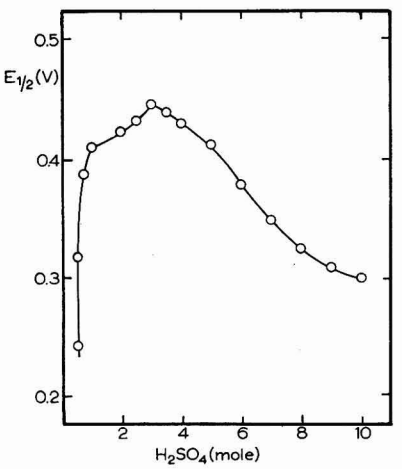

Fig. 7. Change in half-wave potential as $C_{H_2SO_4}$ increases.

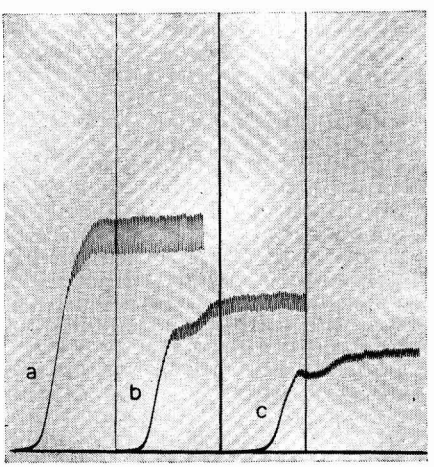

Fig. 8. Polarographic waves of $5 \cdot 10^{-3} N$ IO_3^-: (a), in $1M$; (b), in $3M$; (c), in $5M$ H_2SO_4.

TABLE 3

$E_{\frac{1}{2}}$, I_d, I_{d_1} AND I_{d_2} VALUES FOR $5 \cdot 10^{-3}$ N IO_3^- AS ACID CONCENTRATION INCREASES, AT 25°

$C_{H_2SO_4}$ (M)	$E_{\frac{1}{2}}$ (V)	$I_{d\,tot.}$ (μA)	I_{d_1} (μA)	I_{d_2} (μA)	$100\ I_{d_2} / I_{d\,tot.}$
0.75	+0.385	60	—	—	—
1	+0.410	57.4	—	—	—
2	+0.422	55.7	—	—	—
3	+0.446	47.5	—	—	—
4	+0.431	38.1	32.1	6	15.8
5	+0.412	32.3	25.9	6.35	20.1
6	+0.378	24.55	20.3	4.25	17.4
7	+0.346	20.5	16.05	4	19.5
8	+0.323	16.95	12.7	4.25	25
9	+0.307	14.85	9.9	4.95	33.4
10	+0.294	9.45	5.95	3.55	37.5

(a) From the values of protonic activity of sulphuric acid given in the literature[16] and from the values of K_a for HIO_3, which according to various authors can vary from 0.15 to 0.20, is clear that the larger diffusion current corresponds to a concentration at which we can expect that all the iodate is present as HIO_3. It is excluded that the diffusion current behaviour depends on a change in ionic strength, as well as on the acidity; measurements made at constant ionic strength using H_2SO_4 and Na_2SO_4 mixtures reproduce the behaviour in Fig. 6.

(b) As the I_2/I^- system is independent of the acidity of medium, it is evident that the electrode reaction is conditioned by the iodic acid, the behaviour of which is well known when the protonic activity changes. The shifts of $E_{\frac{1}{2}}$ towards less positive values, after the maximum value, is to be related with the reduction of ionic species more complex than HIO_3.

(c) The appearance of a double reduction process for $C_{H_2SO_4} > 3\ M$ can be related with the presence of polymeric and solvated species of HIO_3. These complex species have been recently discovered by GILLESPIE AND SENIOR[17].

Controlled-potential reduction

Considering the irreversible behaviour of iodic acid reduction, in order to clarify the reduction mechanism, especially in the high protonic activity solutions, we used the controlled-potential reduction method. We used the millicoulometry method which allows us to keep the conditions of the polarographic experiment unchanged and to have data strictly comparable with those obtained by the polarographic method.

The electrolytic reductions at controlled potential have been carried out in solutions of constant concentration of IO_3^- and of variable concentration of H_2SO_4. Reducing these solutions at -0.2V *vs.* S.C.E. and for $C_{H_2SO_4} > 3M$ also at $+$ 0.3 V *vs.* S.C.E., we obtained the data given in Table 4. The extrapolated value for $C_{IO_3^-} = 0$ of the single reductions is in very good agreement with the value of 0.82 C for a 5-electron reduction. Considering that at -0.2 V *vs.* S.C.E. we are at the reduction potential of the I_2/I^- couple, the 5-electron value for HIO_3 reduction confirms that

TABLE 4

CONTROLLED-POTENTIAL COULOMETRY ON 2 ml OF $5 \cdot 10^{-3}$ IO_3^- IN H_2SO_4, AT 25°

1 M H_2SO_4 E = −0.2 V vs. S.C.E.		*3 M H_2SO_4 E = −0.2 V vs. S.C.E.*		*5 M H_2SO_4 E = −0.2 V vs. S.C.E.*		*3 M H_2SO_4 E = +0.3 V vs. S.C.E.*		*5 M H_2SO_4 E = +0.3 V vs. S.C.E.*	
KIO_3 (%)	*Coulomb No.*	*KIO_3 (%)*	*Coulomb No.*	*KIO_3 (%)*	*Coulomb No.*	*KIO_3 (%)*	*Coulomb No.*	*KIO_3 (%)*	*Coulomb No.*
100	0	100	0	100	0	100	0	100	0
93.8	0.0464	95.7	0.042	96.2	0.0302	94.3	0.0352	97.7	0.0245
88.5	0.090	90.7	0.082	92.7	0.0592	91.4	0.069	94.5	0.048
84.3	0.131	85.7	0.120	89.4	0.087	87.9	0.101	91.5	0.0714
79.2	0.1708	82	0.155	85.8	0.104	85	0.132	89.6	0.094
75.1	0.2078	77.7	0.190	82.9	0.130	80.5	0.163	86.5	0.116
70.3	0.241	73.8	0.222	80.3	0.155	77.5	0.192	84.6	0.137
66.3	0.275	69.8	0.253	77.5	0.179	73	0.219	81.5	0.158
62.2	0.306	65.7	0.282	74.6	0.202	72.5	0.245	79	0.178
58.7	0.335	62.2	0.309	72	0.225	63.8	0.300	77.2	0.197
51.2	0.400	57	0.355	65	0.285	55	0.38	70.5	0.25
		50.5	0.405	56.8	0.340			61.5	0.32
				52	0.382			53	0.402
0*	0.815	0	0.83	0	0.805	0	0.84	0	0.86

* extrapolate values for $C_{IO_3^-} = 0$

the electrode process is the one given by the scheme:

$$HIO_3 + 6e + 5H^+ \rightleftharpoons I^- + 3H_2O \qquad (1)$$

$$\tfrac{1}{5}\, HIO_3 + I^- + H^+ \rightleftharpoons \tfrac{3}{5}\, I_2 + \tfrac{3}{5}\, H_2O \qquad (2)$$

i.e. for every 1.2 moles of reduced HIO_3 we have a current transfer in the cell corresponding to 6 electrons, equal to 5 electrons/mole.

Considering the iodine which appears in equilibrium (2) and that the I_2 reduction is complete at −0.2 V *vs.* S.C.E., the total electronic balance reaches 6 electrons/mole as we should logically expect. It is evident that in the electrode process I_2 behaves as if it were not reduced because the I_2 formed is always completely reoxidized by the iodate.

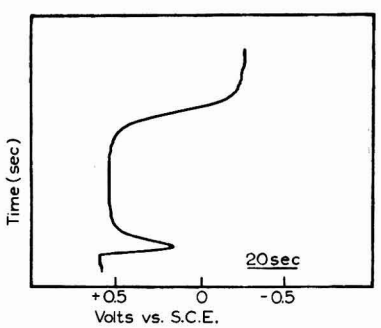

Fig. 9. Chronopotentiogram of $5 \cdot 10^{-3} N$ IO_3^- in $1M$ H_2SO_4.

The value of 5 electrons shows that both a primary electrochemical process (eqn. 1) and a chemical process (eqn. 2), contribute to the HIO_3 reduction. The reduction values at + 0.3 V *vs.* S.C.E., *i.e.*, on the first step of the double wave which appears for $C_{H_2SO_4} \geqslant 3$ *M*, are equal to those found for the same solution at −0.2 V *vs.* S.C.E., and confirm that the double wave does not represent different stages in the reduction of the iodate but it is due to the presence in solution of polymeric or solvated species of the iodate itself which are reduced at different potentials.

Chronopotentiometric measurements

The chronopotentiogram obtained from a $5 \cdot 10^{-3}$ *N* IO_3^- in 1 *M* H_2SO_4 solution is shown in Fig. 10; it is the same as the one reported by ANSON[9]. According to ANSON, the unusual chronopotentiogram can be explained as follows. At the beginning of the electrolysis the iodate is reduced to iodide ion. The iodide reacts with the iodate forming iodine. When the I_2 concentration at the electrode reaches a certain value, the prevailling reaction at the electrode becomes the I_2 to I^- reduction.

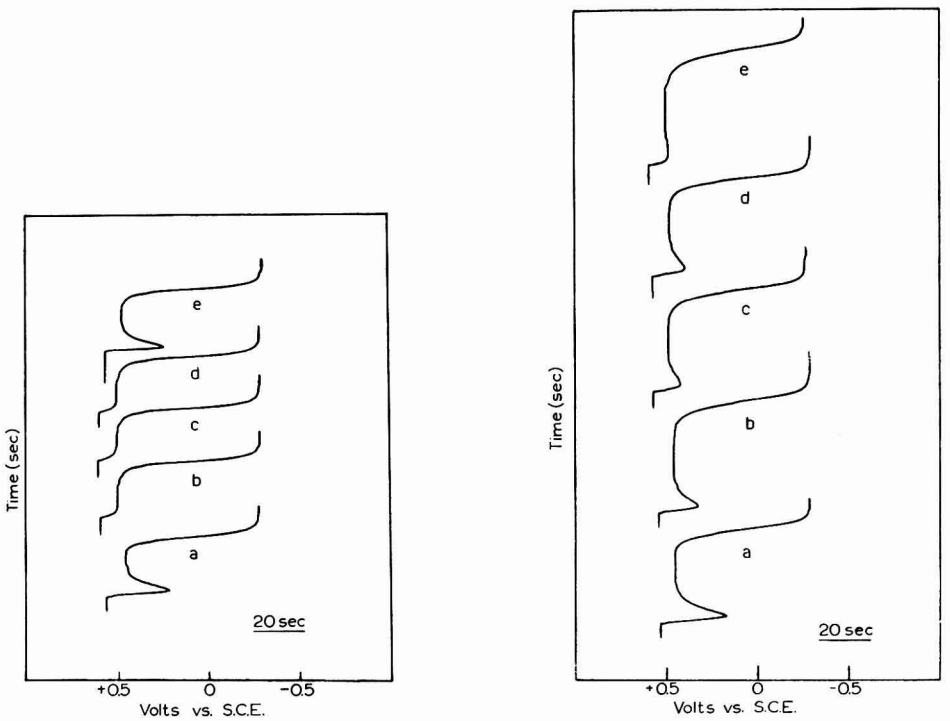

Fig. 10. Chronopotentiograms of $5 \cdot 10^{-3}N$ IO_3^- in 1*M* H_2SO_4: (a), fresh solution; (b), successive recording without agitation; (c), *idem*; (d), *idem*; (e), recorded after agitation for 30 sec.

Fig. 11. Influence of I^- on $5 \cdot 10^{-3}N$ IO_3^- in 1*M* H_2SO_4 at the following concentrations: (a), $1 \cdot 10^{-6}N$; (b), $1 \cdot 10^{-5}N$; (c), $2 \cdot 10^{-5}N$; (d), $4 \cdot 10^{-5}N$; (e), $6 \cdot 10^{-5}N$.

This second reduction takes place at potentials more positive than the preceding one and therefore the electrode potential present a peak. This interpretation which agrees with our polarographic and coulometric data is confirmed by the following experiments which give evidence for the formation of a I_2 layer around the electrode during the iodate reduction.

Making successive recordings on the same solution without renewing the diffusion layer by shaking we find:

(a) disappearance of the peak;

(b) no change of the transition time;

(c) no change of starting potential in the chronopotentiograms following the first;

(d) It is, however, evident (i) that after every recording a quantity of I_2, reconstitutes itself around the electrode and (ii) that the iodine functions as catalyst in iodate reduction and that the iodine formation occurs at the level of the diffusion layer. We have but to renew the diffusion layer by shaking, to obtain the original chronopotentiogram from the iodate solution.

A further confirmation of the role that the I_2/I^- system plays in the iodate reduction are the chronopotentiograms shown in Fig. 11 obtained from the iodate–iodine mixtures. Adding I_2 in solution, we notice a gradual diminution of the peak at less positive potentials and its disappearance for an iodine concentration equal to 1.2×10^{-4} M.

CONCLUSIONS

We can draw the following conclusions from the experimental data. Iodic acid is not directly reduced on a platinum electrode but with a very high overtension. The reduction is strongly catalyzed by traces of I_2, on account of the fact that the presence of the latter allows the substitution of the slow direct reduction with two fast reactions: one of them occurs at the electrode surface (I_2/I^-), the other in the solution (I^-/IO_3^-). It is evident that the iodate has a considerable inertness to direct reduction; such inertness has been revealed chemically in normal titrations, where as a rule we add to the iodate solution to be titrated a small quantity of iodine, so that the iodate may be used as an oxidant.

SUMMARY

The iodic acid reduction in sulphuric medium on platinum micro-electrodes has been studied by polarographic, coulometric and chronopotentiometric methods. The influence of iodide ions, sulphuric acid protonic activity and of ligands of I^-, such as Tl(I) and Hg(II) on the reduction process has been extensively investigated. It is demonstrated that the iodate is not directly reduced but with a very high overtension and that reduction is strongly catalyzed by traces of I_2.

REFERENCES

1 L. W. ANDREWS, *J. Am. Chem. Soc.*, 25 (1903) 756.
2 G. S. JAMIESON, *Volumetric Iodate Methods*, Reinhold Publishing Corporation, New York, 1926.
3 I. M. KOLTHOFF AND J. G. ORLEMANN, *J. Am. Chem. Soc.*, 64 (1942) 1044.

4 I. M. KOLTHOFF AND J. G. ORLEMANN, *J. Am. Chem. Soc.*, 64 (1942) 1970.
5 H. A. LAITINEN AND J. W. SUBCASKY, *J. Am. Chem. Soc.*, 80 (1958) 2653.
6 J. BADOZ AND C. GUILLAUME, *Advances in Polarography*, Vol. I, Pergamon Press, London, 1960, pp. 299–312.
7 R. A. OSTERYOUNG, *Anal. Chem.*, 35 (1963) 1100.
8 R. A. OSTERYOUNG and F. C. ANSON, *Anal. Chem.*, 36 (1964) 975.
9 F. C. ANSON, *J. Am. Chem. Soc.*, 81 (1959) 1554.
10 J. K. MORGAN, G. M. PEARD AND F. C. CULLIS, *J. Chem. Soc.*, (1951) 1865.
11 D. COZZI AND P. G. DESIDERI, *J. Electroanal. Chem.*, 4 (1960) 301; D. COZZI, G. RASPI AND L. NUCCI, *J. Electroanal. Chem.*, 6 (1963) 267, 275.
12 G. CHARLOT, *Selected Constants—Oxydo–Reduction Potentials*, Pergamon Press, New York, 1958.
13 P. G. DESIDERI, *J. Electroanal. Chem.*, 2 (1961) 39.
14 P. G. DESIDERI, *J. Electroanal. Chem.*, 4 (1962) 359.
15 P. G. DESIDERI, *J. Electroanal. Chem.*, 6 (1963) 344.
16 H. S. HARNED AND J. W. HAMER, *J. Am. Chem. Soc.*, 27 (1935) 57.
17 R. J. GILLESPIE AND J. B. SENIOR, *Inorg. Chem.*, 3 (1964) 440.

REDUCTION OF IODATE IN SULPHURIC MEDIUM

II*. THE INFLUENCE OF THE SURFACE OF THE PLATINUM ELECTRODE

PIER GIORGIO DESIDERI
Institute of Analytical Chemistry, University of Florence (Italy)
(Received November 9th, 1964)

INTRODUCTION

In a previous study[1] on iodate reduction in sulphuric acid it was observed that the platinum electrode can absorb iodine and as a consequence of this is able gradually to modify its response. This phenomenon, which can be included in the more general case of the behaviour of solid electrodes depending on the state of the surface, has prompted us to re-examine the iodate reduction process on a platinum electrode superficially modified so that its variations with respect to an untreated electrode may be recorded. Polarographic and chronopotentiometric methods have been used in the investigation.

EXPERIMENTAL

Reagents and apparatus

Reagents and apparatus have been described in a previous study[1].

RESULTS AND DISCUSSION

Electrode pre-treatments

Before every recording the electrode was treated in one of the following ways.

Oxidation. The electrode was made an anode in 1 M H_2SO_4, for various times, with a current density of 320 mA/cm^2.

Cleaning. The electrode previously oxidized under the conditions described above was treated with HI freshly prepared from KI and H_2SO_4, according to ANSON[2].

Reduction. The electrode was made a cathode in 1 M H_2SO_4, with a current density of 320 mA/cm^2, for various times.

The terms "oxidized", "cleaned" and "reduced" refer to the treatments (described above) undergone by the electrode before use.

* Part I, see ref. 1.

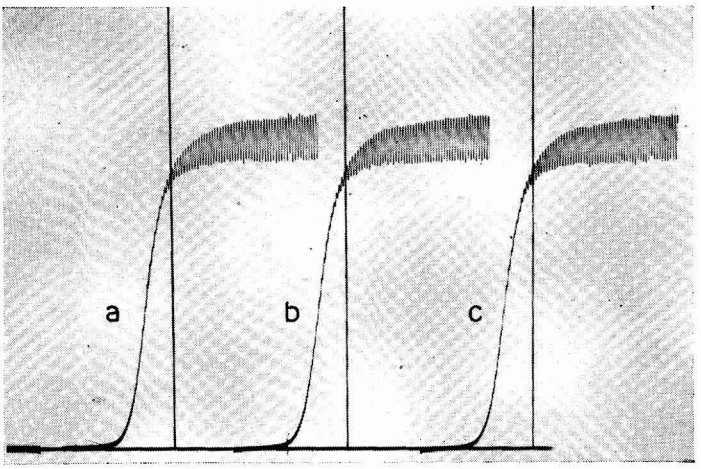

Fig. 1. Polarograms of 0.005 N IO_3^- in 1 M H_2SO_4 on the electrode "reduced" for: (a), 1 min; (b), 5 min; (c), 25 min.

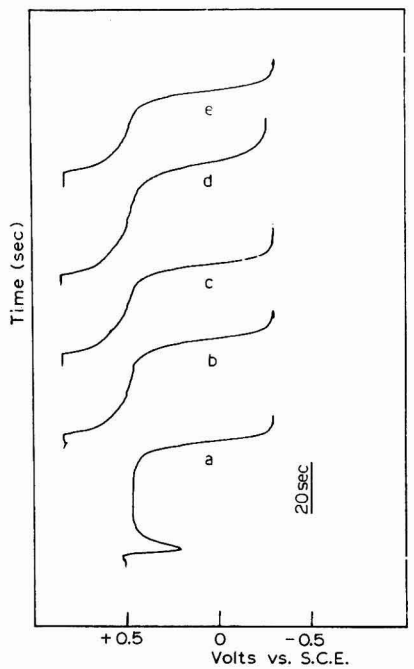

Fig. 2. Chronopotentiograms of 0.005 N IO_3^- in 1 M H_2SO_4 on electrode "reduced" for: (a), 2 min; (b), 4 min; (c), 8 min; (d), 16 min; (e), 32 min.

Effect of treatment time

Reduction. Current–potential curves (Fig. 1) do not show any appreciable variations even for rather long electrode reduction times. The chronopotentiograms

TABLE 1

$E°$, $E_{\tau/4}$ AND τ AS REDUCTION TIME INCREASES KIO_3, 0.005 N IN 1 M H_2SO_4; $i = 6 \cdot 10^{-5}$ A.

Reduction time (min)	*E° (V)*	$E_{\tau/4}$ *(V)*	τ *(sec)*
2	+0.515	+0.460	40
4	+0.815	+0.525	30
8	+0.815	+0.540	30
16	+0.815	+0.575	30.4
32	+0.815	+0.575	20.5
60	+0.815	+0.575	15.5

(Fig. 2), however, show a considerable change of electrode response as treatment time varies. The chronopotentiogram which presents a maximum towards less positive potentials and another towards positive potentials (curve a) as already described by ANSON[3], is obtained for short times. This is characteristic of a "new" platinum electrode and of the "cleaned" electrode. For times longer than 3 min normal-type chronopotentiograms are obtained. The data given in Table I show that both the starting potential and $E_{\tau/4}$ reach a constant value only after treatment for 15 min.

Oxidation. The treatment time has not sensible influence on the electrode response, see the polarograms in Fig. 3 and the time–current curve in Fig. 4. It should be noted, however, that an "oxidized" electrode, even for a very short treatment time, never gives the chronopotentiogram with less positive and more positive maxima, recorded both on the "cleaned" electrode and on the "reduced" electrode for times shorter than 3 min.

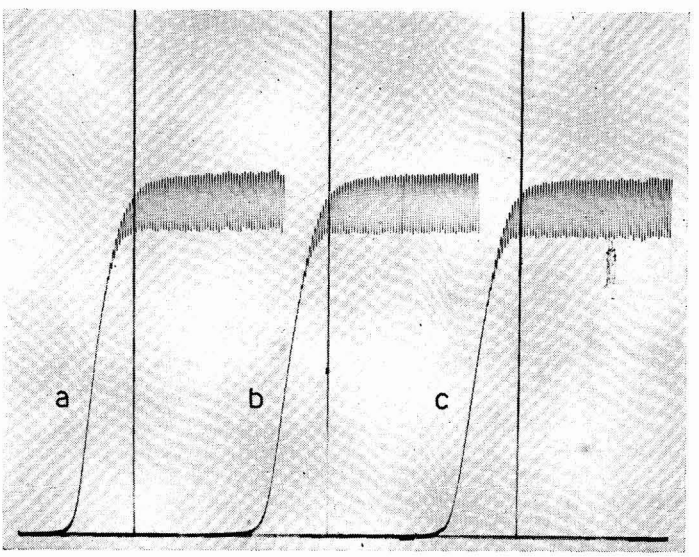

Fig. 3. Polarograms of 0.005 N IO_3^- in 1 M H_2SO_4 on electrode "oxidized" for: (a), 1 min; (b), 5 min; (c), 25 min.

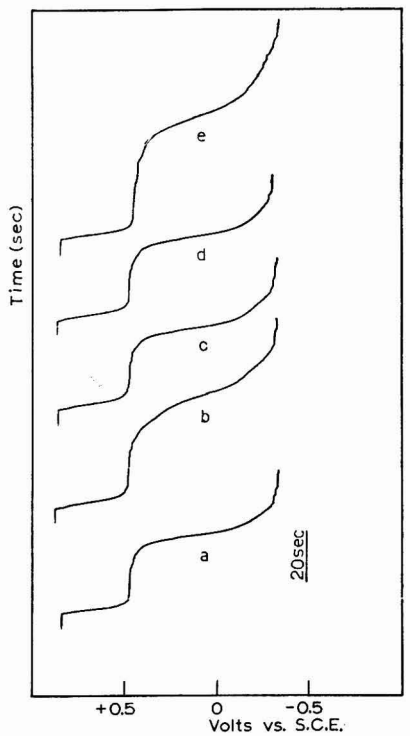

Fig. 4. Chronopotentiograms obtained from 0.005 N IO_3^- in 1 M H_2SO_4 on electrode "oxidized" for: (a), 2 min; (b), 4 min; (c), 8 min; (d), 16 min; (e), 32 min.

TABLE 2

E°, $E_{\tau/4}$ AND τ AS OXIDATION TIME INCREASES

KIO_3 0.005 N in 1 M H_2SO_4; $i = 6 \cdot 10^{-5}$ A.

Oxidation time (min)	E° *(V)*	$E_{\tau/4}$ *(V)*	τ *(sec)*
2	+0.825	+0.465	20.4
4	+0.855	+0.465	26
8	+0.855	+0.465	20.5
16	+0.855	+0.465	20.5
32	+0.855	+0.465	30.4
60	+0.855	+0.465	33.6

The data in Table 2 show that with an "oxidized" electrode the starting potential changes towards more positive values as the treatment time increases, until it reaches a constant value after 4 min. In contrast to the behaviour with the "reduced" electrode, $E_{\tau/4}$ has a constant value after very short treatment times.

As a result of these data the oxidation and reduction of the electrode before use has been protracted for 15 min.

Effect of IO_3^- concentration

The variations in diffusion current as the iodate concentration changes are shown in Fig. 5. They were obtained on "oxidized", "reduced" and "cleaned" electrodes. For a "cleaned" electrode the wave disappears for $C_{IO_3^-} < 0.002$ N, as with a "new" electrode. On a "reduced" electrode the wave is still well-developed for $C_{IO_3^-} = 0.001$ N and on an "oxidized" electrode the sensitivity reaches $C_{IO_3^-} = 0.0005$ N.

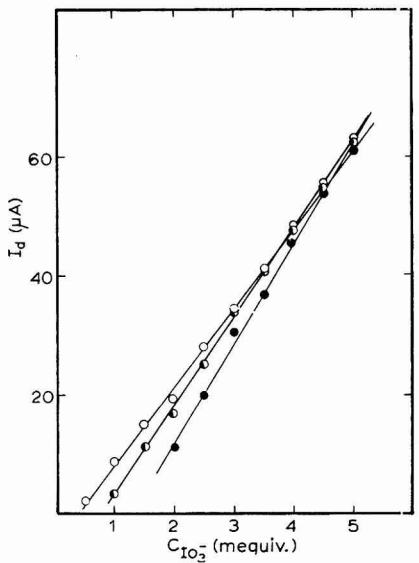

Fig. 5. Variation of I_d as $C_{IO_3^-}$ varies: ○, oxidized electrode; ◑, reduced electrode; ●, cleaned electrode.

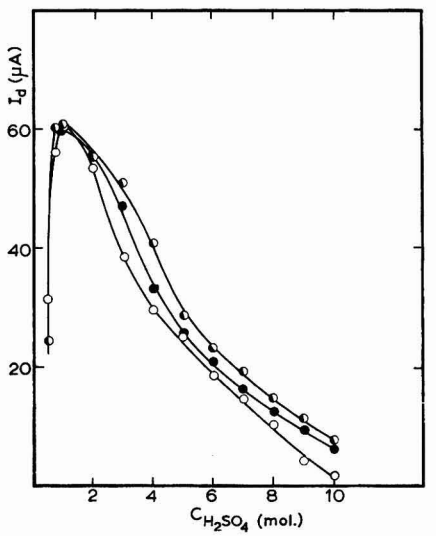

Fig. 6. Variation of I_d as $C_{H_2SO_4}$ increases: ○, oxidized electrode; ●, reduced electrode; ◑, cleaned electrode.

TABLE 3

WAVE SLOPE ON A PRE-TREATED ELECTRODE AS $C_{IO_3^-}$ INCREASES

$C_{IO_3^-}$ (mequiv.)	∂E (mV) / $\partial \log i/(i_d - i)$		
	1	2	3
1	29	—	—
2	19	28.5	38.5
3	12	17	28
4	11	15.5	24
5	9	12	18.5
6	8	10	16

(1) oxidized electrode; (2) reduced electrode; (3) polished electrode.

In a previous study[1] we had noted that the lowest iodate concentration at which a polarographic wave could be obtained was considerably lowered by adding to the solution a very small quantity of iodine; it is, however, evident that on "oxidized" and "reduced" electrodes the modification of the electrode surface favours iodine formation and consequently the catalyzed reaction of iodate. The variation in the slope of the polarographic wave is very interesting since it indicates the different speeds at which the reduction process takes place depending on the superficial state of the electrode (Table 3).

For any one electrode the slope varies gradually as the iodate concentration changes; the behaviour is similar after various treatments (oxidation, reduction and cleaning) but different in absolute value. The slope value increases in the order "oxidized", "reduced", "cleaned".

Effect of sulphuric acid concentration

It can be seen from Fig. 6 that the diffusion current when $C_{H_2SO_4}$ changes is a maximum for $C_{H_2SO_4} = 1\ M$. This is true for all three types of electrode. It is, however, evident that the presence of a maximum for I_d is connected with the total transformation of iodate into iodic acid, as shown in a previous study.

Also the division of the wave into two steps for $C_{H_2SO_4} \geqslant 3\ M$ is shown in an almost equal measure by the three electrodes (Table 4).

TABLE 4

I_d, I_{d_1} AND I_{d_2} ON THE PRE-TREATED ELECTRODE AS $C_{H_2SO_4}$ CHANGES

	Ox. electrode			*Red. electrode*			*Pol. electrode*		
$C_{H_2SO_4}$ (*M*)	I_d (μA)	I_{d_1} (μA)	I_{d_2} (μA)	I_d (μA)	I_{d_1} (μA)	I_{d_2} (μA)	I_d (μA)	I_{d_1} (μA)	I_{d_2} (μA)
1	61	—	—	61	—	—	57.4	—	—
2	53.3	—	—	55.6	—	—	55.7	—	—
3	45.28	38.2	7.28	51	—	—	47.5	—	—
4	36.5	29.4	7.1	48	40	8	38.1	32.1	6
5	35.35	27.1	8.1	31	25.6	5.4	32.3	25.9	6.35
6	24.95	18.85	6.1	24.5	21.2	3.3	24.55	20.3	4.25
7	17.95	14.15	3.8	18.04	14.5	3.54	20.5	16.5	4
8	13	10	3	13.77	12	1.77	16.95	12.7	4.25
9	7.02	4.22	2.8	11.35	8.85	2.5	14.85	9.9	4.95
10	5.64	3.54	2.1	8.75	6.55	2.5	9.45	5.95	3.55

I_d total I_d; I_{d_1}, I_d of the first step; I_{d_2}, I_d of second step.

The three electrodes differ, however, in the behaviour of their half-wave potential with increase in $C_{H_2SO_4}$ (see fig. 7). In all cases $E_{\frac{1}{2}}$ shifts towards more positive values as the protonic activity increases and is a maximum at a definite acidity which is different according to the treatments which the electrode has undergone. The maximum value of the half-wave potential for "cleaned", "reduced" and "oxidized" electrodes is obtained at 3, 4 and 5 *M* H_2SO_4 respectively.

Effect of iodine on the HIO_3 reduction

In the presence of iodine the differences between the three electrodes tend to vanish. For $C_{I_2} = 1 \cdot 10^{-4}$ N, both polarographically and chronopotentiometrically the electrode has a response which is independent of the treatment which it has undergone. This confirms the role of the I_2/I^- system in the iodate reduction and shows clearly that the influence of the surface of the electrode on the reduction process is limited with the initial stage of the process, *i.e.*, with the formation of iodine in the diffusion layer.

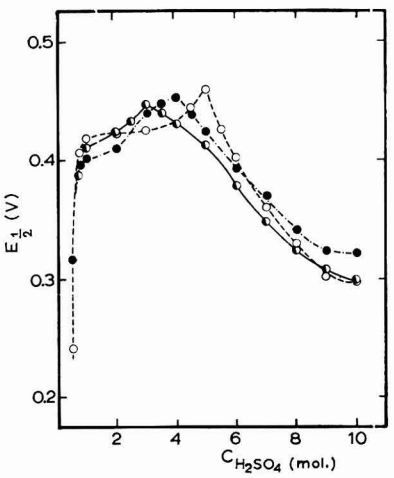

Fig. 7. Variation of half-wave potential as $C_{H_2SO_4}$ increases: ○, oxidized electrode; ●, reduced electrode; ◑, cleaned electrode.

CONCLUSIONS

From the data given above it follows that the iodate reduction occurs in two stages: the first, electrochemical; the second, chemical through the I_2/I^- system. The surface of the electrode affects only the first reduction stage. The differences recorded polarographically concern almost exclusively the reduction speed (wave slope) while considerable variations have been noted chronopotentiometrically. In this case, contrary to what has been stated by ANSON[3], the electrode treatment entirely modifies the chronopotentiogram behaviour.

The influence of surface state of electrode on the first reduction stage is different for the electrodes differently treated (oxidized, reduced, cleaned); the rate of the iodate reduction process decreases passing from the oxidized to the reduced electrode and from this to the cleaned one.

SUMMARY

Iodic acid reduction on platinum micro-electrodes was studied with polarographic and chronopotentiometric methods with reference to the surface state of the electrodes. Treatment and treatment time of the electrodes and influence of sulphuric acidity, iodic acid concentration and iodine on the reduction process, were investigated. It is shown that the modification of the surface state of the electrode influences only the first stage of the reduction process. The role of the I_2/I^- system in the iodic acid reduction is confirmed.

REFERENCES

1 P. G. DESIDERI, *J. Electroanal. Chem.*, 9 (1965) 000.
2 F. C. ANSON, *Anal. Chem.*, 33 (1961) 934.
3 F. C. ANSON, *J. Am. Chem. Soc.*, 81 (1959) 1554.

THE ELECTRICAL DOUBLE LAYER ON INDIUM AMALGAMS IN 0.1 *M* $HClO_4$ AT 25°

JAMES N. BUTLER, MARY L. MEEHAN AND A. C. MAKRIDES
Tyco Laboratories Inc., Bear Hill, Waltham 54, Massachusetts (U.S.A.)
(Received October 12th, 1964)

I. INTRODUCTION

Although the electrical double layer on mercury has been extensively studied[1-9], very little reliable information has been obtained concerning alloy systems. The indium–mercury system is ideal for studying the influence of electrode composition on electrical double-layer structure, for a number of reasons. First, liquid amalgams containing up to 70% In can be prepared at room temperature[10-14], which permits the use of a dropping electrode to provide a clean, reproducible surface for measurement. Second, the zero-charge potential of indium amalgams lies well within the region where the electrode is ideally polarized; therefore the zero-charge potential can be determined accurately by the streaming electrode method and the capacity can then be integrated to find surface charge and interfacial tension. Third, the difference in chemical properties of indium and mercury provides the possibility of a strong effect of electrode composition on specific adsorption of ions and neutral molecules in the double layer.

Although a few measurements of double-layer capacity on thallium amalgams have been reported[15-17], no results have been reported for indium amalgams. This paper gives the results of a preliminary study on the double-layer capacity of indium amalgams containing from 0–64% In, at 25° in 0.1 *M* $HClO_4$. This medium was chosen to correspond to that used for our measurements of hydrogen overvoltage on indium amalgams, which have been reported elsewhere[18].

II. EXPERIMENTAL

Double-layer capacities were measured at a dropping electrode by the method of GRAHAME[1,19]. The dropping electrode was surrounded by a cylindrical platinized-platinum screen. A bridge similar to that described in detail by PARSONS[20] was used to measure the impedance between the drop and the screen. The bridge was adjusted to balance at some moment near the end of the drop lifetime and the bridge-unbalance signal displayed on an oscilloscope and photographed. The age of the drop when the bridge was in balance, and hence the drop area, was obtained by measuring the time on the photograph, using time-marks produced by a signal generator accurate to

0.01%. The a.c. signal applied was about 3 mV in amplitude. The series resistance was approximately 60 Ω, the same value as was calculated from the area of the drop and the conductivity of the solution. The reproducibility of measurements with mercury electrodes, using different capillaries and fresh solution, was about 1%, but the absolute values obtained are probably not so accurate.

The capacity of mercury at the top of the hump near the zero-charge point was found to be 27.4 μF/cm^2. GRAHAME[1,21] obtained 28.0 μF/cm^2; and HANSEN *et al.*[8,22] obtained 28.7 μF/cm^2. Our results are 2–5% lower than these measurements. Our measurement technique differed from that of the previous workers primarily in that their drop lifetimes were approximately 10 sec, whereas ours were 0.5–2 sec. The discrepancy does not result from the variation in mass-flow during drop formation due to back-pressure; correction for this effect was made as described by GRAHAME[23], but the corrected value was 27.2 μF/cm^2, slightly lower than the uncorrected value. Systematic errors may have arisen from stray capacitances and inductances in the bridge and cell, from differences in the way the drops broke off, from precision of the assumption that the drops were spherical throughout their lifetime, or from trace impurities in the solution.

III. CALCULATIONS

The first step in the calculations is to obtain the area of the drop at the moment when the impedance bridge was balanced. A convenient form for the dependence of area on time, which includes a correction for the back-pressure due to interfacial tension, was proposed by GRAHAME[23]. The pressure, P, at the capillary tip results from both the height of the amalgam above the tip and the back-pressure due to interfacial tension:

$$P = \varrho\, gh - 2(\gamma/r) \tag{1}$$

where g is the acceleration of gravity (980.6 dyn/g), h is the height of the column of amalgam, ϱ is the density of the amalgam, γ is its interfacial tension, and r is the radius of the drop at the end of the capillary. The volume flow rate is taken to be proportional to P, and the area of the drop is obtained by integrating the volume flow rate with respect to time, assuming a spherical shape for the drop.

The assumption of a spherical drop is not as inaccurate as it might appear, since as long as the drop retains its cylindrical symmetry, the area/volume ratio is independent of its shape[27]. The error resulting from the normal asphericity of the drop just before it falls can be avoided by discarding values obtained very close to the end of drop lifetime. The principal uncertainty in area occurs when the drop is initially formed and is not yet a complete sphere. This problem can be minimized experimentally by using fine-pointed capillaries instead of the conventional blunt polarographic capillaries[24]. Making the assumption of a spherical drop, the following relation is obtained for the area of the drop as a function of time:

$$A = (36\pi)^{\frac{1}{3}}(k_1 \varrho\, ght)^{\frac{2}{3}}\left\{1 - \frac{3\gamma}{\varrho\, gh}\left(\frac{4\pi\varrho}{3mt}\right)^{\frac{1}{3}}\right\}^{\frac{2}{3}} \tag{2}$$

where k is a proportionality constant, and m is the mass-flow of amalgam through the capillary, which is virtually independent of potential[25]. The proportionality constant

can be evaluated from the drop lifetime, t^*, since the total volume of a drop is simply mt^*/ϱ. Evaluating eqn. (2) at the lifetime of the drop, and calculating the total volume of the drop, the following expression for the proportionality constant is obtained.

$$k_1 = \frac{m}{\varrho^2 gh}\left\{1 - \frac{3\gamma}{\varrho gh}\left(\frac{4\pi\varrho}{3mt^*}\right)^{\frac{1}{3}}\right\}^{-1} \tag{3}$$

This expression may be substituted in eqn. (2) to give an equation for the area of a drop as a function of time. When h is very large, eqns. (2) and (3) together reduce to the usual formula:

$$A = (36\pi)^{\frac{1}{3}}(mt/\varrho)^{\frac{2}{3}} \tag{4}$$

The true area is smaller than the area calculated from eqn. (4) because of the back-pressure.

Since it is sometimes difficult to obtain accurately reproducible drop lifetimes, some averaging procedure for drop lifetime is desirable. The drop lifetime used in eqn. (3) is calculated from the interfacial tension, γ, and an average value for the diameter by the usual formula for the drop-weight measurement of interfacial tension:

$$t^* = (\pi\gamma a/mg) \tag{5}$$

Although more subtle corrections[26] are known for this equation, they are not conveniently expressed in analytic form, and are not necessary for the present calculations. From a number of measurements of drop lifetime, an average value was obtained for the capillary diameter. This agreed with actual measurements of the capillary diameter made using a travelling microsope. From this value, using eqn. (5), t^* is calculated for each point, and used in eqn. (3) to obtain the proportionality constant.

This principal advantage of this averaging method is that only a few drop lifetimes need be actually measured. The capacity bridge can be balanced at the same point in the oscilloscope trace, whether or not the end of the drop actually appears on the oscilloscope screen[1].

In the above equations a value must be assumed for the interfacial tension in the initial phase of the calculation, but once the capacity data has been integrated, a much better value for the interfacial tension is known. To provide the most rapid convergence, the best possible starting values for interfacial tension are required. These are obtained in the present calculation by integrating an assumed quadratic form for the integral capacity, which may be obtained from literature data, or guessed by analogy with smilar systems. The exact values used affect only the rapidity of convergence, not the final answer. The integral capacity is assumed to be given by the quadratic form

$$K = K_0 + K_1\phi_0 + K_2\phi_0^2 \tag{6}$$

where ϕ_0 is the rational potential (potential with respect to the point of zero charge). The interfacial tension is then given by

$$\gamma = \gamma_{max} - 10\left\{\frac{K_0}{2}\phi_0^2 + \frac{K_1}{3}\phi_0^3 + \frac{K_2}{4}\phi_0^4\right\} \tag{7}$$

where γ_{max} is the maximum value of the interfacial tension, which must be measured, obtained from the literature, or estimated by correlation with similar systems. For

mercury in dilute aqueous solutions, $\gamma_{max} = 426.2$ ergcm^{-2}, $K_0 = 27.0$ μFcm^{-2}, $K_1 = 18.65$ μFcm^{-2} V^{-1}, and $K_2 = 9.65$ μFcm^{-2} V^{-2}. The factor 10 is required in eqn. (7) because of the conventional units; 1 μFcm^{-2} V^{-2} is equal to 0.1 erg cm^{-2}.

Further details regarding the relation of drop area to drop lifetime may be found in the literature[27-29].

Once the area of the drop at the point of balance has been calculated, the values of capacity and series resistance read from the bridge can be converted to the desired quantities—capacity per unit area and polarization resistance. The capacity per unit area is simply

$$C = \frac{C_{exp}}{A} \tag{8}$$

The polarization resistance is obtained after correcting the total measured resistance for the resistance of the electrolyte and the resistance of the amalgam in the capillary. If a cylindrical or spherical counter electrode of radius δ surround the drop, then the resistance R of the solution is given by

$$R = \frac{\delta r}{\varkappa A (r + \delta)} \tag{9}$$

where $\varkappa$ is the specific conductance of the electrolyte, r is the radius, and A is the area of the drop at the balance point. The polarization resistance is given by

$$R_{pol} = A(R_{exp} - R - R_{cap}) \tag{10}$$

where R_{exp} is the resistance measured on the bridge, R is given by eqn. (9), and R_{cap} is the resistance of the thread of amalgam in the capillary. R_{cap} may be calculated from the dimensions of the capillary and the resistivity of the amalgam. It is rarely more than one or two ohms.

The next portion of the calculation involves integration of the measured differential capacity values to obtain the surface charge, integral capacity, and interfacial tension.

Measurements of capacity are usually taken at closely-spaced intervals of potential (0.02–0.10 V). Since the values may scatter slightly about a smooth curve, a simple trapezoidal rule was used for the integration instead of a more sophisticated numerical integration algorithm. The surface charge is obtained by integrating the differential capacity:

$$q = \int_0^{\phi_0} C d\phi_0 \tag{11}$$

where ϕ_0 is the rational potential. A second integration gives the interfacial tension:

$$\gamma = \gamma_{max} - 10 \int_0^{\phi_0} q d\phi_0 \tag{12}$$

The absolute value of γ depends, of course, on the value of γ_{max}, which must be obtained independently. The curve of γ_{max} *vs.* indium concentration is assumed to be the same for indium amalgams in aqueous solutions as for indium amalgams in

vacuum[46]. Direct measurements of γ_{max} are now in progress[25]. The integral capacity is obtained from the surface charge:

$$K = \frac{g}{\phi_0} \tag{13}$$

Once these values have been calculated, the interfacial tension is used to recalculate the area of the drop, and better values of the differential capacity, surface charge, integral capacity, and interfacial tension are obtained. The iteration is continued until successive values of interfacial tension agree within 0.01 erg/cm^2. The final values do not depend on the initial assumption of the capacity function (eqn. 6); this affects only the rapidity of convergence.

The next step in the calculation is to find the potential of the outer Helmholtz plane and to calculate the contribution to the capacities from the diffuse double layer. In the absence of specific adsorption, the potential of the outer Helmholtz plane, ϕ_2, is given by the equation

$$K\phi_0 = \sqrt{\frac{2DD_0RTC}{\pi}} \sinh\left(\frac{F\phi_2}{2RT}\right) \tag{14}$$

where K is the integral capacity of the double layer, D is the dielectric constant of the solvent, D_0 (1.1128 $\times$ 10^{-12} C V^{-1} cm^{-1}) is a dimensional constant, R is the gas constant, C is the concentration of a 1–1 electrolyte, T is the absolute temperature, and F is the Faraday constant. Analogous equations have been derived for electrolytes other than simple univalent ones[30], and treatments have been extended beyond the simple Debye–Huckel theory[31–36].

With the constants evaluated and combined, eqn. (14) becomes

$$K\phi_0 = 11.72 \sqrt{C\,\frac{T}{298}} \sinh\left\{19.46\,\phi_2\left(\frac{298}{T}\right)\right\} \tag{15}$$

This equation is most easily solved by iteration using Newton's approximation method.

These calculations were performed on an IBM 7090 digital computer. The detailed program has been given elsewhere[37].

IV. RESULTS AND DISCUSSION

Most of the capacity measurements are plotted in Figs. 1 and 2; the zero-charge potentials used in the calculations are marked with arrows. These were reported in an earlier paper[18], and are listed in the capacity tables. As the concentration of indium decreases, the capacity at a given potential increases. At capacity values above 60 μF/cm^2, the capacity increases with decreasing frequency. Below this value, the capacity varies by less than 2% between 0.5 and 20 kc, except for the 0.002 and 0.005% amalgams, where a strong frequency dependence is observed in the region between 0 and —0.2 V, even at low capacity values. This frequency dependent pseudocapacity results from the reversible dissolution of indium. In the regions where the capacity was independent of frequency, the polarization resistance

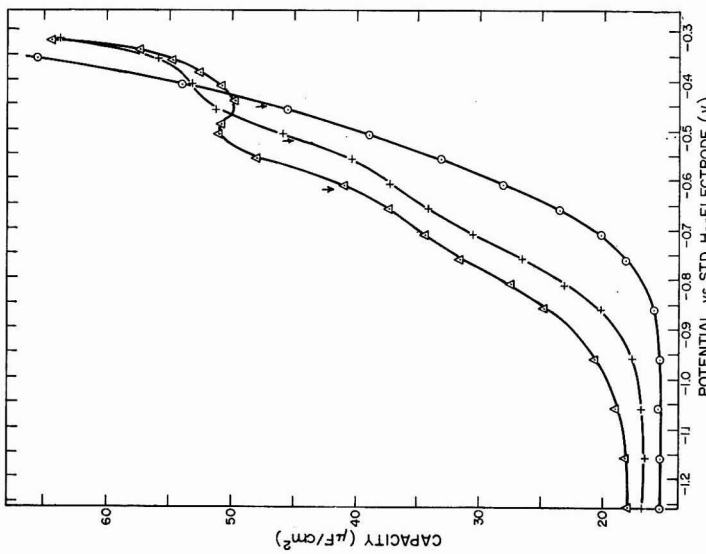

Fig. 2. Differential capacity of concentrated In amalgams at 10 kc. △, 64%; +, 40%; ○, 20%.

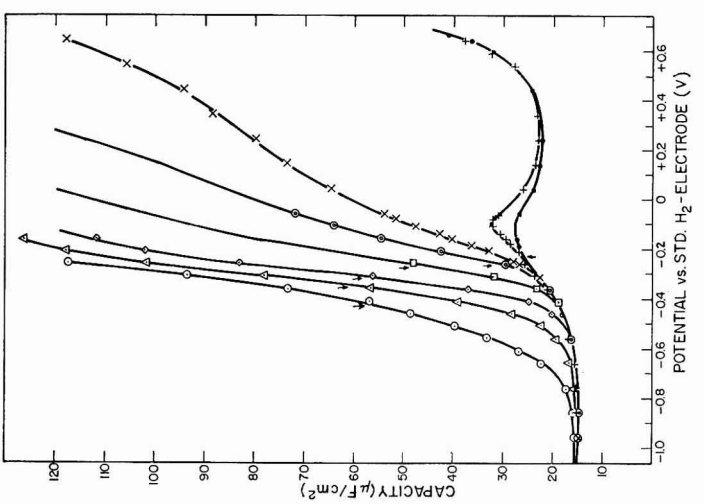

Fig. 1. Differential capacity of indium amalgams containing up to 16.3 mole % In, at 1 kc. ○, 16.3%; △, 3.9%; ◇, 1.0%; □, 0.1%; ◎, 0.01%; ×, 0.005%; +, 0.002% In; ●, 0.001% In (and pure Hg). The potentials given on the figure are 0.065 V more negative than those in the tables, because of the different reference electrode.

was usually less than 0.1 Ω cm². In regions where the capacity increased with decreasing frequency, the polarization resistance was as much as 100 times larger, and increased as the capacity increased.

Selected values of the measured capacity and integrated surface charge are given in Tables 1 and 2. Only values which are independent of frequency from 0.5–20 kc have been included. Amalgams of concentration less than 1% In gave capacity values which were the same as mercury except at potentials where a frequency dependence was observed.

TABLE 1

*Potential (V)**	*Pure mercury*		*0.92 At. %*		*3.9 At. %*		*8.4 At. %*	
	Dif. cap. (μF/cm²)	*Charge (μC/cm²)*	*Dif. cap. (μF/cm²)*	*Charge μC/cm²*	*Dif. Cap (μF/cm²)*	*Charge μC/cm²*	*Dif. cap. (μF/cm²)*	*Charge μC/cm²*
−1.100	16.17	−15.83	15.81	−15.77	15.80	−16.15	15.80	−16.15
−1.000	15.52	−14.25	15.31	−14.21	15.25	−14.60	15.12	−14.61
−0.900	14.57	−12.74	14.81	−12.70	15.08	−13.08	14.68	−13.12
−0.800	14.55	−11.29	14.85	−11.22	15.08	−11.58	14.75	−11.65
−0.700	14.84	− 9.82	15.06	− 9.73	15.60	−10.04	15.38	−10.14
−0.600	15.43	− 8.30	15.83	− 8.18	16.45	− 8.44	17.21	− 8.51
−0.500	16.33	− 6.72	17.33	− 6.52	19.15	− 6.66	23.12	− 6.53
−0.400	18.15	− 4.99	20.46	− 4.61	28.25	− 4.37	36.72	− 3.61
−0.300	20.88	− 3.04	37.05	− 1.95	56.73	− 0.29	62.95	+ 1.32
−0.200	24.83	− 0.76						
−0.100	27.23	+ 1.85						
0.00	26.59	4.54						
+0.100	23.90	7.06						
+0.200	22.40	9.38						
+0.300	21.81	11.59						
+0.400	22.88	13.82						
+0.500	24.55	16.19						
+0.600	28.20	18.83						
E_{ECM} (V)	−0.170		−0.257		−0.295		−0.322	
C_{ECM} (μF/cm²)	25.55		53.42		58.84		56.63	

* All potentials are referred to a reversible hydrogen electrode in 0.1 M $HClO_4$, which is −0.065 V with respect to the standard hydrogen electrode. ECM is the electrocapillary maximum, or zero-charge potential.

Figure 3 shows the capacity of mercury and 63.6% indium amalgam as a function of surface charge. In effect, such a plot normalizes the shift in zero-charge point. The indium amalgam capacity is higher than that of mercury at all values of surface charge, and the difference becomes greater at more positive potential. The "hump" which occurs near the zero-charge point for mercury also appears in the indium amalgam, but at slightly more positive potentials.

Figure 4 shows how the capacity varies with indium concentration at constant surface charge. At the most negative values of surface charge, the capacity is nearly independent of indium content at concentrations less than 20% In. However, as the surface charge becomes more positive, the increase in capacity begins at lower indium concentrations, and the increase is larger. In the concentration range from 1–20%, the zero-charge potential is close to the potential for reversible dissolution

TABLE 2

Potential (V)	*20.0 At. %*		*30.0 At. %*		*39.98 At. %*		*50.0 At. %*		*63.6 At. %*	
	Dif. Cap. ($\mu F/cm^2$)	*Charge ($\mu C/cm^2$)*	*Dif. Cap. ($\mu F/cm^2$)*	*Charge ($\mu C/cm^2$)*	*Dif. Cap. ($\mu F/cm^2$)*	*Charge ($\mu C/cm^2$)*	*Dif. Cap. ($\mu F/cm^2$)*	*Charge ($\mu C/cm^2$)*	*Dif. Cap. ($\mu F/cm^2$)*	*Charge ($\mu C87$)*
−1.300	15.74	−18.81	16.29	−18.66	17.11	−18.76	17.16	−17.88	18.09	−17.87
−1.200	15.63	−17.24	16.18	−17.04	17.03	−17.05	17.09	−16.17	18.23	−16.05
−1.100	15.52	−15.69	16.10	−15.43	16.85	−15.36	16.94	−14.47	18.45	−14.22
−1.000	15.68	−14.13	15.99	−13.82	17.06	−13.66	17.27	−12.76	18.87	−12.35
−0.900	15.58	−12.57	16.52	−12.20	17.80	−11.92	18.81	−10.96	20.76	−10.37
−0.800	16.12	−10.98	17.94	−10.47	20.63	−10.00	22.55	− 8.89	24.98	− 8.08
−0.750	16.95	−10.15	19.45	− 9.54	23.36	− 8.90	25.43	− 7.68	28.29	− 6.75
−0.700	18.32	− 9.26	22.05	− 8.50	26.76	− 7.65	29.17	− 6.30	31.83	− 5.25
−0.650	20.39	− 8.29	25.73	− 7.31	30.90	− 6.20	33.00	− 4.80	34.75	− 3.58
−0.600	23.75	− 7.19	31.21	− 5.88	34.54	− 4.57	35.54	− 3.07	37.67	− 1.77
−0.550	28.54	− 5.88	36.05	− 4.20	37.70	− 2.76	37.30	− 1.26	41.39	+ 0.21
−0.500	33.41	− 4.33	38.80	− 2.33	40.88	− 0.80	42.48	+ 0.75	47.60	+ 2.43
−0.450	39.42	− 2.51	43.85	− 0.27	46.51	+ 1.39	47.37	+ 3.00	51.53	+ 4.91
−0.400	46.04	− 0.37	50.15	+ 2.08	51.98	+ 3.85	50.67	+ 5.45	51.54	+ 7.48
−0.350	54.53	+ 2.14	57.82	+ 4.78	53.68	+ 6.49	51.82	+ 8.01	51.25	+10.03
−0.300	66.30	+ 5.16	62.10	+ 7.78	56.61	+ 9.25	53.47	+10.64	55.07	+12.67
E_{ECM} (V)	−0.392		−0.444		−0.481		−0.518		−0.555	
C_{ECM} ($\mu F/cm^2$)	47.40		44.61		43.02		40.82		41.01	

of indium, and the measured capacity contains a contribution (less than 10 $\mu F/cm^2$) from the dissolution reaction pseudo-capacity. This section of the curve for zero-charge is shown as a broken line in Fig. 4. At positive values of surface charge, the reversible dissolution reaction prevents measurement of true double-layer capacity at concentrations less than 20 mole % In. At concentrations greater than 20%, the capacity decreases as the indium content increases.

The potential of the outer Helmholtz plane, ϕ_2, is of importance in the slow-

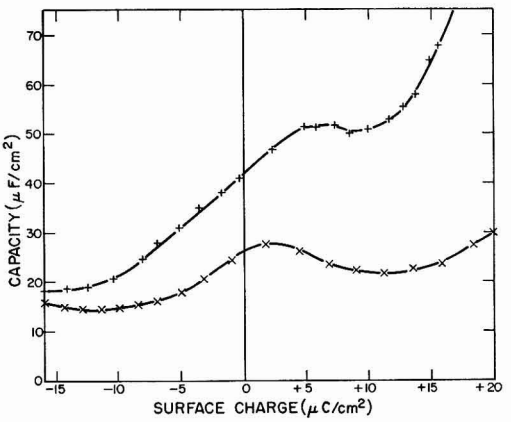

Fig. 3. Comparison of capacity as a function of surface charge for mercury (×) and 63.6% In amalgam (+). Note that the "hump" occurs at approximately the same surface charge.

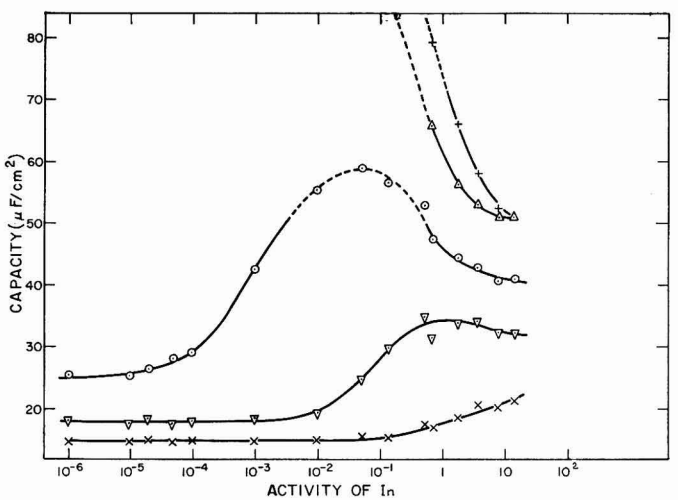

Fig. 4. Capacity as a function of In activity at constant surface charge. +, +10.0; △, +5.0; ○, 0.0; ▽, −5.0; ×, −10.0 $\mu C/cm^2$. The broken portions of the curve indicate that a substantial contribution to the capacity arises from the reversible dissolution of indium.

discharge theory of hydrogen evolution[38,39], as well as in other electrode reactions where electron-transfer is the rate-determining step[15,40,41]. This potential can be calculated as described previously, and the results for mercury and indium amalgams are shown in Fig. 5 as a function of rational potential. Because of the higher surface charge on the amalgam, the value ϕ_2 at a given rational potential is as much as 20 mV larger than on mercury. On the other hand, as can be seen from Fig. 6, the value of ϕ_2 at a given potential relative to the reversible hydrogen electrode (the negative of the hydrogen over-potential) is nearly the same for mercury and the amalgam in the potential region where overvoltage measurements are usually carried out—from −0.9 to −1.2 V. The dotted portions of the curves on Figs. 5 and 6 indicate regions

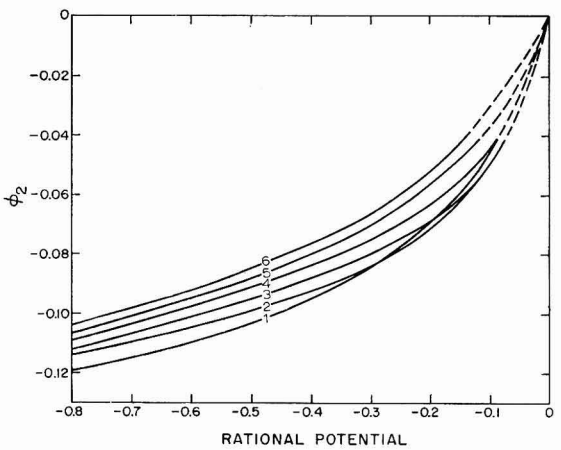

Fig. 5. Potential of the outer Helmholtz plane for Hg and In amalgams as a function of rational potential. (1) 63.6%; (2), 20.0%; (3), 3.9%; (4), 0.92%; (5), 0.094% In; (6), Hg.

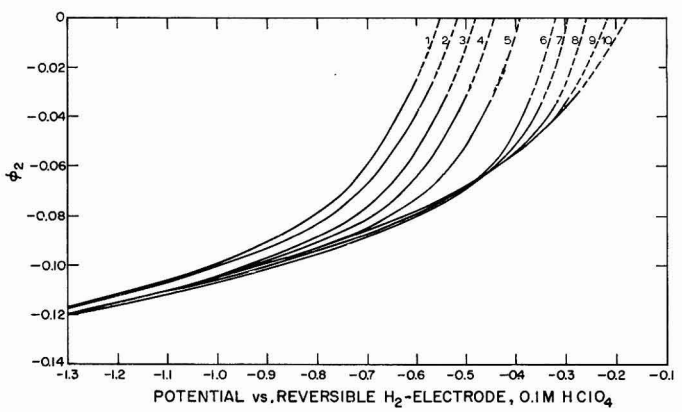

Fig. 6. Potential of the outer Helmholtz plane for Hg and In amalgams as a function of hydrogen overpotential. Note that in the region where overpotential measurements are usually made (−0.8 to −1.2 V) the difference is quite small. (1), 63.6%; (2), 50.0%; (3), 40.0%; (4), 30.0%; (5), 20.0%; (6), 8.4%; (7), 3.9%; (8), 0.92%; (9), 0.094% In; (10), Hg.

where there is probably error due to specific adsorption of perchlorate ion[3]. This region, is, of course, unimportant in considerations of hydrogen over-potential. Thus, even though the zero-charge potential shifts by 0.4 V, the potential drop across the diffuse double layer changes only by 3–10 mV.

In a previous publication[18], we investigated the variation of hydrogen over-voltage on indium amalgams. We analyzed our experimental data in terms of Frumkin's equation[38,39,42]. Since the composition of the electrode and the concentration of hydrogen ion in the electrolyte are constant, we can gather the constant terms of Frumkin's equation into a corrected exchange current i_0':

$$\eta = \frac{1-\alpha}{\alpha}\phi_2 + \frac{RT}{\alpha F}\ln(i/i_0') \tag{18}$$

where

$$\ln i_0' = (1-\alpha)\ln[H^+] - \frac{\alpha F}{RT}g_H + \text{const.} \tag{19}$$

In these equations, α is the cathodic transfer coefficient, i is the current density, g_H is the heat of desorption of a hydrogen atom from the surface of the electrode, and $[H^+]$ is the bulk concentration of hydrogen ions. In our previous paper[18], we assumed $\alpha = 0.500$, which gave values of $-\log i_0'$ that were independent of η.

The corrected exchange current, i_0', is different from the exchange current obtained from the simple Tafel equation because of the term in ϕ_2, which corrects for the potential drop across the diffuse double layer. If $\phi_2 = 0$, eqn. (18) reduces to the simple Tafel equation:

$$\eta = \frac{RT}{\alpha F}\ln(i/i_0) \tag{20}$$

Equation (18) can be cast into the form of a straight line:

$$y = \alpha x + B \tag{21}$$

where

$$y = \frac{RT}{F}\ln i + \phi_2 \tag{22}$$

$$x = \eta + \phi_2 . \tag{23}$$

The slope of this line is α and its intercept is

$$B = \frac{RT}{F}\ln i_0' \tag{24}$$

To obtain the parameters for each of the experiments conducted, the values of ϕ_2 shown in Fig. 6 were used in eqns. 22 and 23 to calculate the functions of x and y. A least-squares straight line was fitted to the function $y(x)$, and from its slope and intercept were obtained the best values for α and $-\log i_0'$. The 95% confidence limits provide an estimate of the probable error in the measurements. These calculations were performed on an IBM 1620 computer. The details have been given elsewhere[37].

In Table 3, the results of these calculations are compared with the parameters

TABLE 3

PARAMETERS FOR HYDROGEN OVERVOLTAGE ON IN AMALGAMS

Mole Fraction In	*Least-squares fit*[c]		$\alpha = 0.500$		
	α	$-\log i_0$	$-\log i_z$	$-\log i_0'$ *(ref. 18)*	$-\log i_0'$ *(this work)*
0.0[a]	0.469 ± 0.003	12.43 ± 0.10	11.13	12.65	12.64
0.084	0.479 ± 0.012	12.27 ± 0.21	9.66	12.53	12.62
0.163	0.496 ± 0.010	12.49 ± 0.17	9.38	12.42	12.55
0.304	0.503 ± 0.016	12.43 ± 0.27	8.59	12.26	12.36
0.522	0.497 ± 0.012	12.20 ± 0.20	7.66	12.09	12.24
0.644	0.478 ± 0.013	11.77 ± 0.22	7.25	11.96	12.13
1.000[b]	0.50 ± 0.02	11.3 ± 0.5	6.5	11.85	11.3

[a] Pure mercury (ref. 43).
[b] Pure solid indium, data obtained at 40–60° extrapolated to 25° (ref. 44).
[c] Errors quoted are 95% confidence limits.

published previously[18]. The previous values were obtained under the assumption that the potential drop across the diffuse double layer at the same rational potential was the same for the amalgam as for mercury, whereas we have shown here that a much better approximation would have been to assume the same potential drop at the same overpotential. For this reason, even the values of $-\log i_0'$ calculated assuming $\alpha = 0.500$, using the accurate capacity data, are slightly different than those published previously.

Another noticeable difference occurs in the value for pure solid indium. The previously published value was extrapolated assuming that the temperature coefficient of overvoltage on solid indium was the same as for mercury. In fact, it its considerably smaller[44], and the smaller value gives $-\log i_0' = 11.3$ at 25°.

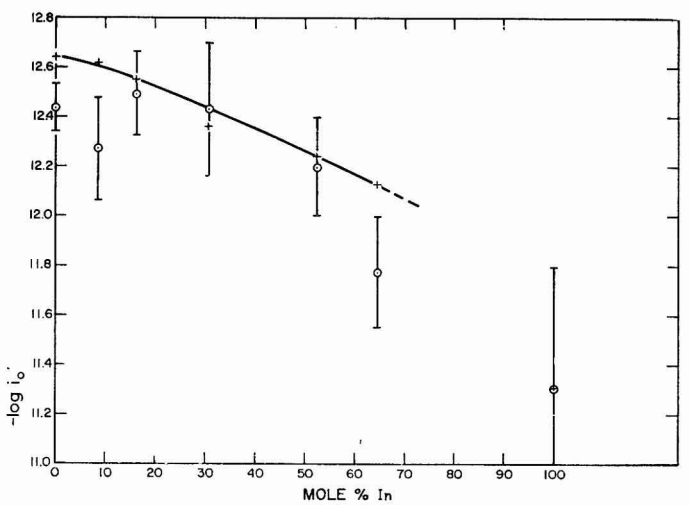

Fig. 7. Exchange current for the hydrogen evolution reaction (corrected for double-layer effects) as a function of amalgam composition. The crosses were calculated with the transfer coefficient, α, fixed at 0.500. The circles were calculated from a least-squares fit of Frumkin's equation to the data. The vertical bars indicate 95% confidence limits.

In Fig. 7 we have compared the values of log i_0' obtained from the least-squares calculation with values calculated assuming a fixed value, $\alpha = 0.500$, as was done in ref. 18. The values of $-\log i_0'$ calculated assuming $\alpha = 0.500$, show an almost linear dependence on indium concentration, whereas the values obtained by the least-squares fit show a rather non-linear dependence, and perhaps even go through a maximum at about 20% In.

This preliminary study leaves many questions still unanswered. Although we have assumed that there is no specific adsorption of ions in the Helmholtz layer, this is not rigorously correct, and perchlorate ion is almost certainly adsorbed to some extent at positive surface charges[3,45]. Whether or not this specific adsorption is entirely responsible for the large change in capacity with indium concentration at constant surface charge (Fig. 4), we cannot unambiguously decide at the present time. The capacity difference might also result from differences in the In–Hg dipole layer in the metallic phase, or from differences in dipole orientation of water in the aqueous phase.

Studies are now in progress to determine the double-layer capacity on indium amalgams in sodium fluoride solutions, since studies on mercury have shown fluoride to be less strongly adsorbed than any other anion[1-3]. The variation of capacity with electrolyte concentration will provide a test of this hypothesis. If fluoride is not specifically adsorbed, then changes in the capacity of the Helmholtz double layer with amalgam composition can probably be attributed to dipole orientation effects.

ACKNOWLEDGEMENTS

This work was supported by the Office of Naval Research, Materials Sciences Division, Contract NOnr-3765(00), ARPA Order No. 302-62. The authors thank Dr. RICHARD PAYNE of the Air Force Cambridge Research Laboratory for several helpful discussions.

SUMMARY

The double-layer capacity of indium amalgams was measured at 25° in 0.1 M $HClO_4$ using a dropping electrode. Fourteen amalgams ranging in composition from 0.001–64.4 mole% In were studied. At indium concentrations below 0.001%, the capacity is identical to pure mercury; at higher concentrations, a pseudo-capacity due to the dissolution of indium is observed at potentials more positive than the In–In^{3+} equilibrium potential. As the concentration of indium varies from 1–70%, the zero-charge potential shifts 0.4 V more negative, and the capacity–potential curve shows a corresponding shift. The capacity–surface charge curve in concentrated indium amalgams shows the same "hump" near the zero-charge point as in pure mercury.

At a surface charge of -10 $\mu C/cm^2$, the capacity varies from 15 $\mu F/cm^2$ for mercury to 20 $\mu F/cm^2$ for 64% indium amalgam. At a surface charge of $+10$ $\mu C/cm^2$, the capacity of a 64% indium amalgam is approximately twice that of mercury.

The potential drop across the diffuse double layer was calculated using the Gouy–Chapman theory. The influence of the diffuse double layer is greater for concentrated amalgams than for mercury. Previous data for hydrogen overvoltage on indium amalgams together with the capacity measurements was used to analyze the effect of the diffuse double layer on the hydrogen discharge reaction.

REFERENCES

1 D. C. GRAHAME, *Chem. Rev.*, 41 (1947) 441.
2 D. C. GRAHAME, *J. Am. Chem. Soc.*, 76 (1954) 4819.
3 D. C. GRAHAME AND B. A. SODERBERG, *J. Chem. Phys.*, 22 (1954) 449.
4 D. C. GRAHAME, *J. Chem. Phys.*, 23 (1955) 1166.
5 D. C. GRAHAME, *J. Am. Chem. Soc.*, 80 (1958) 4201.
6 D. C. GRAHAME AND R. PARSONS, *J. Am. Chem., Soc.*, 83 (1961) 1291.
7 B. B. DAMASKIN, *Usp. Khim.*, 30 (1961) 220–42.
8 R. S. HANSEN, D. J. KELSH AND D. H. GRANTHAM, *J. Phys. Chem.*, 67 (1963) 2316–26.
9 R. PARSONS, *J. Electroanal. Chem.*, 5 (1963) 397–410.
10 W. M. SPICER AND C. J. BANICK, *J. Am. Chem. Soc.* 75 (1953) 2268.
11 H. ITO, E. OGAWA AND T. YANAGASE, *Nippon Kinzoku Gakkaishi*, B15 (1951) 382; C.A. 47 (1963) 12193.
12 L. F. KOZIN AND N. N. TANANAEVA, *Zh. Neorgan. Khim.*, 6 (1961) 909; Eng. Transl.: *Russ. J. Inorg. Chem.* 6 (1961) 463.
13 G. L. EGGERT, *Trans. Am. Soc. Metals*, 55 (1962) 891.
14 B. R. COLES, M. F. MERRIAM AND Z. FISK, *J. Less-Common Metals*, 5 (1963) 41.
15 P. DELAHAY AND M. KLEINERMAN, *J. Am. Chem. Soc.*, 82 (1960) 4509–4514.
16 L. I. BOGUSLAVSKII AND B. B. DAMASKIN, *Zh. Fiz. Khim.*, 34 (1960) 2099–2108.
17 J. N. BUTLER, *J. Electroanal. Chem.*, 9 (1965) 149.
18 J. N. BUTLER AND A. C. MAKRIDES, *Trans. Faraday Soc.*, 60 (1964) 1664.
19 D. C. GRAHAME, *J. Am. Chem. Soc.*, 71 (1949) 2975.
20 R. PARSONS, *Trans. Faraday Soc.*, 56 (1960) 1340–50.
21 D. C. GRAHAME, *Proceedings 3d Meeting CITCE*, (1951) p. 330.
22 R. S. HANSEN, R. E. MINTURN AND A. HICKSON, *J. Phys. Chem.*, 60 (1956) 1185.
23 D. C. GRAHAME, *J. Phys. Chem.*, 61 (1957) 701.
24 D. C. GRAHAME, *J. Am. Chem. Soc.*, 68 (1946) 301.
25 J. N. BUTLER, unpublished work.
26 W. D. HARKINS AND F. E. BROWN, *J. Am. Chem. Soc.*, 41 (1919) 499.
27 G. S. SMITH, *Trans. Faraday Soc.*, 47 (1951) 63.
28 G. C. BARKER AND A. W. GARDNER, *Advances in Polarography*, Pergamon Press, London, 1960, p. 330.
29 J. M. LOS AND D. W. MURRAY, *Advances in Polarography*, Pergamon Press, London, 1960, p. 425.
30 D. C. GRAHAME, *J. Chem. Phys.*, 21 (1953) 1054.
31 J. R. MACDONALD, *J. Chem. Phys.*, 22 (1954) 1317.
32 J. R. MACDONALD AND M. K. BRACHMAN, *J. Chem. Phys.*, 22 (1954) 1314.
33 J. R. MACDONALD, *J. Chem. Phys.*, 29 (1958) 1346.
34 J. R. MACDONALD, *J. Chem. Phys.*, 30 (1959) 806.
35 G. G. ROBERTS AND R. H. TREDGOLD, *Phys. Letters*, 2 (1962) 6.
36 W. B. JEPSON, *J. Chem. Phys.*, 39 (1963) 2377.
37 J. N. BUTLER, *Computer Programs for Calculations Relating to Dropping Amalgam Electrode*, (Tech. Memo #12).
38 A. N. FRUMKIN, *Z. Physik. Chem., Leipzig, A164* (1933) 121.
39 A. N. FRUMKIN, *Discussions Faraday Soc.*, 1 (1947) 57.
40 M. BREITER. M. KLEINERMAN AND P. DELAHAY, *J. Am. Chem. Soc.*, 80 (1958) 5111.
41 R. PARSONS, *Advances in Electrochemistry and Electrochemical Engineering I*, edited by P. DELAHAY, Interscience Publishing Co. Inc., New York, 1961, p. 1.
42 A. N. FRUMKIN, *Advances in Electrochemistry and Electrochemical Engineering I*, edited by P. DELAHAY, Interscience Publishing Co. Inc., New York, 1961, p. 65.
43 B. POST AND C. F. HISKEY, *J. Am. Chem. Soc.*, 72 (1950) 4203.
44 J. N. BUTLER AND M. DIENST, *J. Electrochem. Soc.*, 112 (1965) 226.
45 R. PAYNE, private communication.
46 D. A. OLSEN AND D. C. JOHNSON, *J. Phys. Chem.*, 67 (1963) 2529.

BOOK REVIEWS

Talanta. Issue in honour of the 70th birthday of I. M. KOLTHOFF, February 1964, Volume 11, Pergamon Press, Oxford, London, New York, Paris.

This is a model of a birthday tribute. In 320 pages are collected 24 papers, more than half by Professor KOLTHOFF's former graduate students. The issue begins with a biographical essay by Professor J. J. LINGANE, another former graduate student and an essay by Professor KOLTHOFF himself on the *Status of and Trends in Analytical Chemistry* in which he states his belief in the importance of the scientific approach to analytical chemistry. That there are few analytical chemists unconverted to this view is testimony to the effectiveness of KOLTHOFF's teaching, both in person and through his books, as well as the example he has given in his papers. The volume concludes with a list of the latter up to the present; it reaches the remarkable total of 823.

ROGER PARSONS, University of Bristol

D'Ans–Lax Taschenbuch für Chemiker und Physiker, 3rd ed., Band II, *Organische Verbindungen*, Springer Verlag, Berlin, Göttingen, Heidelberg, 1964, 1177 pages, D.M. 48.

The largest section of this pocket book consists of an alphabetic list of some six thousand six hundred organic and organometallic compounds, together with their formulae, molecular weights, densities, melting and boiling points, refractive indices, solubilities, crystalline forms, optical rotations, etc. Although provision is made for quoting properties such as principal i.r. and u.v. absorption peaks, or pK values, these are given so rarely that the book is useless as a source of such data. Melting and boiling point and formulae indices are provided, and also a section of fifty pages on nomenclature. The volume also contains thermochemical data for about six hundred compounds, and a table of critical constants.

The authors have culled their information from easily available standard sources, and this volume would not therefore, make a significant addition to the resources of any reasonably well-stocked library. The individual worker would find it useful to keep at the bench, but at a comparable price, he could purchase a considerably more versatile and comprehensive handbook.

J. S. LITTLER
Chemistry Department, University of Bristol

Behavior of Electrons in Atoms, by R. M. HOCHSTRASSER, W. A. Benjamin Inc., New York and Amsterdam, 1964, xii + 162 pages, $4.50.

This short monograph appearing in the *General Chemistry Monograph Series*

provides a sound qualitative introduction to the electronic structure of atoms and to the investigation of the energy states of atoms, by means of perhaps the most powerful method of investigating atomic structure *i.e.*, atomic spectroscopy.

In accordance with the scope of this series and the intended level of its readers, the treatment is much more phenomenological–experimental than mathematical. In fact very few mathematical formulae are used and these do not go beyond logarithmic functions. The nine chapters of this monograph are devoted to: elementary presentation of the atomic spectra; interaction between atoms and electrons; quantum theory and atomic structure; Pauli principle, atomic energy terms and states; excitation probabilities and collisions involving excited atoms. The text is very elementary so that undergraduates should have no difficulty in following the reasoning, especially as there are a number of very clear figures which help to explain the text.

G. MILAZZO, Istituto Superiore di Sanità, Roma

CONTENTS

Points of zero charge in equations of electrochemical kinetics
A. N. FRUMKIN (Moscow, U.S.S.R.) 173

Electrolytic separation and colorimetric determination of traces of lead in cobalt using isotopic dilution analysis
A. LAGROU AND F. VERBEEK (Ghent, Belgium) 184

Influence of mercury drop growth and geometry on the a.c. polarographic wave
J. R. DELMASTRO AND D. E. SMITH (Evanston, Ill., U.S.A.) 192

Reduction of iodate in sulphuric medium.
I. The reduction mechanism
P. G. DESIDERI (Florence, Italy) 218

Reduction of iodate in sulphuric medium.
II. The influence of the surface of the platinum electrode
P. G. DESIDERI (Florence, Italy) 229

The electrical double layer on indium amalgams in 0.1 *M* $HClO_4$ at 25°
J. N. BUTLER, M. L. MEEHAN AND A. C. MAKRIDES (Waltham, Mass., U.S.A.) . . . 237

Book reviews 251

ELSEVIER PUBLISHING COMPANY, AMSTERDAM

Printed in The Netherlands by

NEDERLANDSE BOEKDRUK INRICHTING N.V., 'S-HERTOGENBOSCH